eman ta zabal zazu

Universidad del País Vasco
Euskal Herriko Unibertsitatea

Departamento de Fisiología
Facultad de Medicina y Enfermería

Role of endoplasmic reticulum stress in the pathogenesis of polycystic liver disease: new potential therapeutic target

Tesis presentada por

ÁLVARO SANTOS LASO

Donostia – San Sebastián

2019

eman ta zabal zazu

Universidad del País Vasco

Euskal Herriko Unibertsitatea

biodonostia

osasun ikerketa institutua
instituto de investigación sanitaria

Role of endoplasmic reticulum stress in the pathogenesis of polycystic liver disease: new potential therapeutic target

Tesis presentada por
Álvaro Santos Laso

Para la obtención del título de doctor en
Investigación Biomédica **por la**
Universidad del País Vasco/Euskal Herriko Unibertsitatea

Tesis dirigida por
Dr. D. Jesús María Bañales Asurmendi
Dra. Dña. María Jesús Perugorria Montiel

The project exposed in this thesis was performed at Biodonostia Health Research Institute under the supervision of Dr. Jesús Mª Bañales Asurmendi and Dr. María J. Perugorria Montiel. Likewise, Dr. María Begoña Ruiz Larrea, on behalf of the Faculty of Medicine and Nursing of the University of the Basque Country (UPV/EHU), absolutely supported this dissertation.

Álvaro Santos Laso was the recipient of a Ph.D. fellowship (*PRE_2015_1_0126*) from Gobierno Vasco (Basque Country, Spain) and a Short-Term fellowship (*Reference number: 8223*) from the European Molecular Biology Organization (EMBO) (Heidelberg, Germany). This work was funded with grants from Diputación Foral de Guipúzcoa (*DFG15/010*) and Gobierno Vasco (*2015111100*).

"***Vive la vida como si nadie mirase y exprésate como si todo el mundo escuchase***"

(Nelson Mandela)

Agradecimientos

A lo largo de este corto pero intenso camino como es la tesis doctoral, he tenido la oportunidad de encontrar una “nueva familia” que no solo me ha apoyado y arropado en las situaciones difíciles, sino que además ha convertido los buenos momentos en inolvidables. Esto es solo una pequeña muestra de lo agradecido que estoy con todas y cada una de las personas que han compartido conmigo estos años (tanto durante mi etapa de prácticas como durante la etapa pre-doctoral), puesto que no hay suficientes palabras para expresar la gratitud que siento.

Me gustaría comenzar agradeciendo a mis directores de tesis, el Dr. Jesús Mª Bañales (Txus) y la Dra. María J. Perugorria (Matxus). Gracias **Txus** por confiar en aquel niño que cuando te conoció, por allá en 2012, apenas comprendía lo que era la ciencia. Tú fuiste quién me animaste a pasar los veranos en el laboratorio y me diste la oportunidad de continuar mi carrera científica, lo que sin duda me ha ayudado a madurar tanto profesional como personalmente. Agradezco enormemente que durante estos años me hayas formado, hayas pulido mis carencias y me hayas otorgado ciertas responsabilidades; espero no haberte defraudado en ningún momento. No quiero pasar por alto todos los buenos consejos que me has dado (muchos de ellos durante nuestros viajes diarios) y el esfuerzo que haces día a día para que todos nosotros tengamos un futuro más cómodo en este mundo tan competitivo. A ti **Matxus**, quiero darte las gracias por esas largas conversaciones que teníamos, prácticamente a diario, y que tanto me han servido para aprender a pensar por mí mismo y para desarrollar una inquietud por querer saber más y buscarle explicación a cada uno de los resultados que iba obteniendo. Todo esto no hubiese sido posible sin el **Dr. Luis Bujanda**, de quien aprecio enormemente el esfuerzo y dedicación invertidos para que este grupo de investigación se creara. Muchas gracias por interesarte tanto por la investigación básica, por valorar el trabajo que hacemos y por estar siempre dispuesto a ayudarnos.

Quiero agradecer también al Gobierno Vasco por haberme concedido la beca para la realización de este proyecto, así como a la Universidad del País Vasco (UPV/EHU) y al Instituto de Investigación Sanitaria Biodonostia (IISB) por permitirme llevarlo a cabo.

Me gustaría continuar expresando mi agradecimiento a todos mis compañeros del grupo de *hepato* (pasados y presentes). Estoy seguro de que sin vosotros esto hubiese sido mucho más duro, y es que ya sabéis lo que dicen: “Si con nosotros pasas el rato, vas a ser feliz, feliz en hepato”. Gracias por vuestro constante apoyo, por vuestra incansable ayuda, por tener siempre una sonrisa en esos días en los que el ánimo está más bajo, por el gran ambiente que generáis… en definitiva, gracias por ser amigos más que compañeros. **Patri** contigo comenzó todo, has sido como la hermana mayor que nunca he tenido. No solo me has enseñado a trabajar correctamente en el laboratorio, sino que me has cuidado tanto dentro como fuera de él. Tú eras a la que siempre recurría cuando metía la pata porque sabía que eras capaz de solucionar cualquier cosa, demostrándome que los problemas se deben afrontar siempre con ingenio y sosiego. **Oihane**, muchas gracias por esos abrazos que me diste en los que, sin duda, han sido los momentos más dolorosos de estos años. Eres una excelente investigadora y mejor persona con la que he aprendido a perseverar y a luchar día a día, aunque las cosas no saliesen bien. Que puedo decir de **Ander** (Epi), menuda pareja formábamos. Nunca olvidaré esos momentos en los que era imposible que parasemos de reír, como los echo de menos. Trabajar a tu lado ha sido todo un privilegio y espero que a lo largo de estos años se me haya pegado un poquito de toda tu sabiduría, puesto que eras el espejo en el que mirarme día a día. Gracias por enseñarme a relativizar los problemas y tomárnoslo todo un poco a “cachondeo”, sin duda eso me ha ayudado a llevar mejor la presión y el estrés propios de esta etapa. Quiero agradecer también a **Aitor** sus buenos consejos cuando más los necesité, su capacidad para quitar tensión a los momentos difíciles y su participación en el grupo “The last of pHilippines”, un trio (junto con Ander) musical poco afinado, pero que causaba sensación. **Maite**, gracias por estar siempre dispuesta a enseñarme y por hacernos reír con las historias de tus viajes futboleros.

Laura que habría hecho sin ti! Está claro que has sido mi parte Izquierdo durante todos estos años, y es que a pesar de que muchas veces teníamos puntos de vista diferentes, nos entendíamos a las mil maravillas, tanto que sabíamos perfectamente cuando teníamos un mal día sin necesidad de decir nada. Poco a poco te fuiste convirtiendo en mi mano derecha y parte de mi

cerebro, llegando a tener que inventarnos una nueva firma para los correos (Atentamente Lauvaro Izquitos) que hiciese justicia a esta nueva entidad. Muchas gracias por ser mi pepito grillo, la que siempre me decía las cosas aunque no me gustasen, porque sabías que era lo mejor para mí. Gracias por motivarme cuando lo veía todo negro e incluso asumir responsabilidades que no te correspondían. No podía haber compartido tantas horas de trabajo (y fuera de él) con alguien mejor que tú, alguien en quien confiaba más que en mí mismo. Hagas lo que hagas no pierdas tu esencia porque personas como tú no se encuentran todos los días . Gracias **Paula** por preocuparte diariamente por todos y cada uno de nosotros, siendo siempre la primera dispuesta a ayudar sin perder la sonrisa y la paciencia, incluso cuando te bombardeábamos con cientos de preguntas al mismo tiempo. No sé qué voy a hacer sin mi correctora/traductora/agenda oficial y sin esas conversaciones matinales que nos hacían el día un poquito más corto y llevadero. Quiero agradecer también a **Ainhoa** las muestras de cariño que siempre tenía preparadas como el mejor remedio ante un mal día, y toda la alegría y energía que aportaba al laboratorio. A **Ibone**, porque además de ser una estupenda enfermera que me curaba los cortes, quemaduras y pinchazos, siempre tuvo palabras y gestos tranquilizadores cuando más los necesité. A **Javi**, por estar siempre dispuesto a dedicar parte de su tiempo a pensar y razonar conmigo, por enseñarme infinidad de cosas interesantes y por hacerme reír en incontables ocasiones. **Puyi**, nunca olvidaré los momentos graciosos que hemos compartido tratando de enseñarte los dichos españoles. Agradecer también a **Pedrinho** todo el esfuerzo y empeño que ha puesto para que este grupo sea mejor de lo que ya es. Muchas gracias por toda la ayuda y los buenos consejos que me has dado, gracias porque desde el primer día nos ganaste con tu simpatía, alegría y cariño.

No quiero olvidarme de las nuevas incorporaciones al grupo, **Nuno**, **Irene** y **Aloña**, a los que quiero dar las gracias por soportar como nadie mis chistes malos y aportar frescura al laboratorio. Os deseo lo mejor en esta andadura.

Me gustaría dar las gracias también a todos los integrantes del grupo que provienen del ámbito clínico por la predisposición a transcender la labor asistencial, y por el afán y esfuerzo que han invertido para tratar de mejorar la

calidad de vida de sus pacientes. Especialmente agradecer a **Adelaida** esas conversaciones banales sobre futuros negocios que no llevaban a ningún lado, pero que nos hacían soñar y escapar durante unos minutos de la realidad, así como por los dulces que nos solía traer y que tanta vitalidad nos daban.

Quiero agradecer a todas aquellas personas que, a pesar de compartir un breve periodo de tiempo con ellas, han dejado huella en mí. Especialmente, me gustaría mencionar a **Elisa** y **Myrian**, quienes me inculcaron el valor del trabajo bien hecho, y a **Anne**, con quién compartí muchas charlas filosóficas y científicas durante nuestras tardes veraniegas de *running*.

Además de a los integrantes del grupo de Enfermedades Hepáticas (hepato), también me gustaría dar las gracias a todos los investigadores del IISB por su labor diaria en la búsqueda de nuevos avances que mejoren la calidad de vida de los pacientes, por los consejos científicos que me han dado y que, sin duda alguna, han tenido un papel importante en mi desarrollo como investigador, y por sus constantes muestras de cariño. En especial, me gustaría agradecer a **Jaione L.** y a **Lucía**, por ser la solución a muchos de mis problemas y unas grandes consejeras, a **Claudia**, porque, a pesar de darle muchos dolores de cabeza, siempre estaba dispuesta a ayudarme, y a **Eli**, **Carlos, Mariasun** e **Iñaki** (plataforma de animalario) por mostrarme siempre su afecto. No obstante el IISB no solo está formado por investigadores, por ese motivo también quiero dar las gracias a todos mis compañeros/as de la "planta 0" que se esfuerzan día a día para proporcionarnos el mejor soporte económico-administrativo con un trato inmejorable, y especialmente agradecer a **Sandra** su apoyo incondicional, sus lecciones y su interés por el trabajo que desempeñamos. Menos mal que tuve la suerte de dar contigo aquel día. Gracias por la empatía que mostraste y la tranquilidad que me trasmitiste, gracias por no perder la sonrisa ni las formas en ningún momento, a pesar de que estuve acudiendo a ti día sí día también durante mes y medio, gracias por ser una persona maravillosa.

También me gustaría dar las gracias a **Nerea G.**, **Nerea A.** y **Ana** que desde el primer día me acogieron e hicieron mucho más llevadera mi estancia en Edimburgo, consiguiendo que los tres meses se me pasasen volando. Gracias por estar siempre dispuestas a tomar unas "pintas" en el Finnegans o

disfrutar de un *Ceilidh*. Agradecer también a **Scott** su ayuda durante esos meses de estancia y su paciencia ante todos mis ruegos y preguntas.

A mis amigos/as que siempre han mostrado su interés y en especial a **Marina**, quien ha participado activamente en este proyecto.

Por último, quiero dedicar mis últimas palabras de agradecimiento a toda mi familia, especialmente a mi bisabuela **Antonia** quién, a pesar de no saber muy bien lo que hacía, se sentía muy orgullosa de mí, y a mis padres, las dos personas que han hecho posible que ahora esté donde estoy y sea quién soy. **Mamá**, **Xabier**, muchas gracias por ser el faro que siempre ilumina mi camino y el eje imprescindible de mi vida. Gracias por darme un educación basada en principios y valores humanos, por enseñarme a no rendirme nunca y hacerme más fuerte ante la adversidad, por todo vuestro apoyo y cariño incondicional, por las horas al teléfono escuchando mis malos ratos, por todo el esfuerzo y sacrificio que habéis hecho para que pueda tener un futuro mejor, por todo eso y mucho más, gracias de todo corazón. Sois los mejores padres que podía haber deseado. Xabier, aunque desgraciadamente no puedes estar presente y disfrutar de este momento con nosotros, espero que te sientas orgulloso de mí. No puedo terminar sin agradecer a otro de los pilares importantes de mi vida. Gracias **María** por todo el apoyo y cariño que me has dado durante estos años, por la paciencia que has tenido soportando mis momentos de estrés, ansiedad y frustración, por entender mejor que nadie como me sentía. Gracias por compartir conmigo momentos inolvidables, por reconducirme cuando más perdido estaba y enseñarme a disfrutar más de la vida. En definitiva, gracias por estar ahí siempre que lo he necesitado. Estoy seguro de que ésta es solo una de las muchas etapas que nos quedan por recorrer juntos.

Solamente me queda decir muchas gracias a todos!

Abbreviations

4-PBA	4-Phenylbutyric acid
20S core particle	20S proteasome
α-SMA	Alpha-smooth muscle actin
γGT	Gamma-glutamyl transpeptidase
AC6	Adenylate cyclase 6
AC8	Adenylate cyclase 8
ADPKD	Autosomal dominant polycystic kidney disease
ADPLD	Autosomal dominant polycystic liver disease
AE2	Anion exchange protein 2
AEBSF	4-(2-aminoethyl) benzenesulfonyl fluoride
AKT	AKT serine/threonine kinase 1
ALP	Alkaline phosphatase
ALT	Alanine aminotransferase
AMC	7-amino-4-methylcoumarin
ANG-1	Angiopoietin-1
ANG-2	Angiopoietin-2
ANOVA	Analysis of variance
AQP1	Aquaporin 1
ARPKD	Autosomal recessive polycystic kidney disease
ASBT	Apical sodium-dependent bile acid transporter
AST	Aspartate aminotransferase
ATF4	Activating transcription factor 4
ATF6	Activating transcription factor 6
ATP	Adenosine triphosphate
AAVs	Adeno-associated virus
BAs	Bile acids
BSA	Bovine serum albumin
Ca^{2+}	Calcium
$[Ca^{2+}]_i$	Intracellular calcium concentration
$CaCl_2$	Calcium chloride
CAML	Calcium-modulating cyclophilin ligand
cAMP	3',5'-cyclic adenosine monophosphate
cDNA	Complementary deoxyribonucleic acid
CDC25A	Cell division cycle 25 homolog A
CFSE	Carboxyfluorescein succinimidyl ester
CFTR	Cystic fibrosis transmembrane conductance regulator
CHF	Congenital hepatic fibrosis
CHOP	C/EBP-homologous protein
CK-19	Cytokeratin-19
Cl^-/HCO_3^-	Chloride/bicarbonate
CNX	Calnexin

CO_2	Carbon dioxide
COL1A1	Collagen type 1 alpha 1 chain
CRT	Calreticulin
CTGF	Connective tissue growth factor
CXCL1 (Il-8 homolog)	C-X-C motif ligand 1 (interleukin 8-homolog)
DDAs	Disulfide bond disrupting agents
dH_2O	Distilled water
DMEM/F-12	Dulbecco's modified Eagle´s medium/ Ham´s F-12 nutrient mixture
DMSO	Dimethyl sulfoxide
DNA	Deoxyribonucleic acid
dNTP	Deoxyribonucleotide triphosphate
DPBS	Dulbecco's phosphate-buffered saline
DPM	Ductal plate malformation
DPX	Dibutylphthalate polystyrene xylene
DTT	Dithiothreitol
ECM	Extracellular matrix
EDEM	ER degradation-enhancing alpha-mannosidase-like protein
EDTA	Ethylenediaminetetraacetic acid
EGF	Epidermal growth factor
EGFR	EGF receptor
eIF2α	Eukaryotic translation initiation factor 2 alpha
ENA-78	Epithelial-derived neutrophil-activating peptide 78
ER	Endoplasmic reticulum
ERAD	ER-associated degradation
ERDJ4	ER DNAJ domain-containing protein 4
ERK½	Extracellular signal-regulated kinases ½
ERSEs	ER stress response elements
EPAC	Exchange factor directly activated by cAMP
FBS	Fetal bovine serum
FDA	Food and Drug Administration
FGF	Fibroblast growth factor
FITC	Fluorescein isothiocyanate
FPC	Fibrocystin/polyductin
GIIα	Glucosidade II alpha
GIIβ	Glucosidase II beta
GADD34	Growth arrest and DNA damage-inducible protein 34
GAPDH	Glyceraldehyde-3-phosphate dehydrogenase
gDNA	Genomic DNA

GRP78	78-kDa glucose-regulated protein
HDAC	Histone deacetylase
HDAC6	Histone deacetylase 6
HEDJ	Human ER-associated DNAJ
HEPES	4-(2-hydroxyethyl)-1-piperazineethanesulfonic acid
HIF1α	Hypoxia-inducible factor 1 alpha
HNA_2PO_4	Sodium hydrogen phosphate
HRP	Horseradish peroxidase
IBDU	Intrahepatic bile duct units
i.e.	Latin: id est (it is)
IGF-1	Insulin-like growth factor-1
IL-6	Interleukin-6
IL-8	Interleukin-8
IP_3R	Inositol 1, 4, 5-trisphosphate receptor
IRE1α	Inositol-requiring enzyme 1 alpha
IVC	Inferior vena cava
JNK	c-Jun N-terminal kinase
KCl	Potassium chloride
LCV	Liver cystic volume
LDL	Low density lipoprotein
LOH	Loss of heterozygosity
LRP5	LDL receptor related protein 5
MAPK	Mitogen-activated protein kinase
MCP-1	Monocyte chemoattractant protein-1
MEK	Mitogen-activated protein kinase kinase
MEM	Minimum essential medium
miRs	MicroRNAs
M-MLVRT	Moloney-murine leukemia virus reverse transcriptase
MMPs	Matrix metalloproteinases
mRNA	Messenger ribonucleic acid
mTOR	Mammalian target of rapamycin
Na^+	Sodium
NaCl	Sodium chloride
NAFLD	Non-alcoholic fatty liver disease
NHC	Normal human cholangiocytes
NP40	Nonidet P-40
NRC	Normal rat cholangiocytes

P/S	Penicillin/streptomycin
PBC	Primary biliary cholangitis
PC1	Polycystin-1
PC2	Polycystin-2
PCK	Cystic rat cholangiocytes
PCR	Polymerase chain reaction
PDI-P5	Protein disulfide isomerase P5
PDS	Primitive ductal structure
PERK	Pancreatic endoplasmic reticulum kinase
PI3K	Phosphatidylinositol 3-kinase
PKA	cAMP-dependent protein kinase A
PKD	Polycystic kidney disease
PLD	Polycystic liver disease
PPARα	Peroxisome proliferator-activated receptor alpha
PSC	Primary sclerosing cholangitis
qPCR	Quantitative PCR
RER	Rough endoplasmic reticulum
RNA	Ribonucleic acid
RPM	Revolutions per minute
RT-PCR	Reverse transcription PCR
RyR	Ryanodine receptor
SAs	Somatostatin analogues
SDS	Sodium dodecyl sulfate
SDS-PAGE	SDS polyacrylamide gel electrophoresis
SEC63	Translocation protein SEC63 homolog
SEM	Standard error of the mean
SER	Smooth endoplasmic reticulum
SERCA	Sarco/endoplasmic-reticulum Ca^{2+}-ATPase
SOX9	SRY-related HMG box transcription factor 9
SP1	Specificity protein-1
SP2	Specificity protein-2
SR	Secretin receptor
SRP	Signal recognition particle
T2DM	Type 2 diabetes mellitus
T3	3, 3', 5-triiodo-L-thyronine
TEM	Transmission electron microscopy
TGFβ	Transforming growth factor beta
TGR5	G-protein-coupled bile acid receptor 1
TIMPs	Tissue inhibitor of metalloproteinases
TKV	Total kidney volume

TLV	Total liver volume
TM	Tunicamycin
TMEM16A	Transmembrane member 16A
TRPV4	Transient receptor potential vanilloid 4
T-TBS	Tris-buffered saline with 0.1% Tween 20
TUDCA	Tauroursodeoxycholic acid
UDCA	Ursodeoxycholic acid
UGGT	UDP-glucose:glycoprotein glycosyltransferase
UPR	Unfolded protein response
UPREs	UPR elements
UPS	Ubiquitin proteasome system
VEGF	Vascular endothelial growth factor
VEGFR-1	VEGF receptor-1
VEGFR-2	VEGF receptor-2
WNT	Wingless
XBP1	X-box binding protein 1

Table of content

Table of figures and tables

Figures

Tables

Introduction

I.1. The liver and the biliary tract

I.1.1. Physiological functions of the liver

The liver is the largest solid organ of the human body (2-3% of average body weight) and a pivotal hub for maintaining normal physiological homeostasis, which is required to preserve the function of most other organs and thus, to sustain the human life.[1] This organ performs crucial metabolic functions including carbohydrate, lipid and amino acid metabolism.[2] In addition, the liver also serves as a reservoir of glucose, lipids, iron and vitamins.[2] The broad spectrum of functions accomplished by the liver also includes the synthesis and secretion of albumin, transferrin, fibrinogen, apolipoproteins, and other plasma proteins into the blood.[2] A major function of the liver also includes bile production and secretion, participating in nutrient absorption mechanisms and biliary clearance of several organic and inorganic solutes.[3] Furthermore, the liver has a dual blood supply (i.e., the hepatic portal vein and the hepatic artery), which makes this organ an accessible target for several toxic compounds.[4] In this regard, the liver has the ability to eliminate pathogenic and xenobiotic agents, and to regulate the immune response.[4] Of note, hepatic functions are maintained even after massive liver damage, due to the unique capacity of this organ for regeneration.[5]

I.1.2. Macroscopic and microscopic anatomy

The liver is grossly divided into two large lobes (i.e., right and left) and two small central ones (i.e., quadrate and caudate), which are mostly covered by the visceral peritoneum with the exception of the region that is in direct contact with the diaphragm.[2, 6] In the inferior surface of this organ, the porta hepatis consist of a deep fissure whereby the hepatic artery, the portal vein and the sympathetic and parasympathetic innervation fibers, enter into the liver. Moreover, this area serves as the natural exit route of the hepatic vein, the lymphatic vessels and the common hepatic duct.[2, 6] In addition, various ligamentous attachments between the liver and the surrounding structures and organs, hold it in place and restrict its movements.[6] The liver parenchyma is arranged in thousands of hexagonal units named hepatic lobules (**Figure I.1**).[2] Each hepatic lobule represents the functional and structural entity of the liver,

containing a central vein from which cords of hepatocytes radiate towards the peripheral portal triads, where branches of the hepatic artery, the portal vein and the bile duct are closely grouped (**Figure I.1**).[6] In addition, terminal branches of the portal vein and the hepatic artery directly connect with the hepatic sinusoids, which drain oxygen, nutrients, bile acids and hormones, delivered by the venous and arterial blood through the acinus to the lobule´s central vein (**Figure I.1**).[2] Likewise, bile duct branches are involved in the collection and transport of hepatocyte-secreted bile.[2] The sinusoidal network is separated from the cords of hepatocytes by a narrow perisinusoidal space (also called the space of Disse), constituting a scaffold of reticular fibers for hepatocytes and containing nutrient-rich blood plasma, which is in direct contact with hepatocytes improving the absorption.[2]

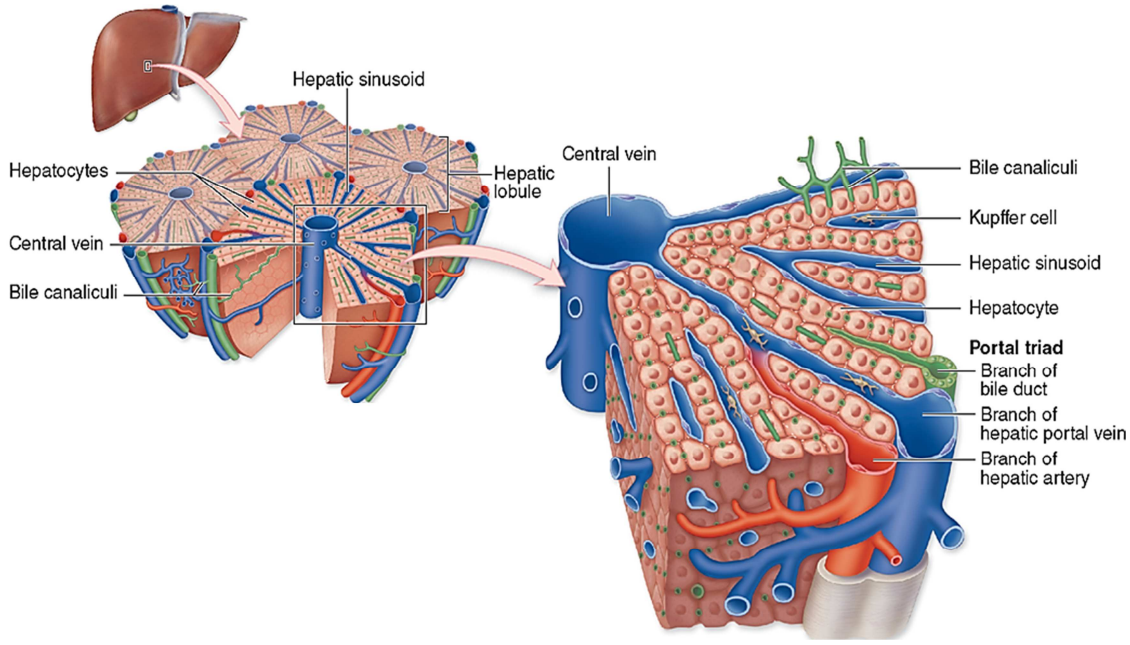

Figure I.1. Microscopic anatomy of the liver. The liver is structured in hexagonal hepatic lobules surrounded by connective tissue and composed of plates of hepatocytes radiating outward from the central vein to the portal triads. (Adapted from Mescher AL *et al*, 2013)[7]

The liver is constituted by several cell types (i.e., parenchymal and non-parenchymal) that cooperatively govern the hepatic function at multiple levels.[1, 2] Hepatocytes and cholangiocytes are the main epithelial cell populations of this organ. Roughly, 70-80% of the liver mass is occupied by hepatocytes, which execute the vast majority of liver functions, whereas cholangiocytes, the cells

lining the bile ducts, only represent the 3-5% of the total liver cells, albeit they perform pivotal functions in the modification and transport of the bile.[1, 2] Unlike, non-parenchymal cells of the liver include Kupffer cells, hepatic stellate cells and sinusoidal endothelial cells that play key roles in immunological, fibrogenic and substance exchange processes, respectively.[1, 2]

As previously mentioned, the hepatocytes initiate the formation and secretion of the primary bile into the canaliculi (i.e., a narrow tubular space between the apical membranes of two adjacent hepatocytes) to subsequently enter the lumen of the canals of Hering, leading to the ductule-canalicular junction.[8] These specialized channels are localized in the proximity of the portal space, and serve as the anatomical and physiological transition from the hepatocyte-lined canaliculi to cholangiocyte-lined ductules (<15µm), which ultimately form the biliary tree (**Figure I.2**).[8, 9] These small structures serially converge at the portal space to form the interlobular ducts (15-100µm), which progressively enlarge to form septal ducts (100-300µm), area ducts (300-400µm) and segmental ducts (400-800µm) (**Figure I.2**).[8, 9] The bile collected from the right and left lobes is subsequently drained to the corresponding hepatic ducts (>800µm), which are the boundary of the intrahepatic biliary tree (**Figure I.2**).[8, 9] Finally, the bile goes through the extrahepatic biliary tree (i.e., common hepatic duct, cystic duct, gallbladder, and common bile duct) ultimately reaching the duodenum (**Figure I.2**), where lipids are digested and absorbed.[8, 9]

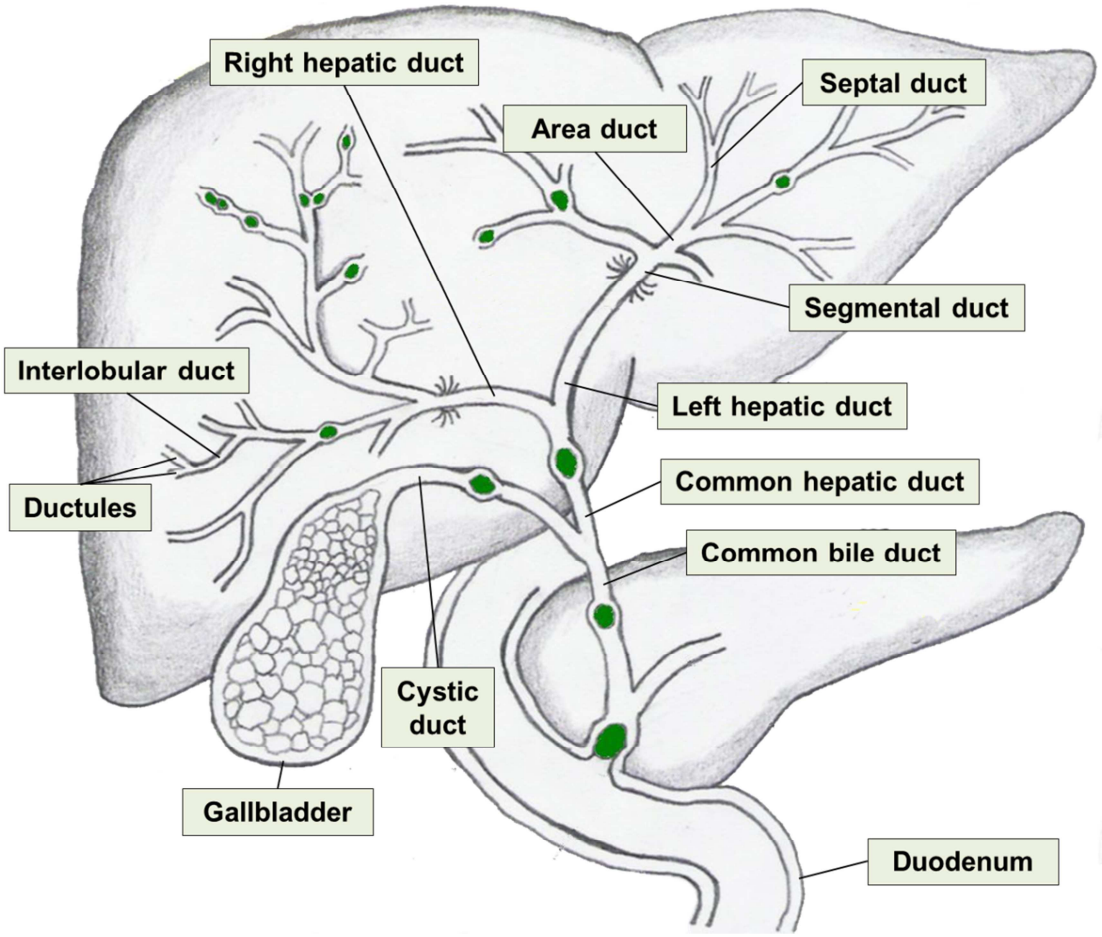

Figure I.2. Biliary tree architecture. The biliary tree consists of a network of intrahepatic and extrahepatic tubular ducts along which the hepatocyte-secreted bile is modified and transported to the duodenum.

I.2. Cholangiopathies

I.2.1. The clinical burden of biliary diseases

The prevalence of chronic liver diseases continues to rise worldwide and currently is the cause of approximately 2 million deaths per year.[10-12] The etiology of these disorders is multifactorial and thus, both males and females of any age, even neonates, are susceptible to undergo chronic liver diseases.[10] Importantly, biliary diseases, also termed as cholangiopathies, are a large category of chronic liver diseases that primarily affect the biliary epithelial cells (i.e., cholangiocytes), ranging from benign conditions with potential curative options to devastating biliary tract cancers with dismal prognosis and poor survival.[10, 11] Even though many of the cholangiopathies are considered rare diseases, a substantial morbidity and mortality is attributed to them, being a

major indication for liver transplantation as curative therapy.[10, 13, 14] Nevertheless, even after successful liver transplantation, patients can be stricken with serious biliary complications such as, ischemic cholangiopathy or strictures and leaks, that can affect to a large percentage of transplant recipients (3-20%), representing an economic burden for the healthcare system.[14, 15] In this regard, the suboptimal methods of diagnosis, the absence of longitudinal registries of patients affected by these pathologies, and the lack of effective medical therapies, make cholangiopathies a relevant clinical and social problem. [10, 13-15]

I.2.2. Etiologic classification of cholangiopathies

Although cholangiopathies are associated with cholestasis, inflammatory and immune responses, and cholangiocyte proliferation, the clinical presentation and the natural course of each of these biliary disorders are unique, due to different etiologies.[13] Thus, cholangiopathies are classified in several categories according to the underlying pathological mechanism (**Figure I.3**).[13, 14, 16] In this regard, the biliary epithelium can be mistakenly attacked by the immune system as occurs in primary biliary cholangitis (PBC), primary sclerosing cholangitis (PSC) and biliary atresia, which are some of the **(1) immune-mediated** cholangiopathies (**Figure I.3**). [14, 16, 17] Importantly, PSC has been widely described as the most important risk factor for cholangiocarcinoma development, a **(2) malignant** cholangiopathy (**Figure I.3**), in which cholangiocytes undergo an oncogenic transformation associated with high-grade of biliary dysplasia.[13, 18] Moreover, exogenous insults can trigger **(3) infectious** cholangiopathies (**Figure I.3**), especially in individuals with acquired immunodeficiency syndrome, who are more susceptible to opportunistic infections with *Cryptosporidium parvum*,[16, 19] or **(4) drug-induced** cholangiopathies (e.g., Amoxicilin/clavulanic, carbamazepine, flucoxacillin…) (**Figure I.3**), which are caused by both the direct toxicity of the drug or by high concentrations of the bile-excreted reactive species.[16, 20] In addition, several circumstances related to iatrogenic factors and systemic diseases can halt the blood supply to the bile ducts, establishing an **(5) ischemic** cholangiopathy (**Figure I.3**).[16, 21] Finally, genetic alterations also have a direct impact on the biliary epithelial cells, being these disorders categorized as **(6) genetic**

cholangiopathies (**Figure I.3**).[16] Of note, this PhD dissertation is strictly focused on genetic biliary diseases and, specifically, on yielding novel insights about the molecular mechanisms involved in the pathogenesis of polycystic liver disease (PLD).

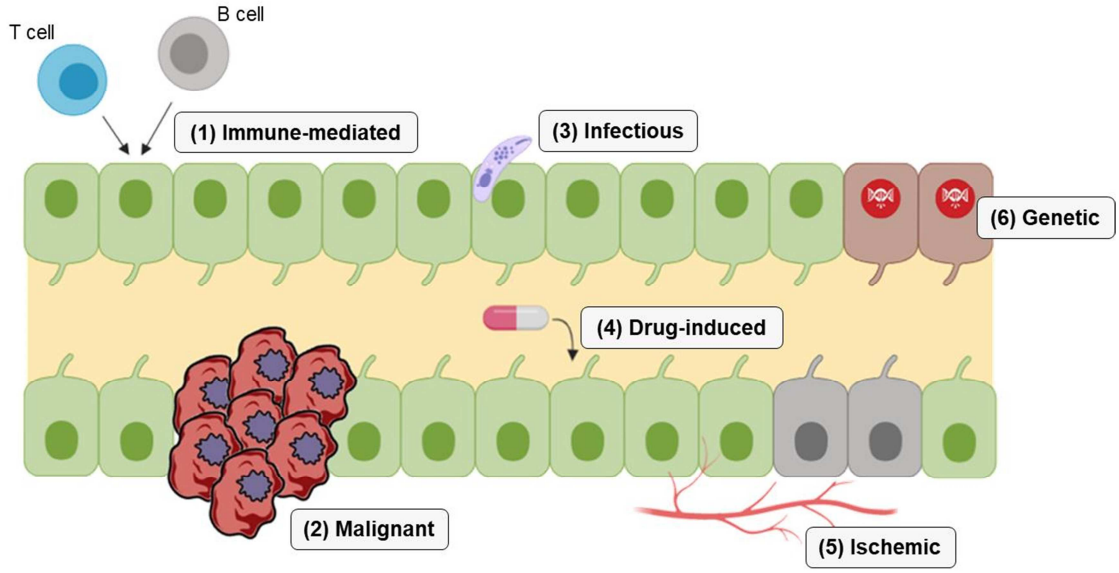

Figure I.3. Classification of cholangiopathies according to their etiology. Cholangiopathies are chronic liver diseases that affect cholangiocytes and are categorized as (1) Immune-mediated, (2) Malignant, (3) Infectious, (4) Drug-induced, (5) Ischemic and (6) Genetic.

I.2.3. Polycystic liver disease

I.2.3.1. Clinical description

PLD comprise a heterogeneous group of inherited genetic cholangiopathies characterized by bile duct dilatation and/or the presence of multiple fluid-filled biliary cysts (>10), which are considered as the leading causes of morbidity.[22-24] Of note, a large rate of patients concomitantly presents polycystic kidney disease (PKD).[22-24] Currently, a worldwide estimation suggests that more than 10 million of people could be affected by PKD, whereas the number of PLD cases diagnosed is much lower than the expected on the basis of PLD-related genetic mutation frequency in the population.[25, 26] However, the exact prevalence of these rare disorders is still largely unknown, due to the incidental clinical detection and the high degree of non-penetrance.[25, 26] In this regard, the vast majority of patients who undergo these diseases remain asymptomatic throughout the years with not requiring therapy, albeit in a minority of them (i.e.,

patients with moderate or severe phenotype), progressive hepatic cystogenesis leads to massive hepatomegaly that triggers intra-cystic complications such as hepatic cysts hemorrhage, infection or rupture, and several pressure-related symptoms including portal hypertension, obstructive jaundice, early satiety, splenic varices, Budd-Chiari syndrome, abdominal pain, dyspnea, gastro-oesophageal reflux and bloating.[23, 24] Despite the infrequency of complications and symptoms, they often seriously compromise the quality of life of patients and can even be life-threatening.[24] Moreover, age, female gender, number of pregnancies and estrogen consumption, have been identified as pivotal risk factors that govern the prevalence, progression (i.e., number and size of hepatic cysts) and severity of the disease.[24, 27, 28] Therefore, the main risk group in the population would be young women (<48) chronically prescribed with oral estrogen containing contraceptives and/or with prior multiple pregnancies, albeit males are also susceptible to be affected with PLD (**Figure I.4**).[24] To date, there are no clinical practice guidelines for the management of PLD and the available therapeutic strategies exert short-term and/or modest beneficial impact. Thus liver transplantation emerges as the only potential curative option for patients with PLD.[22-24]

Figure I.4. Representative images of patients with severe PLD phenotype. Typical clinical manifestations evidenced in symptomatic patients with PLD. Both images were relinquished by the Division of Gastroenterology and Hepatology of the Mayo Clinic (Rochester, Minnesota, U.S.A).

I.2.3.2. Etiology

I.2.3.2.1. Genetics

Germline mutations (i.e., first hit) related to the development of PLD phenotypes are heterozygous and therefore, only one allele of the gene is disturbed whereas the other remains functional (i.e., wild-type).[29] However, the loss of a single allele of any of the PLD-related genes is not sufficient to trigger the disease.[29, 30] Thus, in the context of PLD, it is widely established that the "second-hit" mechanism (also known as Knudson hypothesis) is the driving force of cystogenesis, due to the total loss of the functional gene.[30] This concept, originally described for mutations in a tumor suppressor gene of retinoblastoma cancer,[31] assumes that spontaneous somatic second-hit mutations in the wild-type allele leads to its partial or total inactivation, indicating that PLD is recessive at a cellular level.[29, 30, 32, 33] In this regard, when loss of

heterozygosity (LOH) is induced by the somatic second-hit mutation, cholangiocytes acquire features of liver progenitor cells, which would explain the cystogenesis and the hyperproliferative properties of cystic cholangiocytes.[29, 33] Notably, the rate of LOH varies genetically and phenotypically, due to the different susceptibility of the LOH genomic regions (i.e., 70-kilobase region surrounding the germline mutation), even between cysts of the same patient.[29] Therefore, cystogenesis emerges as an independent process, based on the concept that solely cholangiocytes with somatic second-hit mutations in the LOH genomic region have the ability to develop cysts.[29, 33] Although all cells of the body acquire the germline mutation during the embryological development, it is remarkable that the presence of cysts are evidenced isolated in the liver [i.e., Autosomal Dominant Polycystic Liver Disease (ADPLD)] or in concomitance with renal cysts [i.e., Autosomal Dominant Polycystic Kidney Disease (ADPKD) or Autosomal Recessive Polycystic Kidney Disease (ARPKD), Caroli´s disease or congenital hepatic fibrosis (CHF) in infants] in patients with PLD, indicating that these two organs are more sensitive to the absence of the protein products derived from these PLD-related genes.[29, 30, 33]

ADPLD is a rare disease whose exact prevalence remains still unknown, albeit it is estimated that 1/100,000 individuals undergo this disorder.[25, 26, 30] The ADPLD-related phenotype is caused by different loss-of-function mutations (i.e., splicing, frameshift, nonsense and missense) in a wide genetic spectrum.[32, 34-36] In this regard, *PRKCSH* (Chr. 19p13.2; 18 exons) was the first gene associated with ADPLD, due to its relative high rate of mutations (~20% of patients).[34, 35] *PRKCSH* encodes for the non-catalytic beta-subunit of the ER-enzyme glucosidase II (GIIβ or hepatocystin) (**Table I.1**), which assists the sequentially cleavage of the two innermost glucose residues of a nascent glycoprotein (**Figure I.5**). Thus, the second terminal residue of glucose is cleaved prior to the entry of the glycoprotein into the calnexin (CNX)/calreticulin (CRT) cycle (**Figure I.5**), where these lectins serve as molecular chaperones involved in the folding of the newly synthesized proteins.[30, 37] Once the last residue of glucose is trimmed, the nascent glycoprotein leaves the CNX/CRT cycle and, if it is properly folded, enters the secretory pathway for further post-translational modifications in the Golgi apparatus (**Figure I.5**). Nevertheless, if the

glycoprotein maintains the denatured conformation, the hydrophobic amino acids are exposed, being recognized by the UDP-glucose:glycoprotein glycosyltransferase (UGGT), which reglucosylates the polypeptide to enter again in the folding cycle (**Figure I.5**).[30, 37] Of note, when the native structure is not reached, the nascent protein is targeted for degradation (**Figure I.5**).[37] Glucosidase II is also constituted by a catalytic alpha-subunit (GIIα or PKD3) encoded by the *GANAB* gene (Chr. 11q12.3; 24-25 exons) (**Table I.1**), which have been identified mutated in 2% of the patients with ADPLD.[30, 32, 36] Importantly, both subunits (i.e., GIIα and GIIβ) should be completely functional, in order to allow the ER-enzyme carries out the aforementioned processes involved in the quality control and folding of newly synthesized glycoproteins (**Figure I.5**).[30] Likewise, mutations in other genes encoding for ER-resident proteins have been associated with ADPLD phenotype.[30, 32] Hence, several components of the SEC61-translocon are disrupted as a consequence of mutations in the corresponding encoding genes.[30, 32] One of them is *SEC63* (Chr. 6q21; 21 exons) (~15% of patients), whose protein product is the translocation protein SEC63 homolog (**Table I.1**), an allosteric effector of the SEC61-translocon for channel opening, which is required to allow the co- and post-translational transport of nascent proteins.[30, 32, 38] For this purpose, SEC63 protein acts as a co-chaperone, that interacts and activates the ER luminal Hsp70-type chaperone 78-kDa glucose-regulated protein (GRP78) to ensure the unidirectional transport of the nascent polypeptides through the channel into the ER lumen (**Figure I.5**).[30, 38] More recently, one of the subunits that constitutes the central element of the SEC61-translocon has also been detected mutated in ~1% of patients with ADPLD.[30] This is the beta-subunit of SEC61 encoded by *SEC61B* gene (Chr. 9q22.33; 4 exons) (**Table I.1**) and just, like SEC63 homolog protein, participates in the translocation and integration of proteins in the ER membrane (**Figure I.5**).[30, 32] Notably, the truncated protein product of this gene does not compromise the functionality of the channel, due to the highly conserved alpha- and gamma-subunits, which maintain the structure of the pore.[30, 39, 40] In addition, another novel gene associated with ADPLD phenotype is *ALG8* (Cr. 11q14.1; 13 exons) (~3% of patients), encoding for alpha-1,3-glucosyltransferase (**Table I.1**).[30, 32] This ER integral membrane protein exerts its function between the sites of action of glucosidase II (i.e.,

PRKCSH and *GANAB* genes) and SEC61 translocon (i.e., *SEC63* and *SEC61B* genes), contributing to the attachment of the second residue of glucose to the lipid-linked oligosaccharide, before it is transferred to an asparagine-residue of the nascent polypeptide (**Figure I.5**).[30, 32] Unlike all these ADPLD-related genes, *LRP5* gene (Chr. 11q13.2; 23 exons) encodes for the low density lipoprotein (LDL) receptor related protein 5 (LRP5), which is a transmembrane protein instead of an ER-resident protein (**Table I.1**). Importantly, LRP5 functions as a co-receptor coupled with Frizzled protein family members for transducing signals of the β-catenin-dependent ('canonical') wingless (Wnt) pathway, which is pivotal for many physiological processes.[30, 41, 42] Particularly, only 50% of the ADPLD cases could be attributed to mutations in these genes, suggesting that more underlying mutations remain to be identified.[30]

Furthermore, the hepato-renal phenotypes of the disease (i.e., ADPKD and ARPKD) have also been associated with some aberrant ER-resident proteins, albeit the majority of the protein products of the ADPKD- and ARPKD-causing genes are located in the primary cilium.[23] This sensory tubular organelle extends from the apical membrane of cholangiocytes to the bile duct lumen, containing the mechano- and chemoreceptor polycystin-1 (PC1), as well as the non-selective calcium channel polycystin-2 (PC2).[23, 30] Mutations in *PKD1* (Chr. 16p13.3; 46 exons) (~78% of patients) and *PKD2* (Chr. 4q22.1; 15 exons) (~15% of patients) genes, that encode for these integral membrane proteins, respectively (**Table I.1**), cause ADPKD (~1/10,000 individuals) in which ~85% of the patients present signs of liver disease.[23, 30] Interestingly, PC1 and PC2 form a ciliary complex responsible for governing the intracellular calcium concentration ($[Ca^{2+}]_i$) and therefore, abnormalities in the function of these proteins lead to decreased $[Ca^{2+}]_i$ and, subsequently, increased 3',5'-cyclic adenosine monophosphate (cAMP) levels, promoting cystic cholangiocyte proliferation.[23, 30] Despite being a primary cilium protein, PC2 is also an ER membrane protein (**Table I.1**), where acts both as a calcium release channel (**Figure I.5**) and as a modulator of other ER calcium channels such as the inositol 1,4,5-trisphosphate receptor (IP_3R) or the ryanodine receptor (RyR).[23, 30, 43] Although *PKD1* and *PKD2* are the main contributors to the development of ADPKD phenotype, a modest percentage of these patients harbor *GANAB* (~0.3%) and *LRP5* mutations (**Table I.1**), evidencing the presence of a genetic

cross-over between ADPLD and ADPKD, despite being different disorders.[30] Finally, the recessive form of PLD (i.e., ARPKD) is not a very common disease in the population, affecting around 1/20,000 individuals.[23, 30] Unlike ADPLD and ADPKD phenotypes, ARPKD has been associated with mutations solely in the *PKHD1* gene (Chr. 6p12.3-12.2; 67 exons), whose protein product, fibrocystin/polyductin (FPC), is an integral membrane protein located in the primary cilium (**Table I.1**).[30] Although the exact function of FPC remains elusive, its involvement in the modulation of ciliary PC2 activity has been broadly reported, governing $[Ca^{2+}]_i$ and consequently cholangiocyte proliferation, as well as other cellular processes related to tubular morphogenesis.[30, 44, 45]

Table I.1. Schematic summary of genes involved in polycystic liver disease

Mutated gene	Protein	Localization	Function	Phenotype	Chromosome
PRKCSH	Glucosidase II β-subunit or hepatocystin	ER	N-glycan metabolism	ADPLD	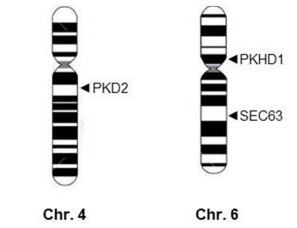
GANAB	Glucosidase II α-subunit or PKD3	ER	N-glycan metabolism	ADPLD or ADPKD	
SEC63	Translocation protein SEC63 homolog	ER	Protein translocation	ADPLD	
SEC61B	Protein transport protein SEC61 β-subunit	ER	Protein translocation	ADPLD	
ALG8	α-1,3-glucosyltransferase	ER	Protein glycosilation	ADPLD	
LRP5	Low density lipoprotein receptor-related protein 5	Plasma membrane	Receptor in canonical Wnt signaling	ADPLD or ADPKD	
PKD1	Polycystin-1	Primary cilium, plasma membrane and cell junctions	Mechano/chemoreceptor linked to calcium signaling and tubulogenesis	ADPKD	
PKD2	Polycystin-2	Primary cilium and ER	Non-selective calcium channel	ADPKD	
PKHD1	Fibrocystin or polyductin	Primary cilium	Receptor coupled to PC1/PC2 complex and involved in tubulogenesis	ARPKD	

Abbrev: ADPKD, autosomal dominant polycystic kidney disease; ADPLD, autosomal dominant polycystic liver disease; ARPKD, autosomal recessive polycystic kidney disease; CHR, chromosome; ER, endoplasmic reticulum; PC1, polycystin-1; PC2, polycystin-2; PKD3, polycystic kidney disease 3; WNT, wingless (Adapted from Lee-Law PY *et al*, 2019).[30]

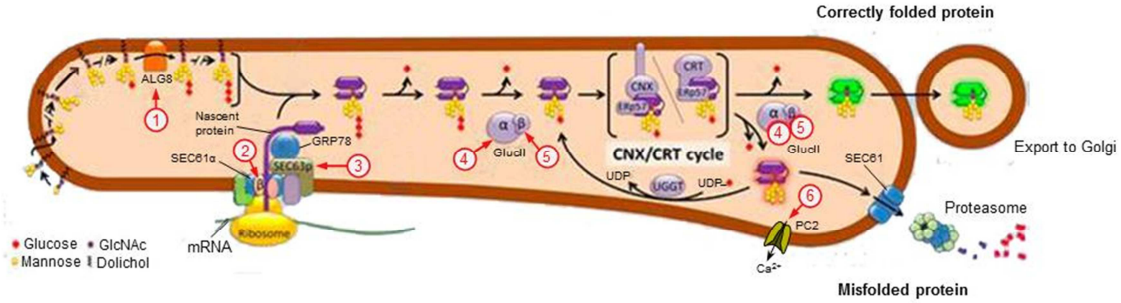

Figure I.5. Role of the ER-resident proteins encoded by the PLD-causing genes in the biogenesis pathway. The addition of the second glucose residue to the lipid-linked oligosaccharide precursor is catalyzed by (1) ALG8, prior to its assembly with the nascent protein translocated through the (2) SEC61/(3) SEC63 subcomplex. Afterwards, the ER enzyme glucosidase II, composed by (4) GIIα and (5) GIIβ, trim the second residue of glucose, allowing the CNX/CRT-mediated protein folding. The functionality of these two molecular chaperones is determine by the ER lumen Ca^{2+} concentration, which is partially regulated through the Ca^{2+} channel (6) PC2. (Adapted from Besse W *et al*, 2017)[32]

I.2.3.2.2. Embriology and ductal plate malformation

In physiological conditions, the embryologic development of the biliary tree commence with the extrahepatic bile ducts, originating from the endodermal hepatic diverticulum on the 18th day of gestation.[46] Once the hepatic diverticulum has a well-defined structure (i.e., 4th week of gestation) (**Figure I.6**), it is divided into a hollow caudal bud (pars cystic) and a solid cranial one (pars hepatica).[46] Later on, the caudal bud grows in length up to 8th week of gestation, becoming the gallbladder, cystic duct, common bile duct and duodenum (**Figure I.6**).[46] The latter, undergoes a rotation to the right side around the 5th week of gestation, causing the common bile duct to be displaced to its definitive position (**Figure I.6**).[46] By contrast, the cranial part of the hepatic diverticulum progresses to the common hepatic duct (**Figure I.6**) and the distal portions of the right and left hepatic ducts, which already exhibit a clearly defined tubular structure in the 12th week of gestation.[46] In parallel, the intrahepatic bile duct system appears in first instance at 7th week of gestation, maintaining luminal continuity with the extrahepatic biliary tree.[46] Despite existing multiple theories about the development of the intrahepatic bile ducts, the most supported one by several research studies postulates the hepatoblastic origin of this bile duct system.[46] In this regard, the monolayer of hepatoblasts (i.e., liver precursor cells) that surround the periportal mesenchyme (**Figure I.7**) acquires strong immunoreactivity to biliary lineage markers, including cytokeratin-19 (CK-19), SRY-related HMG box transcription

factor 9 (SOX9), osteopontin and E-cadherin.[46-48] This cylindrical sleeve of cells, termed ductal plate, is gradually duplicated from the 12th week of gestation onwards, giving rise to a bilayer, where cholangiocytes (portal side) and hepatoblasts (parenchymal side) are separated from each other by a lumen.[46, 48] Importantly, this asymmetrical structure constitutes the primitive ductal structure (PDS) (**Figure I.7**), which demarcates the onset of bile duct morphogenesis.[48] Simultaneously, the PDS undergoes a remodeling process, consisting on the differentiation and maturation of few parts of this structure, whereas other parts are disposed of through apoptotic mechanisms.[46, 48] Importantly, both hepatoblast differentiation to cholangiocytes and PDS remodeling are promoted by Notch, transforming growth factor β (TGFβ) and Wnt signaling pathways,[48-50] as well as, fibroblast growth factor (FGF),[48, 50] transcription factors (i.e., HNF1β and HNF6)[48-50] and microRNAs (i.e., miRNA-30 family).[48, 50, 51]

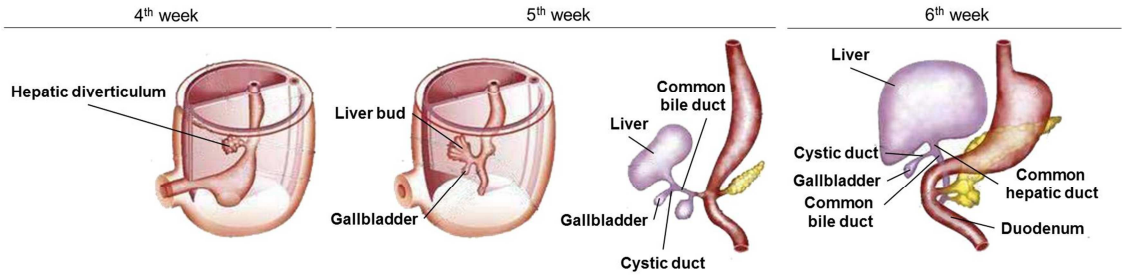

Figure I.6. Different stages in the embryologic development of the biliary tree. The hepatic diverticulum is the anlage of the liver and the biliary system, which matures and differentiates towards completely defined functional structures. (Adapted from Moore KL *et al*, 2015)[52]

The absence of any of the aforementioned regulatory factors and/or the presence of somatic second-hit mutations in the PLD-related genes, lead to a failure in the remodeling process of the PDS during fetal and neonatal development.[48, 49] As a consequence of the ductal plate malformation (DPM), embryonic biliary duct-like structures of variable size are scattered through the liver parenchyma (**Figure I.7**), being considered the trigger factor of hepatic cystogenesis.[23, 48, 49, 53] Of note, several morphogenic defects have been identified as causative of DPM, including **(I)** abnormal differentiation of hepatoblasts, **(II)** impaired maturation of radially asymmetric PDS, and **(III)** anomalous bile duct enlargement (**Figure I.7**).[48, 49, 53] Even though DPM can

occur in different stages of embryogenesis, in all of the aforementioned cases exist a perturbation of cell polarity and formation of cysts (**Figure I.7**).[53] Unfortunately, the exact type of defect that causes DPM in ADPLD and ADPKD remains still obscure, whereas in ARPKD there is an underlying aberrant duct expansion.[23, 50]

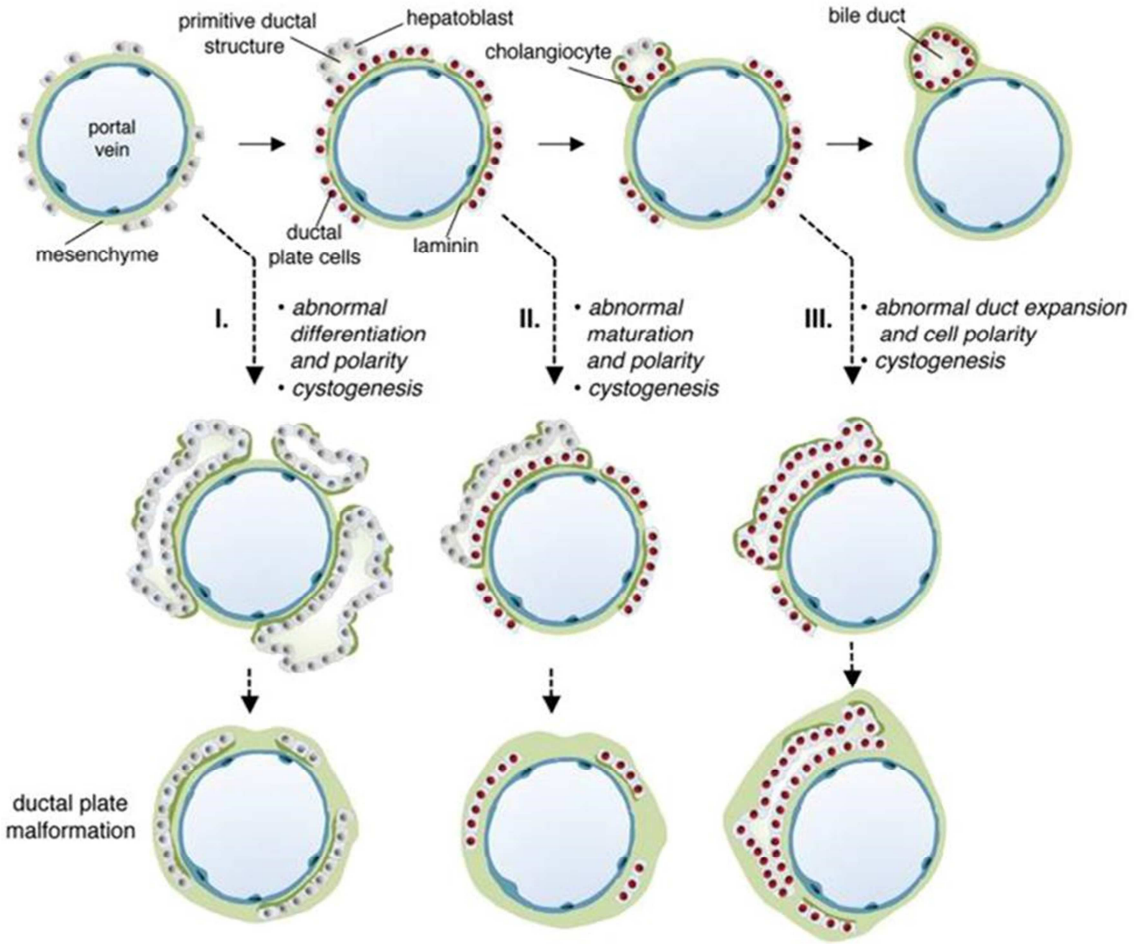

Figure I.7. Classification of DPM based on the 3 different pathogenic mechanisms. A monolayer of liver progenitor cells (i.e., hepatoblasts) encircles the portal vein and differentiates into cholangiocytes constituting the ductal plate. Then, this structure is duplicated to form the PDS (bilayer). Defects in the formation of the ductal plate and/or maturation of the PDS give rise to cystic structures. (Obtained from Raynaud P *et al*, 2014)[53]

I.2.3.3. Clinical management of PLD

The therapeutic strategies available hitherto are intended for patients with severe symptomatic PLD and massive hepatomegaly.[24] The treatment of patients who endure this disease seeks to improve their quality of live and provide long-term relief of symptoms, without compromising liver function.[24]

Accordingly, surgical and pharmacological methods focused on lessening the size and volume of the liver or delaying the progression of the disease, respectively, are employed.[24, 54]

I.2.3.3.1. Surgical approaches

Before conducting the removal of hepatic cysts, it is crucial to carefully evaluate the patient´s condition, because the invasiveness of the procedure implies certain risks and limitations. Indeed, the efficacy of each surgical technique is determined by the distribution, number and size of the cysts.[24, 54] Thus, **aspiration-sclerotherapy** is eligible when symptoms are mainly caused by a dominant cyst (≥ 5cm of diameter).[24, 54, 55] In this regard, after the radiological-guided aspiration of the entire volume of cystic fluid, a sclerosing agent (i.e., ethanol, minocycline or tetracycline) is temporarily administered into the lumen of the dominant cyst (**Figure I.8**), in order to destroy the inner epithelial wall by diminishing the pH inside the cyst. [24, 54-56] In case that multiple large cysts are localized in the anterior segment of the liver, the common therapeutic choice is usually **laparoscopic fenestration**, due to the simple accessibility of the cysts.[24, 54, 57, 58] This technique consists on aspiration of the cystic fluid followed by surgical deroofing of the liver cysts (**Figure I.8**), achieving an instant relief of the symptoms since numerous cysts can be eliminated in a single surgery.[24, 54] Nevertheless, if the cysts are scattered through several segments of the liver, these surgical procedures are not recommended.[24, 54] Accordingly, **segmental hepatic resection** may be considered as a therapeutic option, as long as other segments are less affected by the disease, which allows to preserve the functionality of the liver after surgery (**Figure I.8**).[24, 54, 59, 60] Notably, with hepatic resection up to 65% of the tissue can be resected, implying a substantial reduction in liver size and symptomatology, albeit only patients with severe disease and disabling symptoms are considered for this treatment.[24, 54, 60] Unfortunately, none of these surgical techniques exert long-term benefits, and also postoperative complications (i.e., ascites, bleeding, pleural effusion), recurrence of symptoms and a mortality rate of 2-2.7%, have been associated with these therapies.[24, 54]

Therefore, liver transplantation is the only curative option for patients with PLD, but solely a minority of them is eligible to undergo this intervention.[24, 54]

Since there is a high risk of morbidity and mortality, as well as a shortage of liver donors, this option is intended for patients whose quality of life is extremely limited, due to the severity of the disease.[24, 54] Importantly, a striking 5-years survival rate (>90%) has been reported in both liver and combined liver-kidney transplantations.[24, 61]

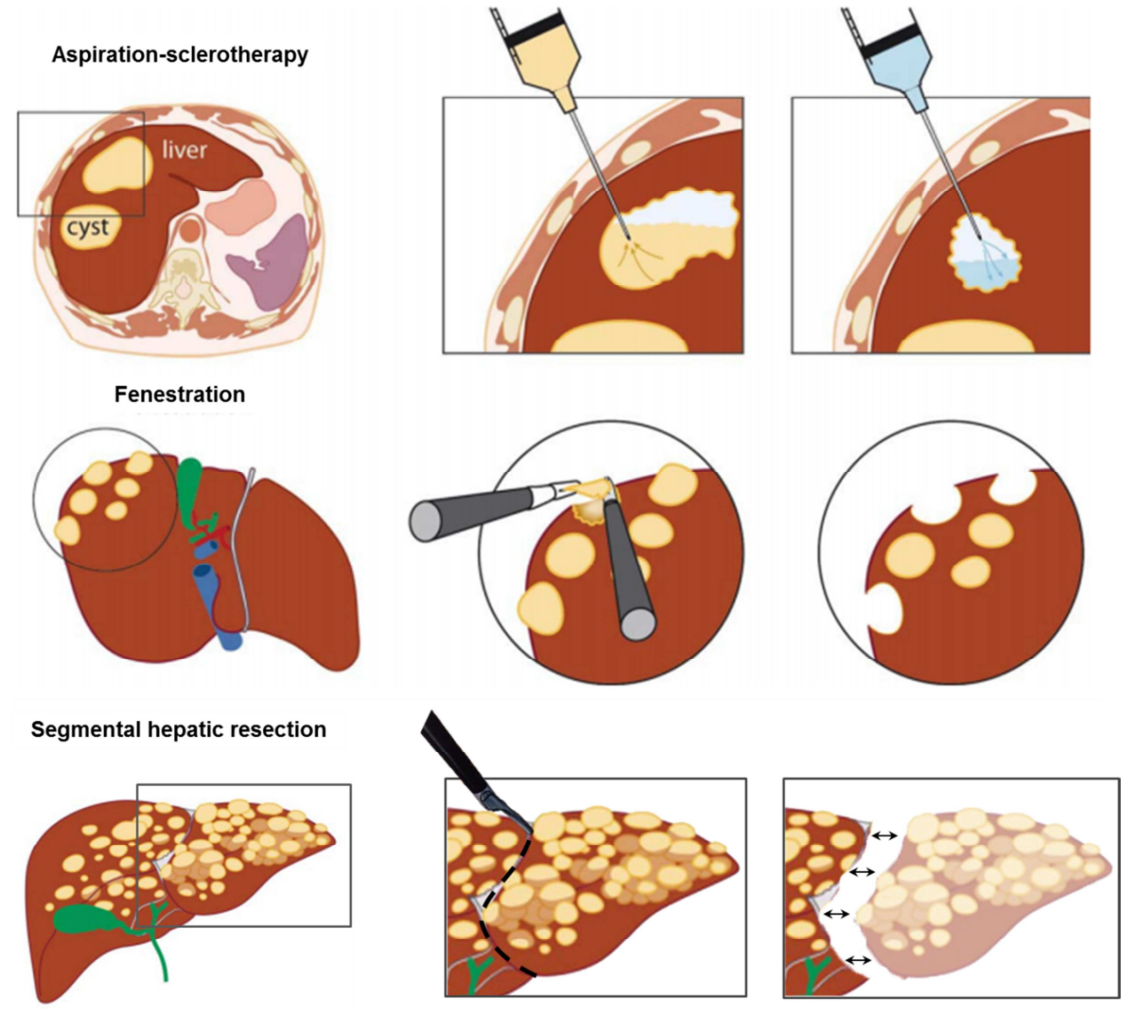

Figure I.8. Surgical therapeutic strategies. Depending on the location, number and size of the hepatic cysts, aspiration-sclerotherapy, fenestration or segmental hepatic resection can be accomplished in order to reduce the size and volume of the liver, alleviating the symptoms of the patients with PLD. (Adapted from Drenth JPH *et al*, 2010)[54]

I.2.3.3.2. Medical therapies

To date, diverse pharmacological strategies have shown promising results in preclinical studies [i.e., inhibitors of matrix metalloproteinases (MMPs),[62] cell division cycle 25 homolog A (Cdc25A),[63] histone deacetylase 6 (HDAC6),[64, 65] and vascular endothelial growth factor receptor 2 (VEGFR2),[66, 67] as well as, transient receptor potential vanilloid 4 (TRPV4) activators[68]], albeit their clinical

benefits have not been demonstrated yet or have not reached the desirable clinical expectations [i.e., mammalian target of rapamycin (mTOR) inhibitors],[69, 70] limiting the available medical treatments for patients with symptomatic PLD.[23] However, normalization of both intracellular cAMP and $[Ca^{2+}]_i$ levels has managed to mildly delay the progression of this disease in several clinical trials conducted with ADPKD and ADPLD patients.[23, 71-73] In this regard, inhibition of the excessive cAMP production in cystic cholangiocytes, by chronic administration of somatostatin analogues (SAs), diminishes both total liver volume (TLV) and total kidney volume (TKV), improving the quality of life of symptomatic patients with PLD.[23, 24] Nevertheless, the maximal therapeutic impact of SAs occurs during the first 6 months of treatment.[23, 24] Indeed, several clinical trials have assessed the extent of the therapy with SAs beyond 6 months (i.e., 12 months, 2 years and 4 years).[23, 24, 72, 74, 75] Although, none of these studies achieved better outcomes, in terms of volume decline, than the treatment for 6 months, the long-term maintenance therapy led to hepatic and renal volume stabilization, and prevented the rebound effect.[23, 24] In order to prolong the beneficial effects of SAs, it has been recently proposed to temporarily interrupt the therapy (i.e., drug holiday), allowing patients to acquire tolerance for these drugs again.[76] Importantly, a similar reduction of the TLV in the different treatment cycles was obtained with this strategy, but when stopping the treatment, a rebound effect correlated with the duration of the drug holiday, occurred.[76] Additionally, chronic administration of SAs cause transient side effects including gallbladder stones, abdominal discomfort, diarrhoea, nausea, vomiting, dizziness and headache.[23, 24] Therefore, this medical therapy is only reserved for patients with moderate to severe disease.[24]

Interestingly, ursodeoxycholic acid (UDCA; 3a,7b-dihydroxy-5b-cholanoic acid) emerges as a potential therapeutic alternative of SAs. Indeed, this endogenous hydrophilic bile acid been shown to have protective properties on both cholangiocytes and hepatocytes,[77, 78] being already approved by the Food and Drug Administration (FDA) for the treatment of chronic cholestatic disorders such as PBC.[79-81] Particularly in PLD, UDCA-mediated restoration of $[Ca^{2+}]_i$ inhibits baseline cystic cholangiocytes hyperproliferation and prevents hepatic cystogenesis progression in an animal model of ARPKD.[82] As a consequence of these beneficial effects of UDCA, an international multicenter phase II clinical

trial was performed, in order to evaluate its potential therapeutic value in PLD patients (i.e., ADPKD and ADPLD) with advanced disease (> 20 cysts and TLV > 2,500 mL).[71, 82] In this regard, oral administration of UDCA halted the increase in both TLV and TKV during 6 months of treatment in advanced symptomatic APDKD patients.[23, 71] Likewise, the increment of liver cystic volume (LCV) was hampered by this therapy.[23, 71] Nevertheless, UDCA had no effect on TLV and LCV in a patient cohort encompassing both severe ADPKD and ADPLD phenotypes.[23, 71] This suggests that solely patients with hepato-renal cystogenesis, and more precisely patients with ADPKD phenotype, could benefit from the medical therapy with UDCA.[23, 71] Unlike SAs, the side effects associated with UDCA administration was negligible (i.e., frequent stools and diarrhoea), as UDCA is an endogenous hydrophilic bile acid with hepatoprotective properties.[23] In this regard, the serological values of some biomarkers of liver injury such as gamma-glutamyl transpeptidase (γGT) and alkaline phosphatase (ALP), underwent a marked reduction after 6 months of treatment.[23, 71]

I.2.3.4. Molecular mechanisms of pathogenesis

I.2.3.4.1. Polycystin-1: a master regulator in the progression of the different PLD phenotypes

Over the years, several studies have described the importance of the functional dosage of PC1 in the clinical features of ADPLD, ADPKD and ARPKD phenotypes, demonstrating its pivotal contribution to hepatic and renal cystogenesis and, consequently, to disease severity.[32, 83, 84] In this regard, recent studies have demonstrated that a critical threshold of PC1 dosage serves as the rate-limiting determinant of cyst progression (**Figure I.9A**). Thereby, the farther below the threshold level PC1 activity falls, the larger the cystic growth rate (**Figure I.9A**).[32, 83] Noteworthy, bile ducts are more sensitive than renal tissue to PC1 deficiency.[32, 84] Thus, mutations in all the causing genes of ADPLD (i.e., *PRKCSH*, *SEC63*, *GANAB*, *ALG8* and *SEC61B*) have been associated with both impaired biogenesis and cilia trafficking of PC1, leading to a reduction in the steady-state protein expression levels (**Figure I.9B**).[32, 83, 84] Importantly, the proportion of this reduction is ultimately governed by the relevance in the biogenesis pathway of each abnormally encoded

protein.[32] Additionally, haploinsufficiency has been considered as an explanatory molecular mechanism of ADPKD severity, since the majority of somatic mutations in *PKD1* gene are likely to be missense.[84, 85] Hence, a partial decline in the functional dosage of PC1 occurs, due to the expression of a truncated full length protein, resulting in a more prominent cystic phenotype and further indicating that, PC1 is a *bona fide* mechanism of cyst formation also in this form of PLD.[84, 85] Curiously, disruption of the stoichiometry of the PC1/PC2 complex, caused by elevated levels of PC1, also induces cystogenesis in ADPKD.[84] More intriguing is the case of ARPKD phenotype, where no ER resident proteins are affected, discarding the premise of a defective biogenesis and transport. Indeed, it has been described that inactivation of *PKHD1* gene does not compromise these processes.[32] Nevertheless, some studies suggest a genetic interaction between *PKD1* and *PKHD1* loci that result in an insufficient functional PC1 amount to prevent the aggravation of the disease (**Figure I.9B**), either because *PKD1* is downstream of *PKHD1* or because their gene product act cooperatively in convergent pathways.[83, 84, 86] Unfortunately, the specific mechanism remains still obscure.

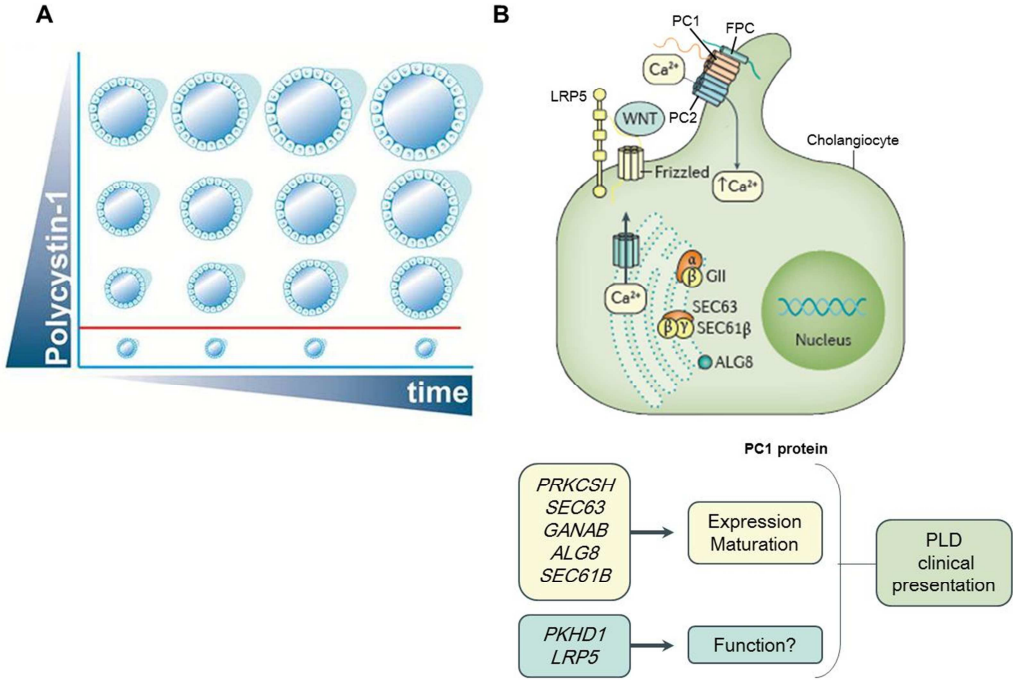

Figure I.9. Impact of PLD-causing genes in PC1 functional dosage. (**A**) Once PC1 is below a critical threshold (depicted by the red line), cystogenesis and, consequently, the severity of the phenotype is governed in a dose and time dependent manner. (**B**) The genes found mutated in PLD compromise the functional PC1 levels by modulating its biogenesis or function, which ultimately govern the clinical presentation of the disease. (Adapted from Perugorria MJ *et al*, 2017 and Fedeles SV *et al*, 2014)[22, 84]

I.2.3.4.2. Primary cilium dysfunction

Primary cilium structural and/or functional abnormalities disturb the detection and transduction of external stimuli towards the inside of cholangiocytes and, consequently, compromise several signaling pathways (i.e., Wnt, Hedgehog, and Notch) involved in differentiation, secretion, proliferation, apoptosis and homeostasis.[23, 87, 88] This non-motile organelle, extending from the apical membrane of cholangiocytes, is constituted by a microtubule-based axoneme (i.e., 9+0 microtubule pattern), which arises from the basal body of the mature centriole in quiescent cells.[23, 88] Notably, the primary cilium harbors several specific receptors and ion channels that attribute to this organelle the features of a mechano-, osmo- and chemosensory cellular structure.[23, 87] In this regard, the mechanosensory capacity of cholangiocyte primary cilium is governed by the PC1/PC2 complex (**Figure I.10A**) and the adenylate cyclase 6 (AC6).[23, 87, 89] Thus, aberrant function of PC1 and/or PC2 proteins, caused by mutations in the corresponding encoding genes (i.e., *PKD1* and *PKD2*, respectively), triggers the hyperproliferation of cholangiocytes and the alteration in fluid secretion/absorption, which is mediated by the dysregulation of both $[Ca^{2+}]_i$ and intracellular cAMP levels.[23, 87, 89] Likewise, $[Ca^{2+}]_i$ is also regulated by TRPV4, that provides the osmosensory activity to the primary cilium (**Figure I.10A**), sensing minimal changes in the bile osmolarity.[87, 89] It has been suggested that polycystins (i.e., PC1 and PC2) and FPC could indirectly modulate the function of this ciliary channel, due to their coassembly in a multiprotein complex.[90] Moreover, several proteins located in the primary cilium accomplish the chemosensory function through the recognition of appropriate ligands present in the extracellular milieu.[87, 89] One of them is the G-protein-coupled bile acid receptor 1 (TGR5) (**Figure I.10A**), whose overexpression in cystic cholangiocytes manages cAMP-mediated proliferation.[91] Finally, disruption of centrosome duplication during the cell cycle is also associated with impaired ciliogenesis (i.e., defects in size and cellular position of the cilium) and the hyperpoliferative phenotype of cystic cholangiocytes (**Figure I.10A**).[23]

I.2.3.4.3. Dysregulated Ca^{+2} and cAMP levels

The PLD-causing genetic mutations are the underpinning of both decreased $[Ca^{2+}]_i$ and increased intracellular cAMP levels, which confer to cystic

cholangiocytes their characteristic hyperproliferative phenotype.[23] Hence, aberrant PC1 and/or PC2 proteins utterly abolish the functionality of the ciliary polycystin complex, hampering the influx of extracellular Ca^{2+} inside cholangiocytes (**Figure I.10B**).[88, 92, 93] Similarly, loss of function of PC2 hinders the entry flow of calcium through the heteromeric PC2-TRPV4 channel.[92, 94] In addition to the primary cilium and as mentioned above, PC2 is also located in the ER membrane, where it functions as a Ca^{2+}-permeable cation channel (**Figure I.10B**), as well as a modulator of the activity of IP_3R (i.e., activation) and RyR (i.e., inhibition) Ca^{2+} channels by the C-terminal domain-mediated interaction.[92, 93] Moreover, IP_3R-dependent Ca^{2+} release is promoted by GIIβ, whereas PC1, when is localized in the ER as shorter cleavage forms, inhibits the activity of this channel.[92, 93, 95, 96] Therefore, abnormalities in the functionality of these proteins may either halt ER Ca^{2+} leak or exhaust the endoplasmic Ca^{2+} storages, compromising the intracellular Ca^{2+} homeostasis. Importantly, this depletion of $[Ca^{2+}]_i$, caused by both the absence of extracellular Ca^{2+} flows and the unavailability of ER Ca^{2+} reservoir, induces the AC6-mediated cAMP synthesis and inhibits phosphodiesterase 1-dependent cAMP hydrolysis (**Figure I.10B**).[23, 92, 97] Consequently, the overproduction of cAMP induces the sustained activation of exchange factor directly activated by cAMP (EPAC) and cAMP-dependent protein kinase A (PKA), two intracellular effectors that mediate cystic cholangiocyte proliferation via Ras/Raf/MEK/ERK½ signaling pathway (**Figure I.10B**).[23, 50, 98, 99]

I.2.3.4.4. Enhanced proliferation and angiogenesis

As mentioned in the previous section, the major driving force of cystic cholangiocyte proliferation is the failure in the management of intracellular cAMP levels, which ultimately induce the Ras/Raf/MEK/ERK½ signaling pathway in an EPAC- and PKA-dependent manner.[23, 50, 98] Nevertheless, this signaling cascade is also involved in angiogenic mechanisms via mTOR and hypoxia-inducible factor 1 alpha (HIF1α) activation, which mediate the production and secretion of the promitotic and angiogenic element vascular endothelial growth factor (VEGF) (**Figure I.10C**).[23, 66, 100] Secreted VEGF interacts with VEGF receptor 1 (VEGFR-1) and VEGF receptor 2 (VEGFR-2), both overexpressed in cystic cholangiocytes, establishing an

autocrine/paracrine loop (**Figure I.10C**), that promotes the enlargement and vascular supply of liver cysts.[23, 50, 66] Moreover, angiopoietin-1 (Ang-1) and angiopoietin-2 (Ang-2) belong to a second family of vascular growth factors, acting in concert with VEGF.[23, 101] In this regard, both angiopoietins compete for a paracrine or autocrine binding with their cognate receptor (i.e., Tie-2), which is overexpressed in cystic cholangiocytes (**Figure I.10C**).[96, 101, 102] Therefore, the net mitogenic and angiogenic effect on liver cysts is determined by the relative balance between Ang-1 and Ang-2.[101] Additionally, cystic fluid of patients with PLD is highly enriched in other factors, including growth factors [i.e., insulin-like growth factor 1 (IGF-1)], cytokines [i.e., interleukin-6 (IL-6) and interleukin-8 (IL-8), and chemoattractant chemokines [i.e., monocyte chemoattractant protein-1 (MCP-1) and epithelial-derive neutrophil-activating peptide (ENA-78)], becoming the cystic epithelium sensitive to them.[23, 50, 96] Interestingly, these factors exert their potent proliferative and angiogenic properties by modulating the expression levels of HIF1α, and consequently the secretion of VEGF, via Ras/Raf/MEK/ERK½ and PI3K/AKT/mTOR signaling pathways (**Figure I.10C**).[102]

I.2.3.4.5. Altered extracellular matrix remodeling

The extracellular matrix (ECM) is a dynamic fibrous network composed by a large variety of proteins and macromolecules (i.e., collagen, elastin, fibronectin, laminin, glycoproteins, proteoglycans and glycosaminoglycans), that provide not only a physical scaffold along which the biliary architecture is organized, but also actively regulates the biological functions of cholangiocytes by integrin-mediated interactions.[103, 104] During pathological condition, the ECM remodeling process may be dysregulated as a consequence of aberrant expression of the most relevant family of ECM-modifying enzymes (i.e., MMPs), their natural inhibitors [i.e., tissue inhibitor of metalloproteinases (TIMPs)] and/or hormones.[50, 62] In this regard, both IL-6 and IL-8, which are contained in the cystic fluid of patients with PLD, establish an autocrine/paracrine interaction with their corresponding plasma membrane receptors (i.e., IL-6R and CXCR1, respectively), triggering the overexpression and hypersecretion of different MMPs (i.e., MMP-1, MMP-3, MMP-10 and MMP-18) (**Figure I.10D**).[23, 50, 62, 96] Likewise, excessive digestion of ECM is also induced by the oestrogen 17β-

estradiol (**Figure I.10D**), which is present in the cystic fluid of female patients.[23, 50, 62, 96] Therefore, the hyperactivity of MMPs weakens the interaction between cystic cholangiocytes and ECM, leaving free space in the liver parenchyma that facilitate hepatic cyst enlargement and, consequently, disease progression.[50, 62, 96, 102]

I.2.3.4.6. Impaired secretion

In the postprandial state, the S-cells placed in the first portion of the small intestine (i.e., duodenum and jejunum) are stimulated to synthesize and secrete secretin into the hepatic portal vein.[9, 105] Moreover, cholangiocytes also express secretin, which is secreted into the hepatocyte-derived primary bile and reabsorbed by the intestinal cells, reaching the enterohepatic circulation.[106] Once in the biliary tract, this gastrointestinal hormone interacts with the G-protein coupled secretin receptor (SR), which is located in the basolateral membrane of cholangiocytes (**Figure I.10E**).[23, 105, 106] Of note, the activation of SR induces the adenylate cyclase 8 (AC8)-dependent cAMP production, contributing to the increased intracellular cAMP levels (**Figure I.10E**) previously reported, and triggering secretin-stimulated choleresis.[9, 105] As mentioned above cAMP activates PKA,[98] which in turn mediates the exocytosis of vesicles containing the chloride channel cystic fibrosis transmembrane conductance regulator (CFTR), the chloride/bicarbonate (Cl^-/HCO_3^-) exchanger anion exchange protein 2 (AE2), and the water channel aquaporin 1 (AQP1), into the apical membrane of cholangiocytes (**Figure I.10E**).[23, 50] Thus, PKA-dependent CFTR phosphorylation leads to the opening of this channel and the efflux of Cl^- into the bile duct lumen, which is subsequently exchanged with HCO_3^- via AE2 (**Figure I.10E**).[9, 23] In turn, secreted HCO_3^- establishes an osmotic gradient that is the driving force for the movement of water through AQP1 (**Figure I.10E**).[9, 23] Although these channels are mainly located in the apical membrane, they also are overexpressed in the basolateral membrane of cystic cholangiocytes (**Figure I.10E**).[107] Therefore, both permanent activation and misslocalization of CFTR, AE2 and AQP1 boost the fluid secretion and its luminal accumulation, promoting bile duct dilatation and cysts expansion in patients with PLD.[23, 50, 107] Furthermore, the unconjugated bile acids (BAs) secreted into the hepatocyte-derived bile are absorbed by cholangiocytes through the apical sodium-

dependent bile acid transporter (ASBT), and released across the basolateral membrane for returning to hepatocytes via the colehepatic shunt.[9, 108] Importantly, the local recycling of BAs causes an adenosine triphosphate (ATP)-dependent $[Ca^{2+}]_i$ increase, which in turn promotes the Cl^- efflux via the Ca^{2+}-activated Cl^- channel transmembrane member 16A (TMEM16A).[9, 108] Hence, highly BAs-concentrated cystic fluid of patients with PLD[23] may trigger the sustained secretion of Cl^- and subsequent flow of HCO_3^- and water, leading to fluid accumulation and cyst enlargement.[109]

I.2.3.4.7. Epigenetics

Alterations in the epigenetic landscape of PLD, attributed to DNA methylation and/or histone modification mechanisms, may govern the expression levels of several microRNAs (miRs)-regulated proteins, that are involved in hepatic cystogenesis.[110] Interestingly, global changes in the miR expression profile have been identified in cystic cholangiocytes, finding the majority of them downregulated (~89%), albeit a small percentage are upregulated (~11%).[23, 50, 111] In particular, both miR-15a and miR-30a are strongly underexpressed, harboring cystic cholangiocytes excessive amounts of their corresponding target proteins [i.e., Cdc25a and epidermal growth factor receptor (EGFR), respectively] (**Figure I.10F**).[23, 50, 112] In this regard, overexpression of Cdc25a and EGFR confers proliferative features to cystic cholangiocytes, contributing to cystic growth (**Figure I.10F**).[23, 50, 51, 112] Contrary, miR-17 is upregulated in ADPKD experimental models, promoting cholangiocytes proliferation and aggravating hepatic cystogenesis through direct repression of *PKD1*, *PKD2* and peroxisome proliferator-activated receptor alpha (*PPARα*).[113, 114] In addition to miRs, aberrant expression of HDAC6 has been associated with the pathogenesis of PLD.[23, 50] This cytoplasmic member of the histone deacetylase (HDAC) family is overexpressed in cystic cholangiocytes, compromising the stability and functionality of the primary cilium via alpha-tubulin deacetylation (**Figure I.10F**).[23, 115] In turn, overexpression of HDAC6 halts the microtubule-dependent transport and degradation of EGFR in cystic cholangiocytes, leading to a prolonged signaling that ultimately triggers ERK½-mediated proliferation.[115, 116] Moreover, deacetylation of β-catenin by HDAC6 triggers its translocation to the nucleus and the Wnt-induced proliferation of cystic cholangiocytes.[23, 115]

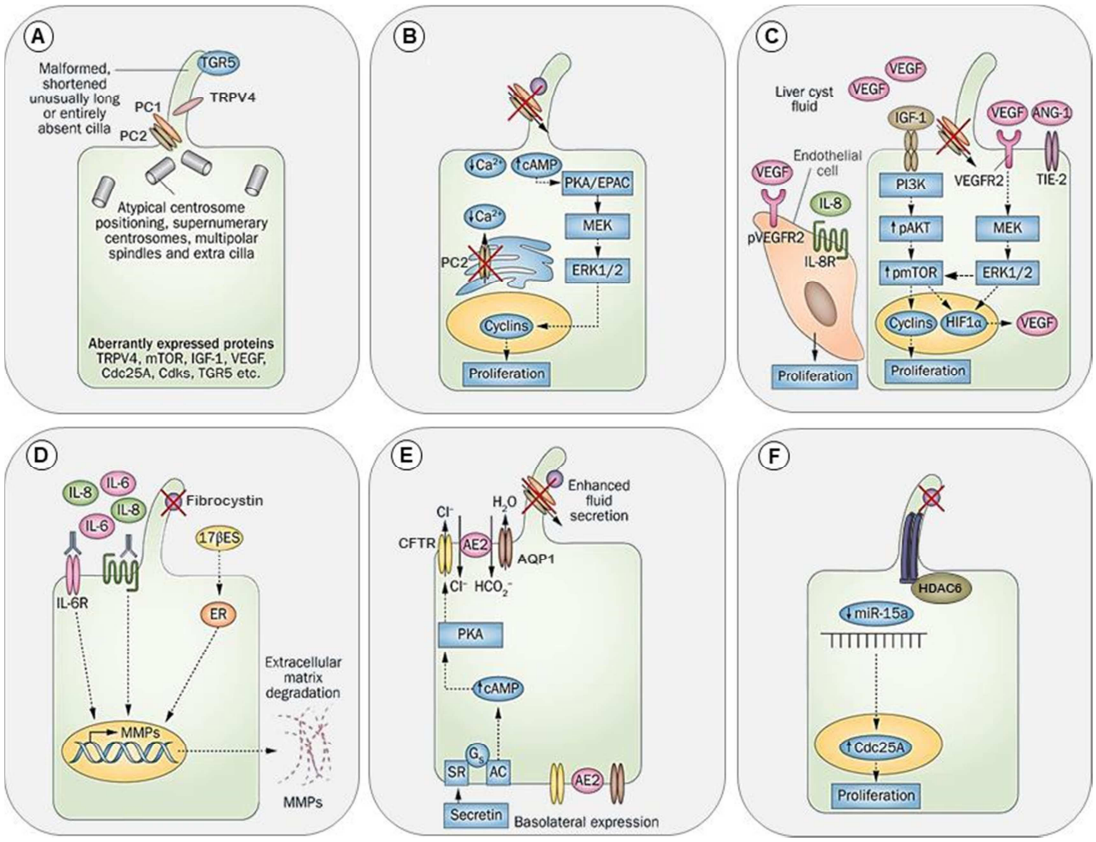

Figure I.10. Panel of the molecular mechanisms involved in cystic cholangiocytes proliferation and hepatic cystogenesis. Several molecular abnormalities confer to cystic cholangiocytes a unique hyperproliferative phenotype. Among them are included (a) primary cilium structural and/or functional abnormalities, (b) decreased $[Ca^{+2}]_i$ and increased intracellular cAMP levels, (c) overexpression of angiogenic factors, (d) hyperactivity of MMPs, (e) augmented fluid secretion and (f) epigenetics modifications. (Adapted from Perugorria MJ *et al*, 2014)[50]

I.3. Pathological role of endoplasmic reticulum

I.3.1. Homeostatic capacity of endoplasmic reticulum

The ER is a highly dynamic intracellular organelle essential for the maintenance of the cellular homeostasis, since it exerts a pivotal role in the storage, biogenesis and metabolism of several macromolecules (i.e., lipids, proteins and carbohydrates) and ions (i.e., Ca^{2+} and K^{+}) (**Figure I.11**).[117-119] Regarding the architecture, the ER is classically subdivided in the ribosome-covered rough endoplasmic reticulum (RER) and the ribosome-free smooth endoplasmic reticulum (SER).[118, 120] Although both the RER and SER are interconnected compartments, their morphological and functional features differ, and even their abundance and cellular distribution varies between different cell lineages.[118, 120] Hence, the SER consists on a polygonal network of tubules where lipid

biogenesis, production of steroid hormones and detoxification enzyme activity occurs.[118, 120] Particularly, glycerophospholipids and sphingolipids involved in the membrane recycling process are chiefly synthesized in this domain of the ER (**Figure I.11**).[118] Likewise, SER-resident enzymes execute the biosynthetic pathway of other more pleiotropic lipids such as cholesterol. In this regard, cholesterol constitutes a major component of the biological membranes, but also serve as a precursor of various steroid hormones, bile salts and vitamin D.[118, 121] Contrary, the RER presents a sheet-like cisternae morphology, whose cytosolic surface is studded with myriad of ribosomes, owing to the involvement of this ER domain in the synthesis of integral membrane and secretory proteins (**Figure I.11**).[117, 118, 120] Thus, the ribosomes translate the information contained in a messenger ribonucleic acid (mRNA) to produce the corresponding nascent polypeptide chain, which contains a signal sequence at the N-terminus recognized by the signal recognition particle (SRP).[117, 118] Once the SRP has bound to the sequence, the SRP-ribosome complex is recruited towards the ER translocation sites, where interacts with the SRP receptor, allowing the co-translational translocation of the nascent polypeptide to the ER lumen (**Figure I.11**) through the translocon (i.e., SEC61B and SEC63).[117, 118] Notably, if the emerging protein is intended to be part or interact with a biological membrane, the translocation is halted at this point and the protein is subsequently embedded into the bilayer.[117, 122] Nevertheless, when the final fate is the secretory pathway, the nascent polypeptide completes the translocation to undergo the ensuing chaperone-assisted folding and the enzymatic modifications (i.e., N-linked glycosilation, disulfide bond formation and oligomerization) within the ER lumen.[117, 120] After that, if the native structure is achieved, the glycoproteins are transported to the Golgi apparatus in a vesicle-mediated process (**Figure I.11**); otherwise they are degraded by the 26S proteasome as a part of the ER-associated degradation (ERAD) pathway.[117, 123] Moreover, the ER operates as the major intracellular reservoir of Ca^{2+} by importing cytosolic Ca^{2+} through the sarco/endoplasmic-reticulum Ca^{2+} ATPase (SERCA) pump (**Figure I.11**).[117, 118, 120] Interestingly, many of the ER-resident chaperones involved in the proper folding of the newly synthesized glycoproteins possess several Ca^{2+} binding sites, where ER free Ca^{2+} binds with high affinity to modulate their activity.[118, 124] For this reason, maintaining an

appropriate concentration (i.e., 100-800µM) of Ca^{2+} within the ER is crucial to preserve a favorable protein folding environment.[117]

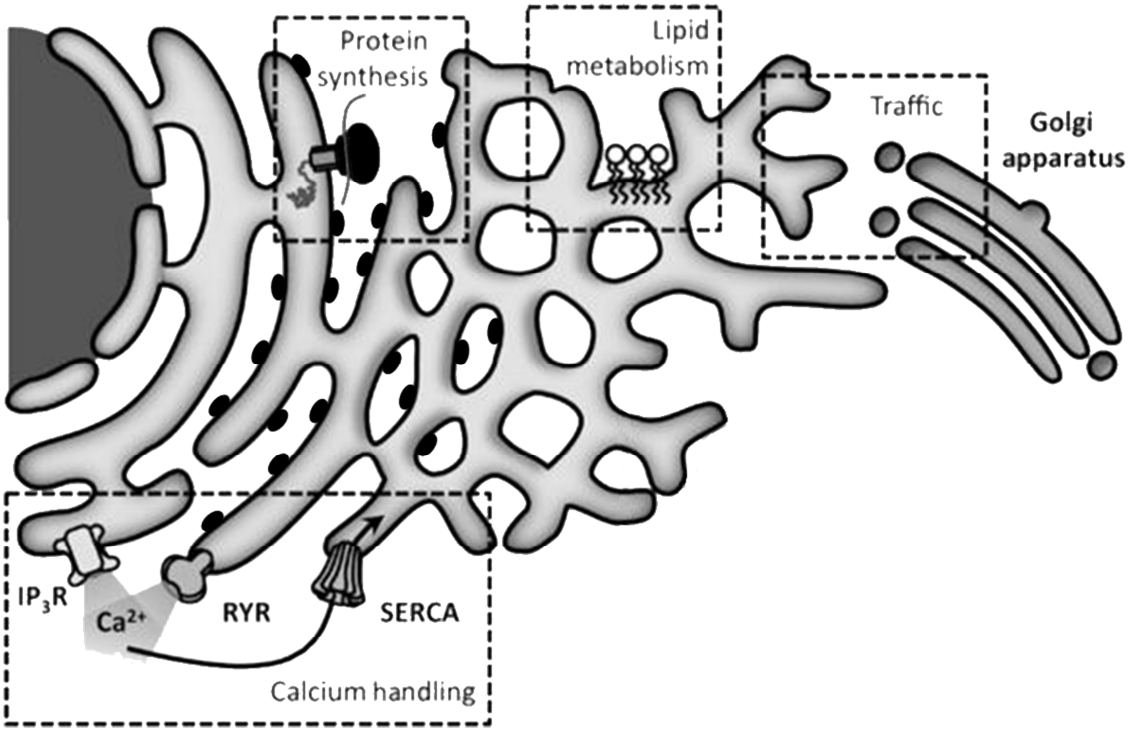

Figure I.11. ER-dependent functions to maintain cellular homeostasis. The ER acts as a multifunctional organelle where lipids are synthesized, proteins are folded and transported, and the Ca^{2+} is stored. (Adapted from Bravo R *et al*, 2013)[118]

I.3.2. Endoplasmic reticulum stress in human diseases

Multiple genetic and/or environmental insults may compromise the aforementioned ER functions, promoting the build-up of aberrant structurally proteins within the ER lumen.[125-127] This establishes a pathological condition termed ER stress, which represents the common underlying mechanism of a large variety of human pathologies (i.e., metabolic disorders, neurodegenerative diseases, cancer and liver diseases, among others) (**Figure I.12**).[125, 128, 129] In this regard, high fat and/or glycemic diets predispose to develop ER stress-mediated type 2 diabetes mellitus (T2DM).[129, 130] Thus, high levels of both glucose (i.e., hyperglycemia) and the saturated free fatty acid palmitate (i.e., hyperlipidemia) hamper the suitable folding of proinsulin through their inhibitory effect on the SERCA pump expression, disrupting the ER Ca^{2+} replenishment capacity and promoting misfolded proinsulin accumulation.[130, 131] Moreover, mutations in ER-resident protein encoding genes, such as *Wfs1*, impair the arrest of the ER stress response, producing β-cells failure and therefore

T2DM.[130] Likewise, genetic mutations in *PSEN1* (i.e., encode for presenilin-1) and *LRRK2* (i.e., encode for LRRK2) coding regions cause ER stress-induced Alzheimer and Parkinson, respectively.[132, 133] Particularly, it has been reported that mutant presenilin-1 interacts and sensitizes the IP_3R to its natural agonist (i.e., IP3), leading to an exaggerated Ca^{2+} leak from the ER, that compromises the folding capacity within this organelle,[134, 135] whereas dysfunctional LRRK2 lacks the GTPase activity needed for the vesicle-mediated trafficking of newly synthesized secretory proteins, and thereby ends up being retained in the ER lumen.[136, 137] Furthermore, a distinguished feature of tumor microenvironment is the sparse oxygen availability (i.e., hypoxia), which causes the accumulation of un/misfolded nascent proteins within the ER, linked to the failure of the oxygen-dependent disulfide bond formation process.[138, 139] In addition, augmented *de novo* lipogenesis is a hallmark of the increasingly prevalent non-alcoholic fatty liver disease (NAFLD), leading to a lipid overload-induced ER stress.[140, 141]

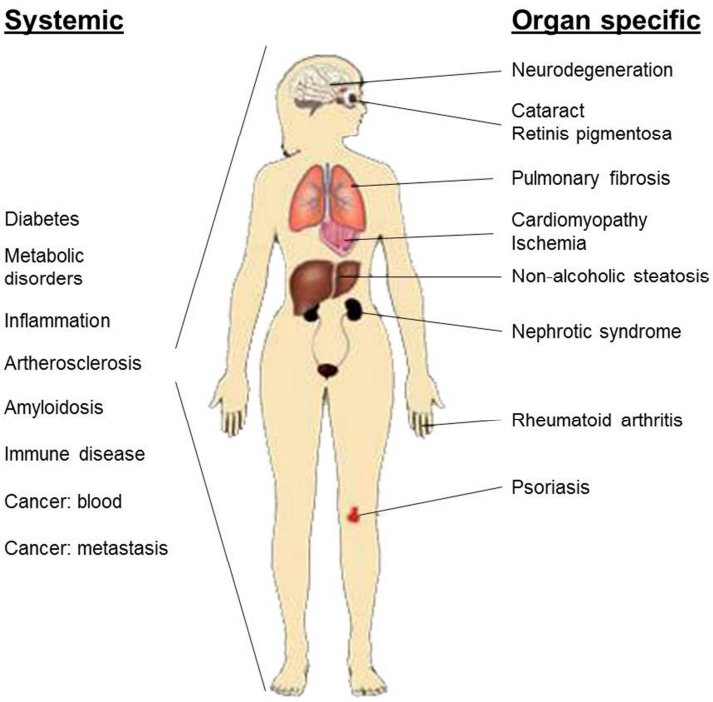

Figure I.12. Human pathologies associated with ER stress. The ER stress underlies the development of several systemic and organ specific human diseases. (Obtained from Lindholm D *et al*, 2017)[128]

I.3.3. Endoplasmic reticulum stress-induced adaptive response

Interestingly, in all these ER stress-related human pathologies an adaptive mechanism, termed unfolded protein response (UPR), is initially activated to abolish the ER stress causing stimulus (i.e., un/misfolded protein accumulation), to restore the proteostasis within this organelle and to preserve the cellular function.[128, 142] For this purpose, the UPR acts through three ER-transmembrane sensors containing a luminal domain, where GRP78 is allosterically associated under non-stressed conditions to maintain them in an inactive state (i.e., competition model) (**Figure I.13**).[142-144] Upon ER stress, the excessive burden of un/misfolded proteins inside the ER lumen competes for binding to GRP78, which ultimately is dissociated from the UPR sensors in order to assist in the folding of the nascent glycoproteins. Accordingly, the signaling of the activated UPR branches is propagated through the cytosolic domains of the sensors (**Figure I.13**).[142-144] The most conserved UPR signaling pathway is initiated by **inositol-requiring protein 1 alpha (IRE1α)**, which in response to the rising burden of aberrant structurally proteins accumulated within the ER, undergoes both the oligomerization and the autophosphorylation needed to generate a stable and active transcription factor called X-box binding protein 1 (XBP1) (**Figure I.13**).[142, 145-147] Once translocated into the nucleus, XBP1 interacts with UPR elements (UPREs) to induce the transcription of a broad spectrum of genes encoding several proteins involved in nascent protein folding [i.e., ER DNA J domain-containing protein 4 (ERdj4), human ER-associated DNAJ (HEDJ) and $p58^{IPK}$], disulfide bond formation [i.e., protein disulfide isomerase P5 (PDI-P5)], in ERAD [i.e., ER degradation-enhancing alpha-mannosidase like protein (EDEM)] and lipid biosynthesis (**Figure I.13**).[142, 145-147] Similarly, **pancreatic ER kinase (PERK)** oligomerizes and autophosphorylates to become active (**Figure I.13**), inducing the inhibitory phosphorylation of eukaryotic translation initiation factor 2 alpha (eIF2α) through the protein kinase activity of its cytosolic domain.[142, 145, 146] In turn, this event boosts the translation of the activating transcription factor 4 (ATF4), which contributes to enhance the protein folding capacity of the ER by increasing the synthesis of the chaperone GRP78 (**Figure I.13**).[128, 142, 145-147] Nevertheless, the PERK-ATF4 axis also upregulates the late expression of various pro-apoptotic

proteins, such as growth arrest and DNA damage-inducible protein 34 (GADD34) and C/EBP homologous protein (CHOP), intended to hasten cell death (**Figure I.13**).[128, 142, 145-148] Unlike IRE1α and PERK, translocation of the **activating transcription factor 6 (ATF6)** from the ER membrane to Golgi apparatus is required for obtaining its transcriptionally active form. Additionally, this implies a sequential cleavage of ATF6 mediated by specificity protein-1 (SP1) and specificity protein-2 (SP2) proteases, in order to release the cytosolic fragment of this transcription factor, which directly controls the expression of UPR target genes through its interaction with ER stress response elements (ERSEs) (**Figure I.13**).[128, 142, 145-148] Thus, the ATF6-dependent signaling branch improves the folding of nascent proteins, reinforces the ERAD machinery and induce the expression of XBP1, albeit under certain conditions also exerts pro-apoptotic effects (**Figure I.13**).[128, 142, 146, 147]

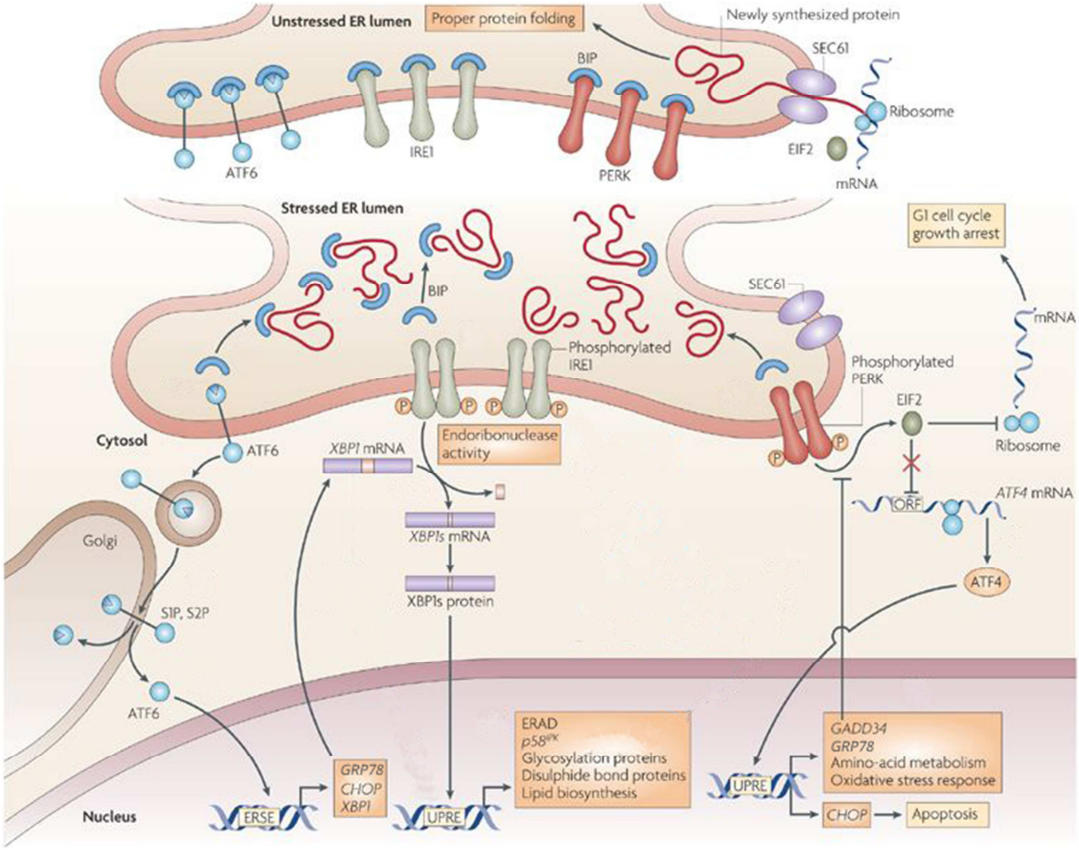

Figure I.13. UPR signaling branches. Upon ER stress, the accumulation of un/misfolded proteins within the ER lumen triggers the activation of the UPR, an adaptive mechanism mediated by three ER-transmembrane sensors (i.e., IRE1α, PERK and ATF6) intended to restore ER homeostasis by improving the protein folding capacity, reinforcing the degradative mechanisms and stimulating lipid biogenesis. However, if the UPR fails to abolish ER stress, the expression of pro-apoptotic mediators (i.e., CHOP and GADD34) is induced, hastening cell death. (Adapted from Todd DJ *et al*, 2008)[146]

Of note, the UPR serves as a double-edged sword process, since it initially focuses on diminishing the burden of un/misfolded nascent proteins built-up within the ER.[142, 143, 149] In this regard, both the protein folding capacity of the ER and the proteasomal degradation are intensified in order to restore ER proteostasis, resolve ER stress and ultimately promote cell survival (**Figure I.14**).[142, 143, 149] Nevertheless, when ER stress levels become chronic and/or excessive, the adaptive responses are not able to handle the overload of aberrant structurally proteins and therefore, the signaling morphs into an alternative program, termed terminal UPR. In this case, the predominance of pro-apoptotic signals end up inducing cell death (**Figure I.14**).[142, 149]

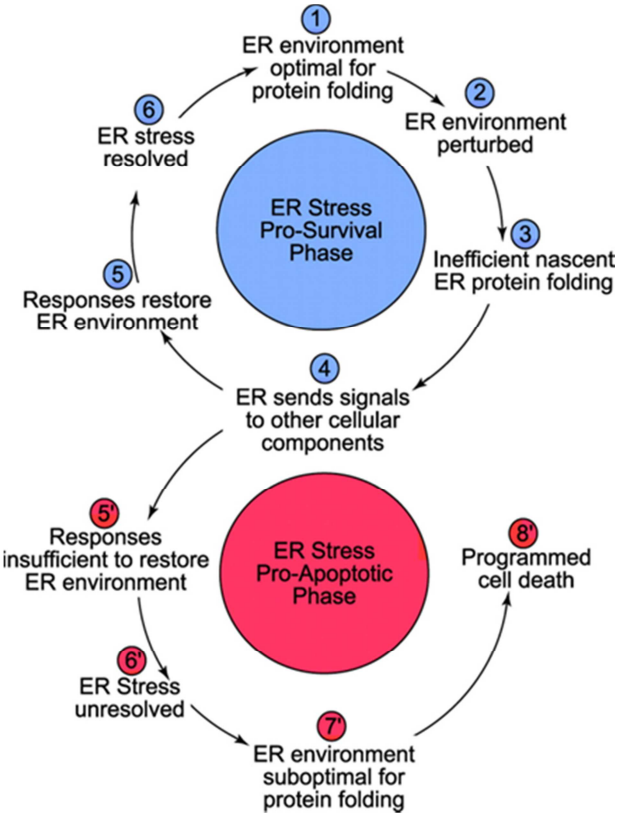

Figure I.14. Pro-survival and pro-apoptotic phases of the UPR. UPR-mediated compensatory mechanisms are intended to promote cell survival. When adverse conditions surpass the adaptive capacity of the UPR (i.e., terminal UPR), cell death is induced. (Obtained from Glembotski CC *et al*, 2007)[150]

Curiously, the vast majority of causing genes for PLD encode for ER-resident proteins involved in folding, trafficking and quality control of newly synthesized glycoproteins, as mentioned above.[32, 151] For this reason, ER stress could have a pivotal role in the etiopathogenesis of this disease. Indeed and as described above in detail (see section I.2.3.4.1), mutations in PLD-related genes impair the biogenesis and/or transport of PC1 to the primary cilium reducing its functional dosage, which is the rate-limiting determinant of cystogenesis and, consequently, of the PLD severity.[32, 83, 84, 151]

I.3.4. Endoplasmic reticulum stress-related molecular therapies

Due to the key role it plays in the onset and progression of a large variety of human diseases, ER stress has become an emerging therapeutic target. That is why many experimental efforts have been allocated, in order to develop different therapies against this pathological process.[152] Currently, the two more established approaches are focused on favoring cell survival by completely abolishing ER stress, when the proper function of the organ is threatened (i.e., pro-survival approach), or inducing cell death by aggravating the preexisting ER stress, as in the case of malignant tumors (i.e., pro-apoptotic approach).[152] In this regard, the pro-survival approach is achieved via chemical chaperones such as 4-phenylbutyric acid (4-PBA) or tauroursodeoxycholic acid (TUDCA), both approved by the FDA to treat urea cell cycle disorders and PBC, respectively.[153] Although the exact mechanism of action of 4-PBA remains unknown, several studies support the involvement of this small molecule assisting in the protein folding of un/misfolded nascent proteins, preventing their aggregation within the ER lumen and restoring the ER-Golgi trafficking.[154, 155] Likewise, TUDCA not only protects against the accumulation of un/misfolded protein aggregates thanks to its amphiphilic structure, but also induces the AKT-mediated inhibition of the PERK-ATF4 axis.[156-158] Moreover, the mechanism of action of other therapeutic compounds consist on intensifying the signaling of the UPR branches to counteract the build-up of un/misfolded nascent proteins within the ER lumen. Among this type of drugs is included salubrinal, a small molecule that indirectly prevents eIF2α dephosphorylation and thereby increases ATF4 expression.[159, 160] Importantly, salubrinal-mediated activation of the PERK-ATF4 signaling branch may balance cell fate between survival and

death, depending on the magnitude or duration of eIF2α phosphorylation.[159] Nevertheless, several anti-apoptotic effects have been attributed to salubrinal by inhibiting the phosphorylation of c-Jun N-terminal kinase (JNK) and p38, as well as caspase 12 activation.[159] In addition, adeno-associated virus (AAV)-mediated gene therapy is currently emerging as an effective and safe tool for ER stress-related pathologies. Indeed, different perspectives of this methodology have been tested in preclinical models in order to restore ER proteostasis, resolve ER stress and promote cell survival.[161] Thus, the aberrant structurally protein overload has been tackled either by improving the ER protein folding capacity through overexpression of both ER-resident chaperones and Ca^{2+} pumps (i.e., GRP78 and SERCA, respectively) or intensifying the degradative pathways via ERAD components overexpression (i.e., HDR1).[161-163] Another perspective of gene therapy based on the administration of AAVs is intended to enhance the signaling of the UPR branches by the AAV-mediated delivery of XBP1 or ATF6.[161, 162]

Contrary, survival of cancer cells has a detrimental impact and, consequently, several pro-apoptotic approaches have been established as anti-carcinogenic therapy.[164, 165] Both inhibitors of the IRE1α RNase domain (i.e., Salicylaldehydes, MKC8866, STF083010 and Toyocamycin)[166-168] and the PERK kinase activity (i.e., GSK2656157)[169, 170] halt the signaling mediated by these UPR sensors, and the subsequent adaptive response against the overload of aberrant structurally proteins inside the ER lumen.[164, 171] Likewise, the proteolytic activation of ATF6 may be averted by the administration of different compounds, that either promote the retention of this UPR sensor in the ER membrane (i.e., Ceapins),[164, 172] or prevent its SP1- and SP2-mediated cleavage [i.e.,4-(2-aminoethyl) benzenesulfonyl fluoride (AEBSF)].[164, 173] Therefore, nuclear translocation of the transcriptional active fragment of ATF6 is hampered, increasing the sensitivity of cancer cells to ER stress. In addition to block the signaling of the three UPR branches, GRP78 also emerges as a potential therapeutic target for different cancers, due to its role in the modulation of the un/misfolded protein burden.[164, 174] Thus, direct interaction of HA15 and HKH40A molecules with GRP78 inhibits the ATPase activity and induces the proteasomal degradation of this ER-resident chaperone, respectively, diminishing the functional dosage available for protein folding.[175, 176]

Additionally, other compounds such as thapsigargin are not a direct target against ER-resident chaperones, but hinder the correct folding of nascent proteins by depleting the ER Ca^{2+} levels via SERCA inhibition.[177, 178] Importantly, the pro-apoptotic effects derived from failures in managing the ER protein burden are not only attributed to a compromised folding capacity, but also to the lack of co-translational modifications such as N-glycosilation (i.e., tunicamycin) and disulfide bond formation [i.e., disulfide bond disrupting agents (DDAs) and dithiothreitol (DTT)].[164, 178, 179] Finally, another anti-carcinogenic strategy that causes proteotoxicity in cancer cells consists on the administration of ERAD-targetable drugs.[164] Notably, those with inhibitory effects on the ubiquitin proteasome system (UPS)-dependent degradation (i.e., Bortezomib, Carfilzomib, Ixazomib and Marizomib) have been widely employed as a therapy in different cancers.[180, 181]

Hypothesis & Objectives

The majority of the mutated genes that cause PLD encode for ER-resident proteins, mainly in ADPKD and ADPLD phenotypes. In this regard, partial or complete loss of protein function disrupts the folding, maturation and trafficking of nascent proteins, triggering an ER stress state. Therefore, this dissertation aims to examine whether ER stress underlies the pathogenesis of PLD and determine the effects derived from its modulation.

Hence, the following objectives are proposed to be assessed:

I. Molecular and ultrastructural characterization of the ER in both healthy and polycystic biopsies and cultured cholangiocytes isolated from human and rat specimens.

II. Analysis of the expression levels of the UPR signaling factors in the presence or absence of ER stress modulators.

III. Evaluation of the impact of ER stress modulation, either by inhibitory and/or inducing agents of ER stress, in cell fate of primary cultures of human cholangiocytes.

IV. Ascertain the role of ER stress regulation in the development and progression of hepatic cystogenesis in PCK rats.

Materials & Methods

M.1. Human samples

Cystic wall tissue were gathered from ADPLD patients (n=16) diagnosed with heterozygous *PRKCSH* (c.1341-2A>G or c.292+1G>C) or *SEC63* (1702delGAA) mutations at the Radboud University Medical Center (Nijmegen, The Netherlands). Germline mutations were identified in the genomic DNA (gDNA) purified from peripheral blood, by direct sequencing with the BigDye Terminator v1.1 Cycle Sequencing Kit (Thermo Fisher Scientific) according to the manufacturer's manual on an *ABI 3730* capillary sequencer (Applied Biosystems). In turn, the mutations were verified through the restriction fragment length polymorphism technique, in a group of healthy controls with a similar ethnic background (European).[182] Furthermore, healthy human gallbladder (n=14) and liver (n=14) tissues were obtained from metastatic colon cancer patients, whom underwent surgical resections performed at Donostia University Hospital (San Sebastian, Spain) and were used as controls. **Table M.1** summarizes the main demographic and clinical features of the patients included in the study.

The research project was approved by the corresponding Clinical Research Ethics Committee of the supporting institutions (MSA-MMR-2017-01 and 2012/317), and all patients signed a written informed consent for the use of their samples for biomedical research.

Table M.1. Demographic and clinical features of the study cohort

Variable	PLD (n=16)	Gallbladder (n=14)	Healthy liver (n=14)
Age, mean ± SEM	51.25 ± 3.07	63.36 ± 3.63	66.36 ± 2.02
Age, range	35 - 71	31 - 79	55 - 80
Gender			
Female (%)	14 (87.50)	5 (35.71)	7 (50.00)
Male (%)	2 (12.50)	9 (64.29)	7 (50.00)
Germline mutation			
PRKCSH (%)			
c.1341-2A>G	4 (25.00)	-	-
c.292+1G>C	1 (6.25)	-	-
SEC63 (%)			
1702delGAA	1 (6.25)	-	-
Other (%)	8 (50.00)	-	-
Unknown (%)	2 (12.50)	-	-
Number of cysts (%)			
<10	2 (12.50)	-	-
10-40	5 (31.25)	-	-
>40	8 (50.00)	-	-
Unknown	1 (6.25)	-	-
Biochemistry, mean ± SEM			
ALT (U/L)	39.07 ± 7.80	55.86 ± 12.96	25.29 ± 3.49
AST (U/L)	30.00 ± 4.57	58.50 ± 16.53	26.17 ± 3.06

M.2. PLD animal model

M.2.1. PCK rat

The PCK rat [PCK/CrljCrl-*Pkhd1*^{pck}/Crl (Charles River Laboratories Inc.)] arises from a Sprague Dawley [Crj:CD (SD)] rat strain that spontaneously underwent a splicing mutation (IVS35–2A3 T) in the *PKHD1* orthologous gene, mimicking features of human ARPKD and ADPKD phenotypes.[183-188] Accordingly, this widely described rodent model is characterized by sequential biliary tree remodeling that results in progressive bile duct dilatation, focal budding and

massive development of cysts, that are initially connected to bile ducts, albeit during disease progression the majority of cysts are isolated.[185] Furthermore, biliary cystogenesis leads to liver hyperplasia (i.e., tissue weight and volume) without affecting the parenchymal volume.[185] In the early life stages of the PCK rat (i.e., less than 8 weeks-old), renal and hepatic cysts, that are accompanied by interstitial and portal fibrosis, already become evident.[188] Additionally, the progression of the disease is associated to impaired hepatic and renal function, which is determined by increased serological values of creatinine, blood urea nitrogen, bilirubin, cholesterol, triglycerides, ALP and aspartate aminotransferase (AST).[185, 186] Therefore, the PCK rat emerges as a suitable rodent model for the study of hepato-renal cystogenesis with an age-dependent disease severity.

M.2.2. Chronic treatment of PCK rats with ER stress modulators

8 weeks-old PCK male rats (Charles River Laboratories Inc.) were divided in the following 4 groups *i)* control (n=12), *ii)* treated with 4-PBA (n=12), *iii)* treated with TM (n=12) and *iv)* dually treated with 4-PBA and TM (n=12). Concurrently, a wild-type group of Sprague Dawley (Charles River Laboratories Inc.) rats (n=12), of the same age and gender as the previous ones, were included in the study as negative control of the disease.

4-PBA (Scandinavian formulas) is highly soluble in water and thus, was administered to the animals in drinking water at 100mM. Fresh water supplemented with 4-PBA was replaced every 4 days for 20 weeks. Water intake was periodically measured in both control and 4-PBA treated groups, evidencing equal water consumption. In this regard, each PCK rat drank a daily average of 27ml of water containing the drug. Therefore, each rat received an average dose of 500mg/day ($\bar{x}$:1g/kg/day), which has been widely used for the treatment of different animal models[189-192] and it is comparable to the clinical dose employed in humans.[193] On the other hand, TM (Sigma-Aldrich) was injected intraperitoneally twice per week during 20 weeks at the non-toxic dose of 0.02mg/kg/day.[194] 5% Isoflurane (AbbVie) in inhaling oxygen (flow of 0.3L/min) was used to induce anesthesia prior to TM administration. Animal weight was checked once a week in order to adjust the TM dose. All animals

were maintained under standard animal housing conditions with a 12 hours light/dark cycle and given standard chow and water *ad libitum*.

Additionally, a previously published *in vivo* study[82] was used in order to evaluate the potential impact of UDCA (Sigma-Aldrich) on ER stress alleviation. Briefly, PCK male rats (8 week-old) were divided into 2 groups: *i*) control (n=10) and *ii*) treated with UDCA (n=10). UDCA was mixed in chow and administered for 5 months at a high dose of 25mg/kg/day, which is normally well tolerated and safe, and is employed in clinical practice for the treatment of cholestatic liver diseases.[79-81, 195-197] Animal weight was monitored daily to adapt UDCA dose. In parallel, wild-type rats (n=12) matched on age and gender were used as negative control of the disease.

Monthly, blood from rat tail was collected in order to determine serum levels of ALP, AST, alanine amino transferase (ALT), albumin, total protein, urea and creatinine using the *COBAS Integra® 400Plus* analyzer. In addition, the physical condition of the animals was visually monitored throughout the whole study. After treatment, rats were slaughtered and the hepatic tissue was subsequently analyzed histologically and molecularly.

The experimental procedures that employed 4-PBA and TM treatments were approved by the Animal Experimentation Ethics Committees of both Biodonostia Health Research Institute (CEEA_17/009) and the Guipuzcoa Government (OH-17-19), while UDCA administration to the animals was approved by the Ethics Committee of the Foundation for Applied Medical Research (CIMA, University of Navarra). Both *in vivo* studies were performed in conformity with the institution's guidelines for the use of laboratory animals.

M.3. Histological analysis

After sacrifice, the hepatic tissue from the wild-type and PCK rats chronically treated with 4-PBA and TM were cut in small pieces, placed in histological cassettes (Leica) and fixed with 4% paraformaldehyde solution for 24 hours. Afterwards, the samples were processed using the MTM tissue processor (Slee Medical GmbH) and embedded in paraffin (Thermo Fisher Scientific), in order to get tissue sections of 5µm of thickness for hematoxylin-eosin stain using the *HM355S* microtome (Thermo Fisher Scientific).

M.3.1. Hematoxylin-eosin staining

Paraffin embedded samples were immersed at room temperature in xylene (VWR) three times of 5 minutes each, to dissolve and remove the paraffin from the tissue sections. Then, the slides were passed through solutions of decreasing ethanol (VWR) concentration (100%, 96% and 70%; 2 minute in each) with a final wash in DPBS 1X (Gibco - Thermo fisher scientific), in order to hydrate the tissue. Samples were stained with Harris Hematoxylin (Merck) for 5 minutes, followed by a wash with tap water and subsequent incubation with Eosin (Merck) for 5 minutes at room temperature. Thereafter, samples were washed again with tap water and dehydrated with increasing grade ethanol solutions (70%, 96% and 100%) for 2 minutes each. Finally, tissue sections were incubated with xylene for 5 minutes two times and mounted with dibutylphthalate polystyrene xylene (DPX) mounting medium (Sigma-Aldrich). The stained tissue was visualized in a *Nikon Eclipse 80i* optical microscope equipped with a *Nikon Digital Sight DS-U2* camera and the NIS-Elements AR 3.2 software (all three from Nikon). Later, hepatic cystogenesis was quantified from the captured images using the ImageJ software 1.50 (NIH, Bethesda, MA, USA).

M.4. Primary biliary cell isolation, culture and treatments

M.4.1. Isolation of normal and cystic human cholangiocytes

Normal and cystic cholangiocytes from human liver specimens were isolated according to a procedure previously described by our group.[198] Briefly, small pieces (~1mm^3) of liver tissue were subjected to a mechanical and chemical digestion by incubating the samples at 37ºC with shaking (140rpm) for 30 minutes in a solution containing Dulbecco's modified Eagle's medium/Ham's F-12 nutrient mixture (DMEM/F-12) + GlutaMAX medium (Thermo Fisher Scientific), 3% fetal bovine serum (FBS), 1% penicillin-streptomycin (P/S) (both from Gibco – Thermo Fisher Scientific), 0.1% bovine serum albumin (BSA), 17mg pronase, 12.5mg type IV collagenase and 3mg DNase (all four from Sigma-Aldrich). Next, sequential filtrations were performed through 100µm and 40µm sterile nylon cell strainer (Falcon – Corning), collecting those tissue

fragments trapped between the two pore-sizes, which were incubated for another 30 minutes in the aforementioned digesting solution, but containing 13mg hyaluronidase (Sigma-Aldrich) instead of pronase. Afterwards, successive filtrations of the tissue samples were repeated to obtain intrahepatic bile duct units (IBDU) ranging from 40µm to 100µm. IBDUs were washed with fully-supplemented DMEM/F-12 medium (**Table M.2**) to inactivate enzyme traces. Finally, cells were seeded in thin collagen-coated cell culture flasks (Corning) using the same growth medium.

M.4.2. Characterization of human cell lines

Normal human cholangiocytes (NHC) were isolated from liver tissue adjacent to a local hepatic adenoma gathered during a surgical resection performed at the Mayo Clinic (Rochester, MN, USA) and validated as healthy tissue by an experienced pathologist.[198] On the other hand, two different primary cell lines of cystic human cholangiocytes (i.e., ADPKD and ADPLD) were used. ADPKD cholangiocytes were isolated from a patient carrying a missense mutation (c.2515C>T) in exon 22 of *GANAB* gene,[36] who underwent a hepato-renal transplant at the "Clínica Universidad de Navarra" (Pamplona, Spain), while ADPLD cholangiocytes isolation was performed from a cystic wall of a patient with a splice site mutation (c.292+1G>C) in intron 4 of *PRKCSH* gene.[34] In this case, the cystic tissue sample was resected by laparoscopic fenestration at the Radboud University Medical Center (Nijmegen, The Netherlands). Of note, the isolated human cholangiocytes were extensively characterized by molecular techniques as previously described by our group.[62, 82, 99, 198, 199] In all three cases, liver tissue came from women and their extraction and use was done according to the guidelines approved by the Ethics Committees of each hospital and prior signature of the pertinent written informed consents.

M.4.3. Establishment of normal and PCK cholangiocyte cell lines

Normal rat cholangiocytes (NRC) and cystic rat cholangiocytes (PCK) were isolated from liver tissue of wild-type and PCK male rats. Before cellular isolation, *in situ* liver perfusion was performed in order to digest the ECM. The animal was anesthetized with 5% Isoflurane (AbbVie) in inhaling oxygen (flow of 0.3L/min) along the procedure. Briefly, the portal vein was surgically exposed

and cannulated with a 18G intravascular catheter (BD Insyte), and was subsequently connected to the infusion tube of the *Model EP-1 Econo* perfusion pump (Bio-Rad). Afterwards, the inferior vena cava (IVC) was cut below the liver and the perfusion buffer [10mM 4-(2-hydroxyethyl)-1-piperazineethanesulfonic acid (HEPES), 2.7mM KCl, 135mN NaCl and 250µM HNa_2PO_4 (all from Sigma-Aldrich)] was infused through the liver at a flow rate of 10mL/min and 37ºC. Then, the perfusion buffer was supplemented with 10mM $CaCl_2$ and 50mg of collagenase type IV (Sigma-Aldrich), and the infusion flow rate was reduced to 5mL/min. During this step, the IVC was clamped both below the liver and above the diaphragm, in order to direct the solution through the liver and prevent the perfusion of other organs, achieving complete digestion of the liver tissue. Once the perfusion was completed, the liver was carefully removed. Finally, the isolation of NRC and PCK cholangiocytes was performed according to the previously mentioned protocol used for human cells (see section M.4.1).

M.4.4. Cell culture conditions and treatments

Human (i.e., NHC, ADPKD and ADPLD) and rat (i.e., NRC and PCK) cholangiocytes were harvested in thin collagen-coated cell culture flasks (Corning). For this purpose, ultrapure water was used to prepare a solution containing 0.1% of glacial acetic acid (Corning) and 50mg/L of rat tail collagen type I (Corning). After filtering the collagen solution by 0.22µm pore size sterile filter system (Corning), cell culture flask surface was covered with the collagen solution for 3 hours (1 hour for cell culture plates). Thereafter, the collagen was removed and DPBS 1X (Gibco - Thermo Fisher Scientific) was added. Cholangiocytes were grown in monolayer with fully-supplemented DMEM/F-12 medium (**Table M.2**) and in a controlled environment (i.e., 37ºC, 5% CO_2 and 75% relative humidity). Once 90% of confluence was reached, the cells were passaged using 0.05% trypsin-EDTA (Gibco – Thermo Fisher Scientific), while the cellular surplus were frozen in a solution containing FBS (Gibco – Thermo Fisher Scientific) with 10% DMSO (Sigma-Aldrich). All cell lines were tested for mycoplasma and were negative all along the experiments.

Table M.2. Composition of the fully-supplemented DMEM/F-12 medium

Reagent (Company)	Concentration
DMEM/F-12+GlutaMAX (Gibco – Thermo Fisher Scientific)	1% (v/v)
Fetal Bovine Serum (FBS) (Gibco – Thermo Fisher Scientific)	5% (v/v)
MEM-non essential aminoacids 100X (Gibco – Thermo Fisher Scientific)	1% (v/v)
Lipid mixture 1000X (Sigma-Aldrich)	0.1% (v/v)
MEM vitamins solution (Gibco – Thermo Fisher Scientific)	1% (v/v)
Penicillin/Streptomicyn (Gibco – Thermo Fisher Scientific)	1% (v/v)
Soybean Trypsin Inhibitor (Gibco – Thermo Fisher Scientific)	0.05mg/mL
Insulin Transferrin Selenium (Gibco – Thermo Fisher Scientific)	1% (v/v)
Bovine Pituitary Extract (Gibco – Thermo Fisher Scientific)	30µg/mL
Dexamethasone (Sigma-Aldrich)	393ng/mL
3, 3', 5-triiodo-L-thyronine (T3) (Sigma-Aldrich)	3.4µg/mL
Epidermal Growth Factor (EGF) (Gibco – Thermo Fisher Scientific)	25ng/mL
Forskolin (Ascent-Scientific)	4.11mg/mL

Normal and cystic human and rat cholangiocytes were seeded in thin collagen-coated cell culture plates (Falcon – Corning) with fully-supplemented DMEM/F-12 medium (**Table M.2**). Once the cells were attached (approximately 6 hours), cholangiocytes were incubated overnight with quiescent medium [DMEM/F-12 + GlutaMAX with 3% FBS and 1% P/S]. Afterwards, human cholangiocytes were treated with 5mM 4-PBA and/or 2.4µM TM in quiescent medium. Finally, NHC, ADPKD and ADPLD cholangiocytes were harvested and collected at different time-points for mRNA expression analysis, as well as functional assays. Likewise, normal (i.e., NRC) and cystic rat (i.e., PCK) cholagiocytes were treated with UDCA (100mM), in order to perform gene expression experiments.

M.5. Gene expression measurement

M.5.1. Total RNA isolation

Total RNA from liver tissue and cells in culture was isolated following the same proceeding. Small tissue pieces (~20mg) or cultured cholangiocytes (~2-3x10^5 cells/well) seeded in thin collagen-coated 6-well plates (Corning) with fully-supplemented DMEM/F-12 medium, and subsequently starved with quiescent medium overnight, were lysed using 1mL of cold Tri-Reagent® (Sigma-Aldrich).

Worth mentioning that the tissue fragments were also mechanically homogenized using a pellet mixer (VWR), while the lysis of cholangiocytes was assisted by scraping. Then, samples were frozen at -80ºC for 24 hours in order to contribute to tissue and cell lysis. Once the samples were thawed, 200µl of cold chloroform (Merck Millipore) was added to each tube, which was vigorously vortexed for 20 seconds to mix the two phases. A subsequent incubation of 10 minutes at room temperature was carried out, followed by a centrifugation at 14,000rpm and 4ºC for 15 minutes. Afterwards, the aqueous phase was transferred into a new clean tube in which 0.5mL of cold 100% 2-propanol (PanReac AppliChem) was added. Both solutions were blended by inversion and incubated for 10 minutes at room temperature. Thereafter, the tubes were centrifuged at 14,000rpm for 15 minutes at 4ºC and the supernatant was discarded. Next, the RNA pellets were washed by slightly vortexing with 1mL of 75% ethanol (VWR) and centrifuged at 14,000rpm for 15 minutes at 4ºC. After removing the supernatant, the RNA pellets were air-dried at room temperature and dissolved with 20µL (for cell pellets) or 300µL (for tissue pellets) of UltraPure™ DNase/RNase-free distilled water (DNase/RNase-free dH_2O) (Invitrogen – Thermo Fisher Scientific). Finally, RNA concentration and purity were quantified by ultraviolet spectrophotometry using the *NanoDrop® ND-1000* apparatus (Thermo Fisher Scientific).

M.5.2. Reverse transcription polymerase chain reaction (RT-PCR)

Complementary DNA (cDNA) was synthesized by retrotranscription of 1µg of total RNA according to different protocols for human liver tissue or rat liver samples and cells in culture.

M.5.2.1. RT-PCR for human tissue samples

The highly efficient SuperScript® VILO™ cDNA Synthesis Kit (Thermo Fisher Scientific) was used to generate first-strand cDNA from human tissue biopsies. Total RNA (1µg) was combined with 10X SuperScript® Enzyme Mix (2µL/sample) and 5X VILO™ Reaction Mix (4µL/sample). Afterwards, DNase/RNase-free dH_2O was added until reaching a final volume of 20µL and a three step protocol [*i*) 10 minutes at 25ºC, *ii*) 1 hour at 42ºC, and *iii*) 5 minutes at 85ºC] was carried out in a *Veriti 96-Well* thermal cycler (Applied Biosystem).

The obtained cDNA was diluted to a final concentration of 12.5ng/µL with DNase/RNase-free dH_2O.

M.5.2.2. RT-PCR for rat tissue and cell samples

A multistep RT-PCR was implemented for rat liver tissue and cultured cholangiocytes. Briefly, total RNA (1µg) underwent DNase treatment by adding 1µL of DNase I Amplification Grade (Invitrogen – Thermo Fisher Scientific) and 1µL of 10X DNase I Reaction Buffer (Invitrogen – Thermo Fisher Scientific) for 20 minutes at 37ºC, in order to remove gDNA contamination. Then, the DNase I reaction was stopped through magnesium chelation with 1µL of 25mM Ethylenediaminetetraacetic acid (EDTA) (Invitrogen – Thermo Fisher Scientific) for 10 minutes at 65ºC, 1 minute at 90ºC and cooled at 4ºC. Afterwards, the cDNA was synthesized by adding 30µL of RT-PCR master mix [buffer 5X, 8µL; random primers 100ng/µL, 4µL; deoxyribonucleotide triphosphate (dNTP) mix, 4µL; DTT, 2µL; RNase OUT, 1.2µL; moloney-murine leukemia virus reverse transcriptase (M-MLVRT); 1.2µL (all from Invitrogen –Thermo Fisher Scientific); DNase/RNase-free dH_2O, 9.6µL] to each tube which were incubated under the following conditions: 37°C for 60 minutes, 95°C for 1 minute and kept at 4°C. All the steps were performed using the *Veriti 96-Well* thermal cycler (Applied Biosystem). Finally, a concentration of 12.5ng/µL was achieved by diluting the cDNA with DNase/RNase-free dH_2O.

M.5.3. Quantitative PCR (qPCR)

Expression levels of various genes of interest were determined by qPCR analysis. In order to do so, a master mix containing 10µL of iQ™ SYBR® Green Supermix (Bio-Rad), 0.6µL of 10µM stock solution of each forward and reverse primer (**Table M.3**) and DNase/RNase-free dH_2O until a final volume of 17µL per sample was prepared and placed into a Hard-Shell® 96-well PCR plate (Bio-Rad). Thereafter, 3µL (i.e., 37.5ng) of the previously synthetized cDNA was added to the plate and, subsequently, the amplification products were detected in the *CFX96 Touch™* apparatus (Bio-Rad), following the iQ™ SYBR® Green Supermix standard protocol (same for all genes): *i*) denaturation of the cDNA and activation of the enzyme were induced by heating the plate at 95ºC for 10 minutes, *ii*) amplification of cDNA was carried out during 40 cycles of 3 steps

consisting in 95°C for 15 seconds, 60°C for 30 seconds (annealing) and 72°C for 45 seconds (extension), *iii*) incubation of 15 seconds at 95ºC followed by *iv*) a gradual increase of the temperature from 60ºC to 93ºC (in 1ºC increments) was established to plot the melting curve profile. Finally, the CFX Maestro™ Software (Bio-Rad) was used to collect and analyze the resultant data. Of note, *Glyceraldehyde-3-phosphate dehydrogenase (GAPDH)* was used as a housekeeping control for data normalization and gene expression was determined using the ΔCT method. The mRNA expression levels are displayed as percentage relative to the control group (100% of expression).

Table M.3. Primers sequences employed for qPCR (all from Sigma-Aldrich)

	Primer name		Sequences
Human primers			
	ATF6	Forward	5'-GCTGGATGAAGTTGTGTCAGAG-3'
		Reverse	5'-GCTTCTCTTCCTTCAGTGGC-3'
	CHOP	Forward	5'-TCTTCATACATCACCACACC-3'
		Reverse	5'-CTTGTGACCTCTGCTGGTTC-3'
	GAPDH	Forward	5'-CCAAGGTCATCCATGACAAC-3'
		Reverse	5'-TGTCATACCAGGAAATGAGC-3'
	GRP78	Forward	5'-GAGCTGTGCAGAAACTCCGGCG-3'
		Reverse	5'-ACCACCTGCTGAATCTTTGGAATTCGAGT-3'
	IRE1α	Forward	5'-AGGGACAGGAGGGAATCGTA-3'
		Reverse	5'-CAGTCCCTAATGCCACACCT-3'
	PERK	Forward	5'-CAGGCAAAGGAAGGAGTCTG-3'
		Reverse	5'-AACAACTCCAAAGCCACCAC-3'
	XBP1	Forward	5'-GCAGGTGCAGGCCCAGTTGTCAC-3'
		Reverse	5'-CCCCACTGACAGAGAAAGGGAGG-3'
Rat primers			
	α-Sma	*Forward*	5'-CGCCATCAGGAACCTCGAGAAG-3'
		Reverse	5'-ATCATCACCAGCAAAGCCCG-3'
	Atf6	Forward	5'-TCTTCAACTCAGCACGTTCC-3'
		Reverse	5'-GCTTCTCTTCCTTCAGTGGC-3'
	Chop	Forward	5'-AGTCATGGCAGCTGAGTCTC-3'
		Reverse	5'-CTGACTGGAATCTGGAGAGC-3'
	Col1a1	*Forward*	5'-GACTGTCCCAACCCCCAAA-3'
		Reverse	5'-CTTGGGTCCCTCGACTCCTA-3'
	Ctgf	*Forward*	5'-CTAGCTGCCTACCGACTGGA-3'
		Reverse	5'-GCCCATCCCACAGGTCTTAG-3'

Cxcl1 **(*Il-8* homolog)**	*Forward*	5'-ACTCAAGAATGGTCGCGAGG-3'
	Reverse	5'-ACGCCATCGGTGCAATCTAT-3'
Gapdh	Forward	5'-TGTGAACGGATTTGGCCGTA-3'
	Reverse	5'-ATGAAGGGGTCGTTGATGG-3'
Grp78	Forward	5'-GAGCTGTGCAGAAACTCCGGCG-3'
	Reverse	5'-ACCACCTGCTGAATCTTTGGAATTCGAGT-3'
Il-6	*Forward*	5'-CATTCTGTCTCGAGCCCACC-3'
	Reverse	5'-AGTCCCAAGAAGGCAACTGG-3'
Ire1α	Forward	5'-GACTATGCAGCCTCACTTCC-3'
	Reverse	5'-CAAGACATCCCCAGATTCAC-3'
Perk	Forward	5'-TTTCACTGTGGAGTCCCTTC-3'
	Reverse	5'-CTGGTACTCCCATTCTAGGC-3'
Xbp1	Forward	5'-GCAGGTGCAGGCCCAGTTGTCAC-3'
	Reverse	5'-CCCCACTGACAGAGAAAGGGAGG-3'

Abbrev: α-Sma, alpha-smooth muscle actin; ATF6, activating transcription factor 6; CHOP, C/EBP-homologous protein; Col1a1, collagen type 1 alpha 1 chain; Ctgf, connective tissue growth factor; Cxcl1, C-X-C motif ligand 1(interleukin 8-homolog); GAPDH, glyceraldehyde-3-phosphate dehydrogenase; GRP78, 78 KDa glucose-regulated protein; Il-6, interleukin 6; IRE1α, inositol-requiring enzyme 1a; PERK, pancreatic endoplasmic reticulum kinase; XBP1, x-box binding protein 1.

M.6. Protein expression assessment

M.6.1. Protein extraction from liver tissue

Liver tissue (~20mg) from wild-type and PCK rats was lysed in 400µl of Nonidet P-40 (NP40) Cell Lysis Buffer (Invitrogen – Thermo Fisher Scientific) and mechanically homogenised using a pellet mixer (VWR). Homogenised tissue was placed in a rotator (Stuart) for 30 minutes at 4ºC. Next, samples were sonicated (JP Selecta) two times for 15 seconds and centrifuged for 15 minutes at 14,000rpm at 4ºC. Supernatant was placed in a new tube for cell debris removal and total protein was quantified.

M.6.2. Protein extraction from culture cells

Normal and cystic cholangiocytes (~2-3x10^5cells/well) from human and rat origin were seeded in thin collagen-coated 6-well plates (Corning) and harvested in fully-supplemented DMEM/F-12 medium. After overnight starvation with quiescent medium, cells were washed once with DPBS 1X (Gibco – Thermo Fisher Scientific) and lysed with 80µL of cold NP40 Cell Lysis Buffer

(Invitrogen – Thermo Fisher Scientific) assisted by scraping. Whole cell extracts were collected and frozen at -80ºC to contribute with cell membrane disruption. When thawing, the samples were centrifuged at 14,000rpm for 10 minutes at 4ºC to discard cellular debris, and the total amount of protein was quantified from the cellular supernatant.

M.6.3. Protein quantification

Protein concentration was measured using the Pierce™ BCA Protein Assay Kit according to the manufacturer´s instructions (Thermo Fisher Scientific). Briefly, an aliquot of each protein sample was diluted 1:5 (for cells) or 1:40 (for tissue) with dH_2O and placed in a 96-well plate (Corning). Simultaneously, a calibration curve was prepared (ranging from 0 to 2mg/mL of BSA). Likewise, the vehicle solution (i.e., NP40) was included in the plate as blank sample. Afterwards, a mixture of the A and B reagents (in a proportion 1:50) of the BCA kit was prepared and 200µL of the blend was added to each well. Finally, the plate was incubated for 30 minutes at 37ºC in darkness and the absorbance was measured at 570nm in a *Multiskan Ascent®* spectrophotometer (Thermo Fisher Scientific).

M.6.4. Protein electrophoresis and immunoblotting

In order to detect the proteins of interest in the whole protein extract, 20µg of total protein was denaturalized by adding 5X Protein Loading Buffer [250 mM Tris pH 6.8, 10% SDS, 50% glycerol (all three from Applichem Panreac), 0.05% bromophenol blue (Probus) and 500mM 2-mercaptoethanol (Sigma-Aldrich)] and heating at 95ºC for 5 minutes. Then, protein samples were separated in a sodium dodecyl sulfate polyacrylamide gel electrophoresis (SDS-PAGE) at 12.5% and electro-transferred onto a 0.2µm pore-size nitrocellulose membrane (Bio-Rad). Thereafter, the membrane was blocked in Tris-buffered saline with 0.1% Tween® 20 (T-TBS) containing 5% skim milk powder (for the non-phosphorylated form) or 5% BSA (for the phosphorylated form) (both from Sigma-Aldrich) for 1 hour at room temperature. An overnight incubation of the membrane at 4ºC was performed with the anti-phospho-p44/42 MAPK (ERK½) primary antibody (Rabbit; Cell Signaling), diluted 1:1000 in the corresponding blocking solution. Next, the membrane was washed 3 times with T-TBS and,

subsequently, incubated for 1 hour at room temperature with an anti-rabbit horseradish peroxidase (HRP)-conjugated secondary antibody (Cell Signaling) at 1:5000 dilution in blocking solution. After washing, the antigen was exposed using the Novex® ECL HRP Chemiluminiscent Substrate Reagent Kit (Invitrogen – Thermo Fisher Scientific) and the emitted chemiluminescence was pre-visualized and captured in the *iBright™ FL1000* imaging system (Thermo Fisher Scientific). Once the membrane was stripped in the stripping solution [1M Tris pH 6.8, 10% SDS (both from Applichem Panreac), dH_2O and 2-mercaptoethanol (Sigma-Aldrich)] for 30 minutes at 50ºC with shaking, the procedure was repeated, incubating the membrane with the anti-p44/42 MAPK (ERK½) primary antibody (Rabbit; Cell Signaling), diluted 1:1000 in 5% skim milk powder solution. Thereafter, a 1:5000 dilution of an anti-rabbit secondary antibody (Cell Signaling) was employed to detect the non-phosporylated form of the protein. Again, the antigen was exposed using the Novex® ECL HRP Chemiluminiscent Substrate Reagent Kit (Invitrogen – Thermo Fisher Scientific) and the emitted chemiluminescence was captured in the *iBright™ FL1000* imaging system (Thermo Fisher Scientific). Finally, protein signal was quantified with the ImageJ software 1.50 (NIH, Bethesda, MA, USA). β-actin protein levels were detected using the anti-β-actin primary antibody (Mouse; Sigma-Aldrich) and used as loading control. Results are displayed as percentage relative to the vehicle-treated group which is set as 100% of expression.

M.7. Transmission electron microscopy

Ultrastructural visualization of ER morphology in normal and cystic cholangiocytes was accomplished by transmission electron microscopy (TEM) in collaboration with the group of Prof. Nicholas F. LaRusso (Cholangiopathies laboratory at Mayo Clinic, Minnesota, USA).[200] Succinctly, human (i.e., NHC, ADPKD and ADPLD) and rat (i.e., NRC and PCK) cholangiocytes in culture were fixed with 2% glutaraldehyde in 0.1M phosphate-buffered saline for 1 hour at room temperature, followed by a post-fixation step in 1% osmium tetroxide for 1 hour on ice. After dehydration with increasing graded series of ethanol (70%, 95% and 100%), cholangiocytes were infiltrated and embedded with Spurr´s resin. Then, ultrathin sections were cut on a *Leica EM UC7* ultramicrotome and

stained with 2% aqueous uranyl acetate for 15 minutes and 2.5% lead citrate for 3-5 minutes, in order to examine the ER ultrastructure using the *JEOL JEM-1400* (JEOL) transmission electron microscope. Finally, ImageJ software 1.50 (NIH, Bethesda, MA, USA) was used to quantify the total surface area occupied by the ER in each TEM micrographs by calculating the sum of the area (µm2)/ length (µm) ratio of each ER portion present in the captured images.

M.8. Flow cytometry-based cell proliferation assay

Proliferation rate of NHC, ADPKD and ADPLD cholangiocytes was determined by flow cytometry technique using the CellTrace™ CFSE Cell Proliferation Kit (Invitrogen – Thermo Fisher Scientific). The CFSE dye reacts with intracellular amines, emitting green fluorescence (Ex 492nm/Em 517nm). The label is stably inherited by daughter cells through successive cell divisions, thus diminishing the fluorescence intensity in each generation (**Figure M.1A**). Every generation of cells will appear as a different peak on a flow cytometry histogram (**Figure M.1B**)

Briefly, cultured cholangiocytes were trypsinized from a T75 flask (Corning) and counted using a Neubauer improved chamber (Marienfeld). Once the specific number of cells was selected, a centrifugation was performed at 1,500rpm for 5 minutes at room temperature, followed by the removal of the supernatant. Afterwards, the cellular pellet was resuspended in sterile 0.1% BSA (Sigma-Aldrich) in DPBS 1X (Gibco – Thermo Fisher Scientific) at a concentration of $1x10^6$cells/mL, and stained with 5mM CFSE (2µL/mL) for 10 minutes at 37ºC. Then, 5 volumes of cold quiescent medium were added to each tube, which were incubated 5 minutes on ice in order to quench the staining. Next, human cholangiocytes were washed 3 times (centrifugation at 1,500rpm for 5 minutes) with quiescent medium and seeded in a thin collagen-coated 12-well plate ($3x10^4$cells/well). When cells were attached, 5mM 4-PBA (Sigma-Aldrich) or 2.4µM TM (Sigma-Aldrich) treatment was added and incubated for 48 hours. After this, the cells were trypsinized, resuspended in DPBS 1X (Gibco – Thermo Fisher Scientific) according to the advised concentration by the flow cytometer manufacturer´s instructions, and placed in a U-bottom 96-well plate (Falcon). Finally, fluorescence signal was detected using

the 525/30nm filter of the *Guava Easycyte 8HT* flow-cytometer (Merck Millipore) and analyzed with the Incyte™ 3.1 software (Merck Millipore). Of note, negative (i.e., non-stained cells) and positive (i.e., cell stained just before the flow cytometry) controls were used to accurately adjust the cytometer settings. Results are represented as percentage relative to the vehicle-treated cells (100% of proliferation).

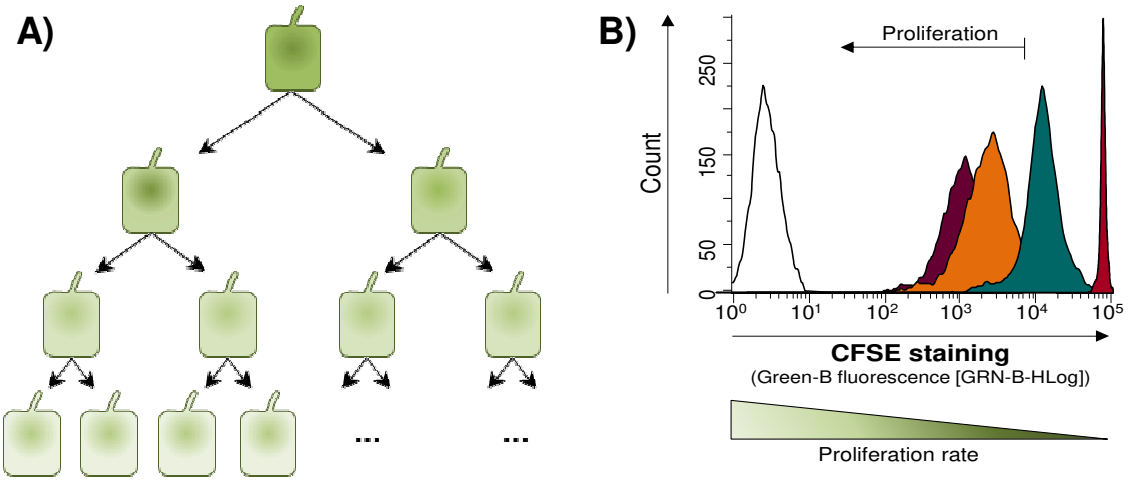

Figure M.1. Flow cytometry proliferation tracing with CFSE dye. (**A**) The basis of the assay consists on the progressive loss of the initial staining in each cell division as the dye is equally distributed among the daughter cells. (**B**) Representative histogram displaying stained and grown cholangiocytes for different times: 24 h (blue), 48 h (orange) and 72 h (purple). Non-stained (white) and newly stained (red) cholangiocytes are used as controls. As cells divide, lower staining intensisty is detected in each cell division.

M.9. Cell death appraisal

Apoptosis-induced cell death was evaluated in normal and cystic human cholangiocytes by two different approaches.

M.9.1. Annexin V and TO-PRO-3 staining

Early and late stage of apoptosis were identified by flow cytometry using a dual fluorescent staining method with FITC Annexin V (BioLegend) and TO-PRO™-3 iodide (Invitrogen – Thermo Fisher Scientific). FITC labeled Annexin V fluorescent dye (Ex 494nm/Em 520nm; green) has a strong and specific Ca^{2+}-dependent affinity for the phosphatidylserine residues translocated to the outer leaflet of the plasma membrane during early apoptosis (**Figure M.2**),[201-203] while TO-PRO™-3 iodide fluorescent dye (Ex 642nm/Em 661nm; red) has a

very strong affinity for dsDNA upon loss of membrane and nuclear integrity, indicating late apoptosis (**Figure M.2**).[201, 203] Briefly, $3.5x10^4$ human cholangiocytes (i.e., NHC, ADPKD and ADPLD) per well were seeded in a thin collagen-coated 24-well plate with fully-supplemented DMEM/F-12 medium (**Table M.2**). Once the cells were attached, an overnight starvation in quiescent medium was accomplished and then, the cells were treated with 5mM 4-PBA (Sigma-Aldrich) and/or 2.4µM TM (Sigma-Aldrich) for 48 hours. In parallel, a positive cell death control was included by adding 2µg/mL of puromycin dihydrochloride (Sigma-Aldrich). Afterwards, the cells were trypsinized and centrifuged at 1,500rpm for 5 minutes at room temperature, discarding then the cell supernatant. Cholangiocytes were washed once with cold DPBS 1X (Gibco – Thermo Fisher Scientific) and resuspended in 1:10 dH_2O-diluted Annexin V Binding Buffer (BioLegend) at a concentration of $1x10^6$cells/mL. Next, the cells were placed in a U-bottom 96-well plate (Falcon) and stained with 100µg/mL of FITC Annexin V fluorescent dye (5µL/well) for 15 minutes at room temperature in the dark. Thereafter, cholangiocytes were incubated in darkness for 15 minutes on ice with 1µM TO-PRO™-3 iodide fluorescent dye (5µL/well) and, subsequently, diluted with Annexin V Binding Buffer at the recommended concentration, according to the flow cytometer manufacturer´s instructions. Finally, the differentially stained cell populations were distinguished, setting up the appropriate filters (525/30nm and 661/15nm) in the *Guava Easycyte 8HT* flow-cytometer (Merck Millipore). The apoptotic rate of human cholangiocytes was analyzed with the Incyte™ 3.1 software (Merck Millipore). Single stained samples were used to establish the levels of fluorescence compensation. Results are shown as relative to vehicle-treated cells.

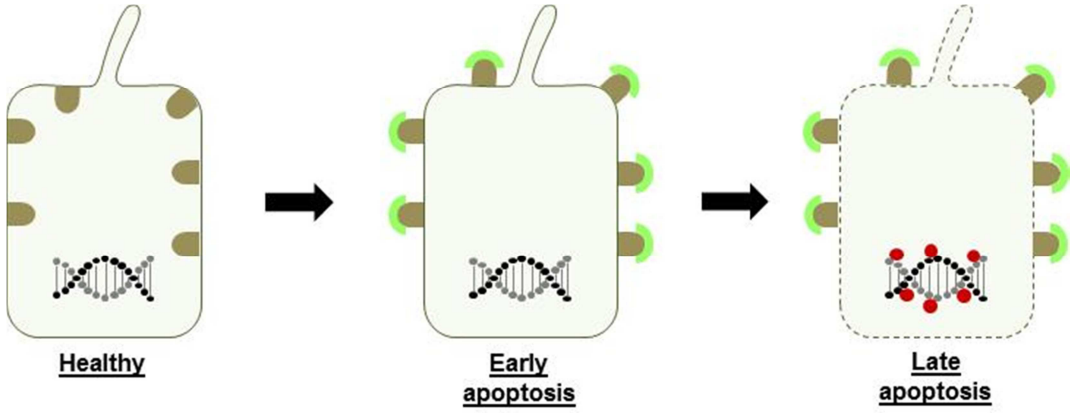

Figure M.2. Overview of cellular apoptosis detection method. Phosphatidylserine residues (brown) exposed at the plasma membrane surface serve as targets for the binding of FITC Annexin V fluorescent dye (green) [Early apoptosis], while TO-POR®-3 iodide (red) staining occurs when the membrane integrity is disturbed and the dsDNA becomes accessible to the fluorescent dye [Late apoptosis].

M.9.2. Caspase activity

The Caspase-Glo® 3/7 assay (Promega Corporation) was accomplished to quantify the activity of caspase 3 and caspase 7, the major executioners of both extrinsic and intrinsic apoptosis pathways. In order to do so, $2.5x10^3$ human cholangiocytes per well were seeded in a thin collagen-coated 96-well plate (Corning) with fully-supplemented DMEM/F-12 medium (**Table M.2**). Afterwards, cells were starved with quiescent medium overnight and treated with 5mM 4-PBA (Sigma-Aldrich) for 48 hours. Then, 75µL of the luminogenic caspase 3/7 substrate were added to each well and shook for 30 seconds at 400rpm in the *Tehtnica Vibromix 301EVT* orbital shaker (Labolan). After 30 minutes of incubation at room temperature in darkness, the luminescence intensity was measured in the *PHERAstar* luminometer (BMG Labtech) plate reader. Results are displayed as percentage relative to the vehicle-treated cells which is set as 100% of expression.

M.10. Proteasome activity

The proteasomal chymotrypsin-like activity of the 20S core particle sub-complex (20S proteasome) was assessed from whole cell protein extracts and rat liver tissue samples, using the Proteasome Activity Assay Kit (Abnova). Briefly, 5µg of the extracted and quantified protein as previously mentioned (see sections M.6.1, M.6.2 and M.6.3), were added to a Nunc™ F96 MicroWell™ White

Polystyrene Plate (Thermo Fisher Scientific) and a final volume of 50µL per well was adjusted with the Proteasome Assay Buffer. Of note, a paired well of each sample was treated with 1µL of the proteasome inhibitor MG132, completely suppressing the proteolytic activity of the proteasome and differentiating it from other protease activity present in the sample. Simultaneously, a calibration curve was prepared [ranging from 0 to 100pmol of 7-amino-4-methylcoumarin (AMC) standard] in the same plate. Likewise, Jurkat cell lysate and the vehicle solution (i.e., NP40 Cell Lysis Buffer) were included as positive control and blank sample, respectively. Afterwards, 1µL of the AMC-tagged peptide substrate (i.e., Succ-LLVY-AMC) was added to each well, being proteolytically cleaved and the AMC released. Finally, the kinetics of fluorescence emitted by the free AMC (Ex 350nm/Em 440nm) was measured at 5 minutes intervals for a total of 120 minutes in the *Infinite® 200 PRO* plate reader (Tecan) by setting up the suitable filters (Ex 360/35; Em 450/10) with the i-control™ Microplate Reader Software (Tecan). Importantly, during the measurement process the plate was kept at 37ºC in darkness. Results are shown as percentage relative to the control cell line or to vehicle-treated cells.

M.11. Statistical data analysis

Results were statistically analyzed using the GraphPad Prism 6.01 software (GraphPad Software). Once the normal distribution of the data was assessed with Shapiro-Wilk test, the statistical difference between two data sets was determined using the parametric unpaired Student´s T test or the non-parametric Mann-Whitney test, depending on the result of the normality test. On the other hand, when more than two data sets were compared one-way analysis of variance (ANOVA) with Tukey´s *post hoc* test or Kruskal-Wallis with Dunn´s *post hoc* test were implemented for the analysis of normally and non-normally distributed data, respectively. Data are indicated as mean ± standard error of the mean (SEM). Significant differences between comparatives were considered when $p<0.05$.

Results

R.1. Characterization of ER stress in PLD

R.1.1. UPR-related factors are overexpressed in human PLD biopsies and cystic cholangiocyte cultures

First, the mRNA expression levels of the main UPR sensors (i.e., *ATF6*, *PERK* and *IRE1α*) and effectors (i.e., *CHOP*, *GRP78* and *XBP1*) were analyzed in a cohort of healthy human liver tissue samples (n=14) and gallbladder tissue specimens (n=14), and in cystic wall biopsies of patients with ADPLD (n=16) (**Table M.1**). Of note, when cystic samples were compared with healthy liver tissue, we only observed a marked increase in the PERK signaling pathway (i.e., mRNA expression of *PERK* and *CHOP*). However, when a more suitable control group as healthy gallbladder tissue was employed,[204] a significant upregulation in the mRNA levels of the three ER stress sensors (i.e., *ATF6*, *PERK* and *IRE1α*) and some of the downstream effectors (i.e., *CHOP*, *GRP78* and *XBP1*), was detected (**Figure R.1A**). Additionally, NHC were also included in the analysis, since they constitute a specific and pure cellular population of healthy cholangiocytes, displaying expression similarities with the gallbladder group and thus, detecting significant differences with PLD tissue samples (**Figure R.1A**). Likewise, increased transcript levels of the UPR factors (i.e., sensors and effectors) were also found in primary cultures of cystic human cholangiocytes (i.e., ADPKD and ADPLD), as compared to NHC (**Figure R.1B**).

These data pinpoint that cystic samples (i.e., tissue and cells) from human ADPKD and ADPLD phenotypes are characterized by ER proteostasis disturbance and concomitant ER stress, as revealed by the activation of the UPR signaling system.

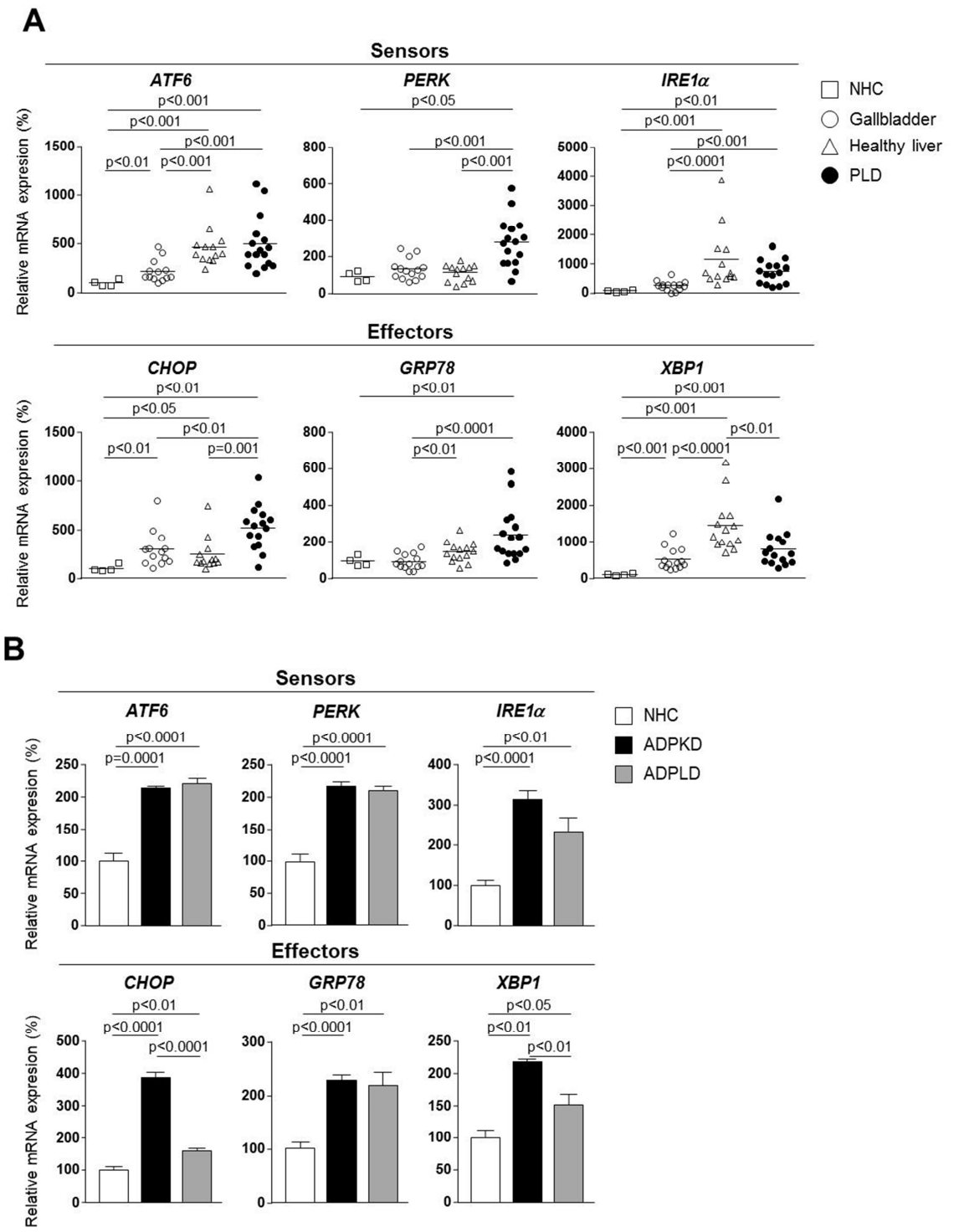

Figure R.1. Assessment of the UPR signaling in human polycystic disease. mRNA expression analysis of the main UPR sensors and effectors in (**A**) healthy controls [liver (n=14), gallbladder tissue (n=14) and NHC (n=4) samples] and ADPLD cystic wall tissue (n=16), as well as, in (**B**) normal (n=6) and cystic (n=6) human cholangiocytes in culture. (**A-B**) mRNA expression values are normalized to NHC (100%). **Abbrev:** ADPKD, autosomal dominant polycystic kidney disease; ADPLD, autosomal dominant polycystic liver disease; ATF6, activating transcription factor 6; CHOP, C/EBP-homologous protein; GRP78, 78-kDa glucose-related protein; IRE1α, inositol-requiring enzyme 1 alpha; NHC, normal human cholangiocytes; PERK, pancreatic endoplasmic reticulum kinase; XBP1, x-box binding protein 1.

R.1.2. Upregulation of the UPR-related factors in rat PLD liver tissue and cystic cholangiocytes in culture

In addition to analyze the UPR signal activation in the dominant traits of the disease (i.e., ADPKD and ADPLD phenotypes), the transcript levels of the main UPR-related sensors and effectors were also determined in an experimental model of ARPKD. As in human samples, the ARPKD phenotype was also associated with an ER stress situation and the concomitant upregulation of the main UPR factors. In this regard, the mRNA expression levels of *Atf6*, *Perk*, *Chop* and *Grp78* were significantly increased in liver tissue samples obtained from PCK rats (i.e., animal model of ARPKD), in comparison to the expression levels observed in liver tissue samples from wild-type rats (**Figure R.2A**). Despite no significant differences were found in the Ire1α signalling pathway between healthy and diseased liver tissue, the transcript levels of both *Ire1α* and *Xbp1* were also mildly increased (**Figure R.2A**). Likewise, ER stress was also evidenced in cystic cholangiocytes isolated from PCK rats. As shown in **Figure R.2B**, except for *Atf6*, the transcript levels of the UPR sensors and effectors were found increased in cystic rat cholangiocytes (i.e., PCK), when compared to healthy ones (**Figure R.2B**).

Hence, the activation of the UPR signaling system also indicates the presence of aberrant ER proteostasis and ER stress in the recessive inheritance traits of PLD.

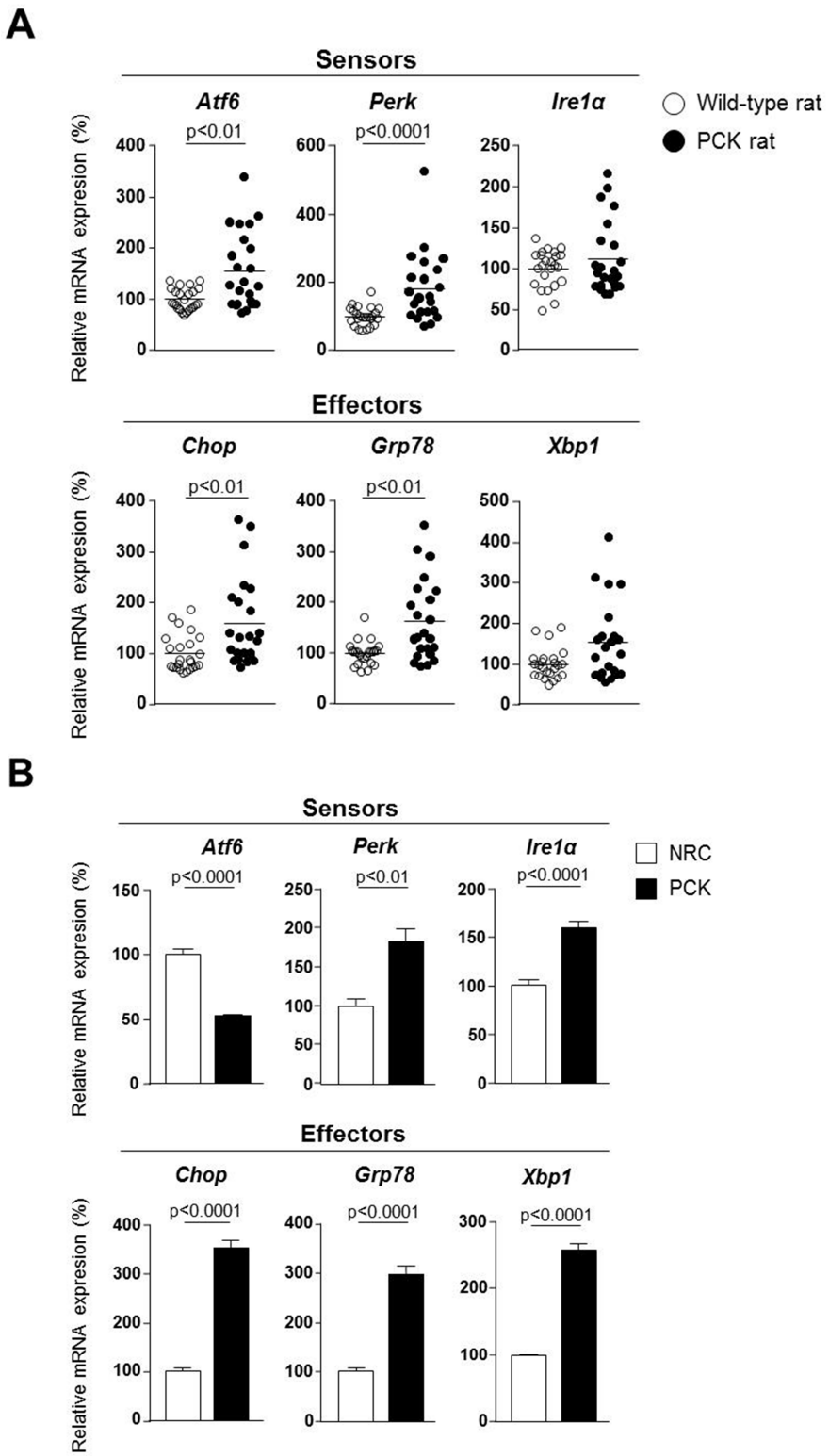

Figure R.2. Analysis of the UPR signaling in polycystic experimental murine models of ARPKD. mRNA expression measurement of the main UPR sensors and effectors in (**A**) wild-type (n=24) and PCK rats (n=23), as well as, in (**B**) normal (n=6) and cystic (n=6) rat cholangiocytes in culture. mRNA expression values are normalized (**A**) to the group of wild-type rats (100%) and (**B**) NRC (100%). **Abbrev:** ATF6, activating transcription factor 6; CHOP, C/EBP-homologous protein; GRP78, 78-kDa glucose-related protein; IRE1α, inositol-requiring enzyme 1 alpha; NRC, normal rat cholangiocytes; PCK, cystic rat cholangiocytes; PERK, pancreatic endoplasmic reticulum kinase; XBP1, x-box binding protein 1.

R.1.3. Intersecting role of ER stress and ubiquitin-proteasome system in PLD

The activation of the UPR boosts the ERAD-mediated clearance of structurally aberrant proteins accumulated in the ER lumen.[205] Interestingly, an integrated component of this degradative pathway is the UPS,[206, 207] which ultimately degrades the terminally misfolded proteins retrotranslocated from the ER,[142, 206] in order to alleviate the burden of structurally aberrant proteins accumulated in this organelle and, consequently, the ER stress.[207] In this regard, the chymotrypsin-like protease activity of the 20S proteasome, the structure which harbors the mechanism for ATP-dependent protein degradation,[208-210] was evaluated upon basal and pathological conditions using a fluorescence-based assay. Notably, the 20S proteasome was significantly hyperactivated in human cystic cholangiocytes (i.e., ADPKD and ADPLD), as compared to NHC (**Figure R.3**).

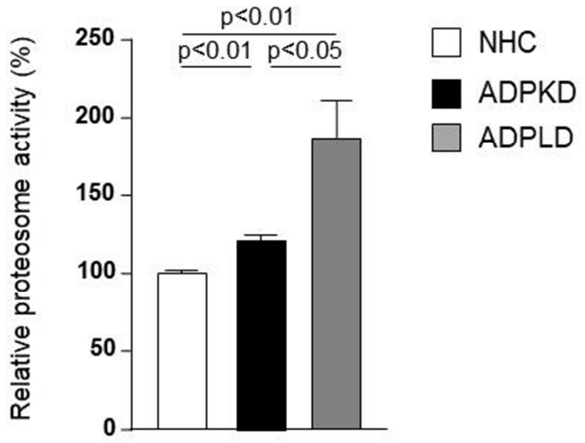

Figure R.3. UPS-mediated degradation of protein overload in the ER of human cholangiocytes in culture. AMC fluorescence intensity in NHC, ADPKD and ADPLD cholangiocytes (n=4-5) in basal conditions. The AMC fluorescence intensity detected with this method is proportional to the chymotrypsin-like protease activity of the 20S proteasome. The values of the AMC fluorescence signal are normalized to NHC (100%). **Abbrev:** ADPKD, autosomal dominant polycystic kidney disease; ADPLD, autosomal dominant polycystic liver disease; AMC, 7-amino-4-methylcoumarin; NHC, normal human cholangiocytes.

Furthermore, this adaptive mechanism was also found to be hyperactivated in liver tissue samples obtained from PCK rats, as compared to wild-type rats (**Figure R.4**).

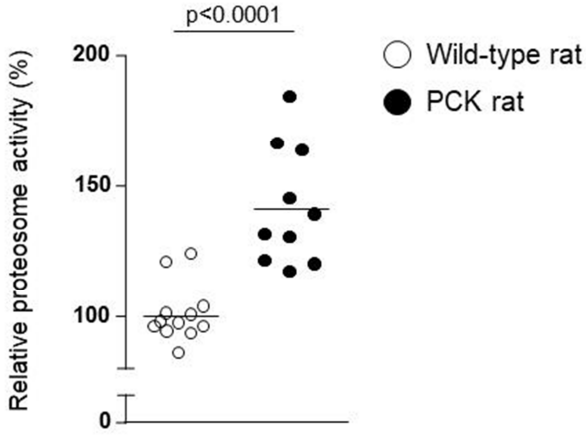

Figure R.4. UPS-mediated degradation of ER protein overload in rat liver tissue. AMC fluorescence intensity in both wild-type (n=12) and PCK rat liver biopsies (n=10) in basal conditions. The AMC fluorescence intensity detected with this method is proportional to the chymotrypsin-like protease activity of the 20S proteasome. The values of the AMC fluorescence signal are normalized to the group of wild-type rats (100%). **Abbrev**: AMC, 7-amino-4-methylcoumarin.

These data suggest that the 20S proteasome is able to modulate its proteolytic activity, in order to counteract an increased demand on protein degradation and thus, to abolish the ER stress by restoring the protein homeostasis within the ER lumen.

R.1.4. Cystic cholangiocytes exhibit marked ER enlargement

Considering that the overexpression of the main UPR factors (**Figure R.1 and R.2**) and the hyperactivation of the 20S proteasome (**Figure R.3 and Figure R.4**) previously identified suggest aberrant ER proteostasis, protein accumulation within the lumen of this organelle and concomitant ER stress, the morphological and ultrastructural features of the ER were further analysed. In this regard, TEM micrographs from primary cultures of normal and cystic cholangiocytes were captured. As expected, normal cholangiocytes isolated from both, healthy human individuals (i.e., NHC) and wild-type rats (i.e., NRC), exhibited a typical narrow ER lumen (**Figure R.5A**). On the other hand, under pathological conditions (i.e., ADPKD, ADPLD and PCK cholangiocytes), a pronounced dilatation of the ER lumen was detected (**Figure R.5A**), being this

phenotype a well-documented adaptive morphological mechanism linked to ER stress management.[118, 152] Accordingly, the total ER surface area underwent a significant 1.79, 1.47 and 1.62-fold increase in ADPKD, ADPLD and PCK cholangiocytes respectively, compared to the corresponding controls (**Figure R.5B**).

Therefore, these data support the concept that un/misfolded proteins are accumulated within the ER lumen of cystic cholangiocytes, triggering ER stress and morphological alterations in this organelle.

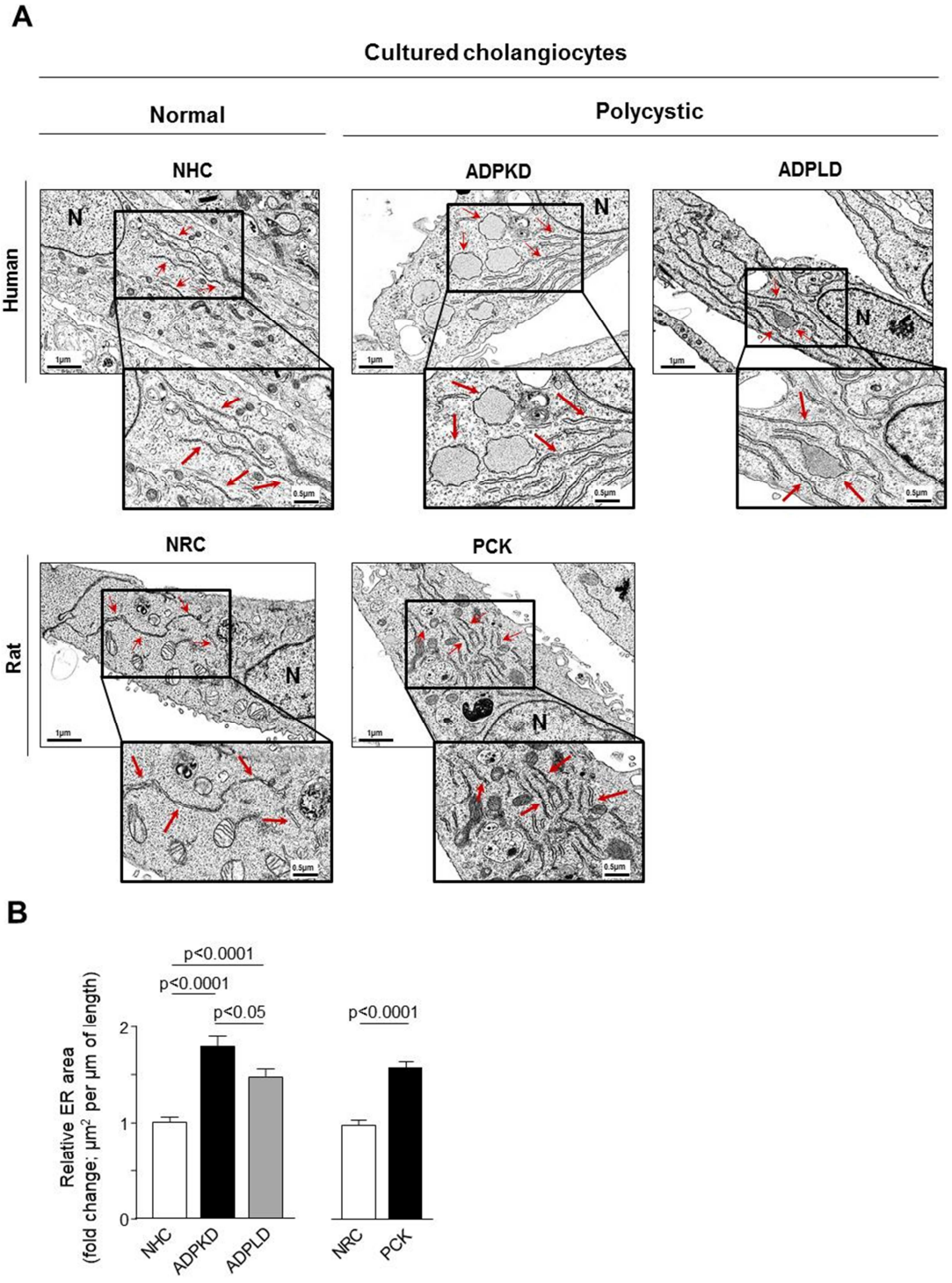

Figure R.5. Morphological analysis of the ER in human and rat cholangiocytes in culture. (**A**) Representative ultrastructural micrographs captured by TEM, showing the ER morphology (red arrows) in primary cultures of normal and cystic cholangiocytes isolated from humans and rats. (**B**) Quantification of the ER lumen surface area in both human [NHC (n=47), ADPKD (n=28) and ADPLD (n=28)] and rat [NRC (n=49) and PCK (n=52)] cholangiocytes. ER area values are normalized to NHC and NRC. Scale bar in (**A**) indicates 1µm for the overview micrographs at 20kx and 0.5µm for the zoomed (40kx magnification) quadrants. **Abbrev:** ADPKD, autosomal dominant polycystic kidney disease; ADPLD, autosomal dominant polycystic liver disease; ER, endoplasmic reticulum; NHC, normal human cholangiocytes; NRC, normal rat cholangiocytes; PCK, cystic rat cholangiocytes.

R.1.5. Adaptive mechanisms elude cell death

Even though signs associated with ER stress (i.e., UPR activation, 20S proteasome hyperactivity and ER lumen enlargement) were identified in human ADPKD and ADPLD cholangiocytes in culture, no significant differences in the apoptotic rate between cystic cholangiocytes and NHC were evidenced (**Figure R.6**). This suggests that the three aforementioned adaptive mechanisms cooperate in order to restore proteostasis within the ER, preventing a sustained ER stress condition and its deleterious effects.

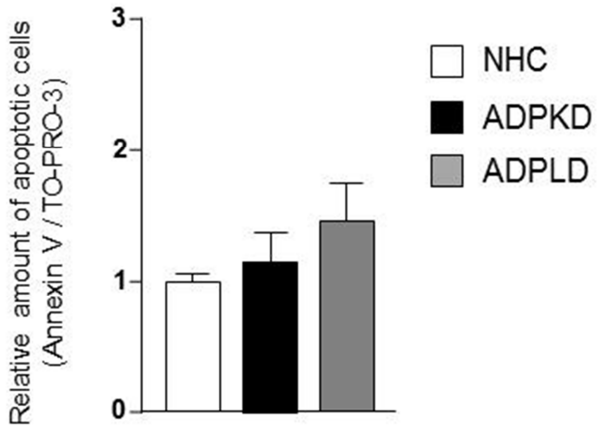

Figure R.6. Basal apoptosis rate in normal and cystic human cholangiocytes. NHC, ADPKD and ADPLD cholangiocytes were dually stained with Annexin V and TO-PRO-3 24 hours after seeding them (n=6). The apoptotic rate is normalized to NHC. **Abbrev:** ADPKD, autosomal dominant polycystic kidney disease; ADPLD, autosomal dominant polycystic liver disease; NHC, normal human cholangiocytes.

R.2. Modulation of the protein-folding burden

To gain further insights into the involvement and the impact of ER stress in the pathogenesis of PLD, we focused on elucidating the effects derived from the regulation of the ER misfolded protein cargo. Thus, the outcome of the treatment with both an ER stress inhibitor (i.e., 4-PBA; 5mM) and an ER stress inducer (i.e., TM; 2.4µM) were analyzed.

R.2.1. Modulation of ER stress rules the UPR signaling and the 20S proteasome activity in vitro

As the UPR appears to be the onset of the ER stress compensatory response, the mRNA expression levels of the sensors and the effectors of this integrated intracellular signaling system was analyzed in the presence and/or absence of the aforementioned protein folding modulators. Curiously, the *in vitro* treatment of normal and cystic human cholangiocytes with 4-PBA and TM exhibited heterogeneous effects on the transcript levels of the UPR sensors (i.e., *ATF6*, *PERK* and *IRE1α*) (**Figure R.7A**), whereas the expression of the effectors (i.e., *CHOP*, *GRP78* and *XBP1*) was more finely regulated (**Figure R.7B**). While the mRNA levels of *IRE1α* were uniformly induced by 4-PBA and TM in both normal and cystic cholangiocytes, the expression of the other two UPR sensors remained unaltered in NHC and ADPKD cholangiocytes. On the other hand, TM incubation caused a remarkable induction of the transcript levels of the UPR effectors (i.e., *CHOP*, *GRP78* and *XBP1*) in NHC, ADPKD and ADPLD cholangiocytes, which was notably attenuated by 4-PBA when both compounds were administered in combination (**Figure R.7B**). Moreover, treatment with 4-PBA significantly reduced the expression of *CHOP*, *GRP78* and *XBP1* in ADPKD, but not in ADPLD cholangiocytes (**Figure R.7B**). Furthermore, the mRNA levels of *GRP78* and *XBP1* were greatly diminished in NHC after the administration of this chemical chaperone (**Figure R.7B**). This difference between NHC and ADPKD cholangiocytes induced by 4-PBA could be attributed to the prominent ER stress condition of the cystic cholangiocytes at basal level, further highlighting the effects of this chemical chaperone.

A

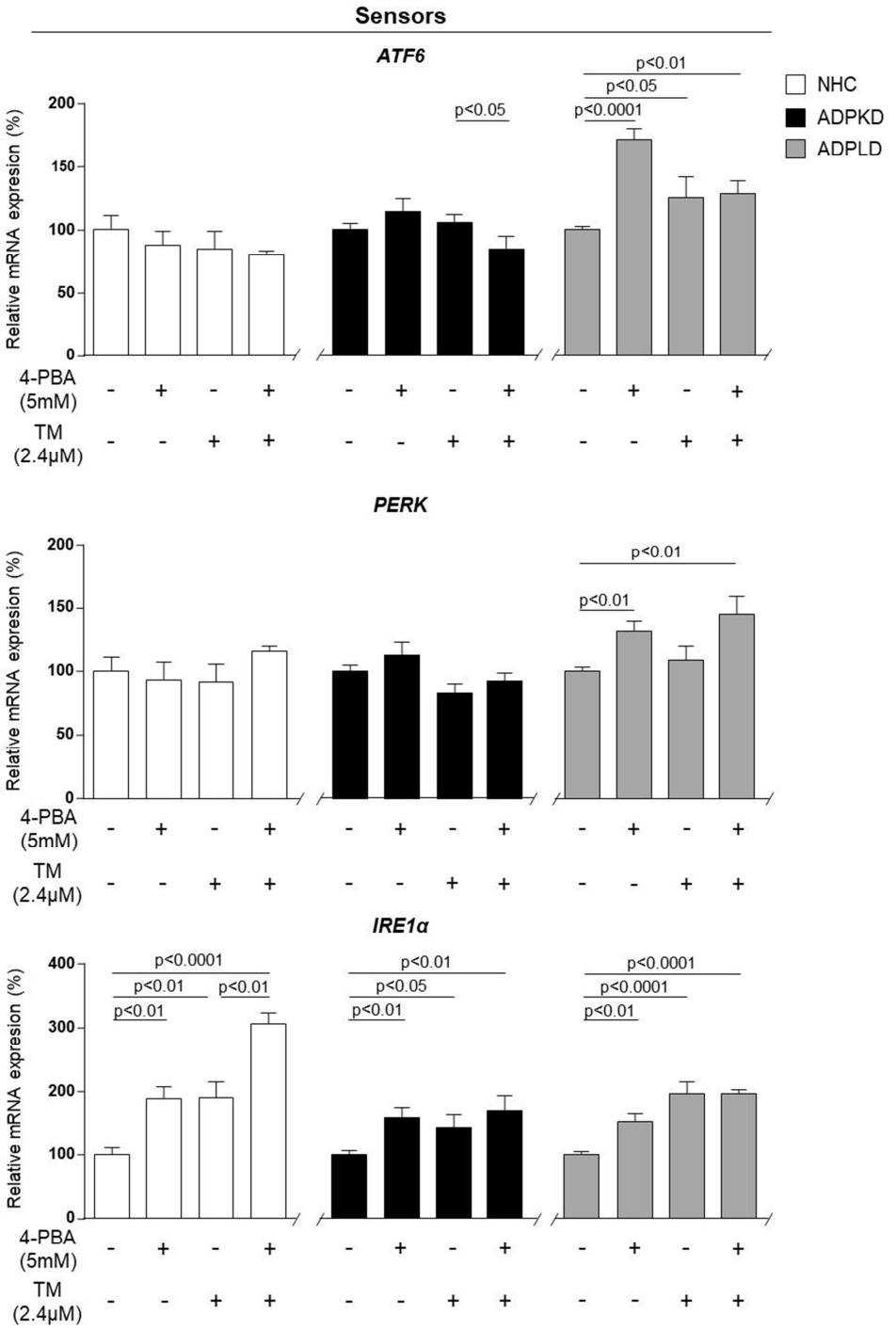
Sensors
ATF6
PERK
IRE1α
NHC
ADPKD
ADPLD
Relative mRNA expresion (%)
4-PBA (5mM)
TM (2.4μM)
p<0.05
p<0.01
p<0.05
p<0.0001
p<0.0001
p<0.01
p<0.05
p<0.01
p<0.0001
p<0.0001
p<0.01

B

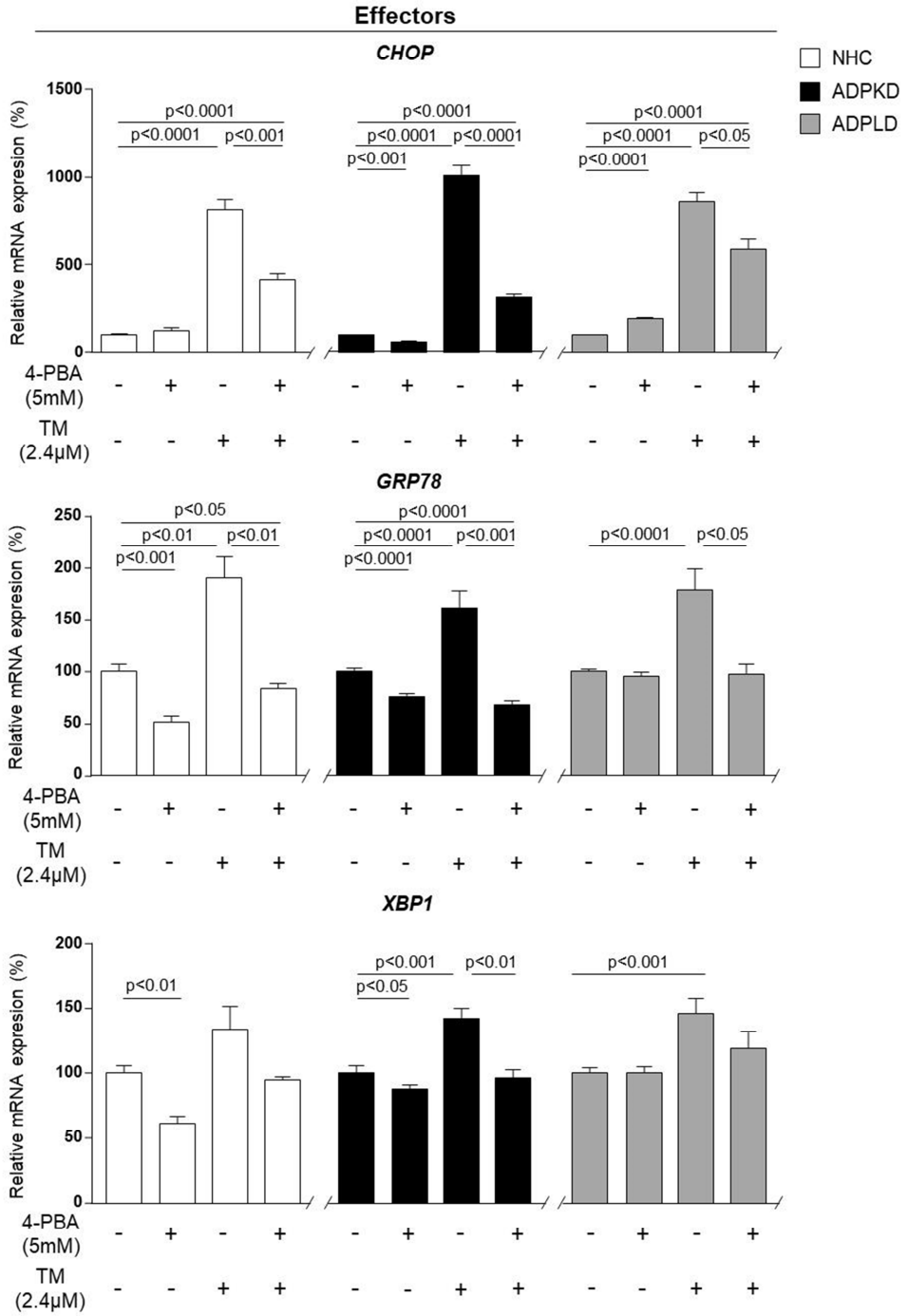

Figure R.7. Chemical modulation of the UPR signaling system in primary cultures of human cholangiocytes. mRNA expression levels of the UPR (**A**) sensors and (**B**) effectors in normal (n=5) and cystic (n=4-5) human cholangiocytes after 24 hours of treatment with 4-PBA, TM or both compounds in combination. Each treated condition was compared with the corresponding vehicle-treated control. **Abbrev:** 4-PBA, 4-phenylbutyric acid; ADPKD, autosomal dominant polycystic kidney disease; ADPLD, autosomal dominant polycystic liver disease; ATF6, activating transcription factor 6; CHOP, C/EBP-homologous protein; GRP78, 78-kDa glucose-related protein; IRE1α, inositol-requiring enzyme 1 alpha; NHC, normal human cholangiocytes; PERK, pancreatic endoplasmic reticulum kinase; TM, tunicamycin; XBP1, x-box binding protein 1.

In addition and as previously mentioned, the cellular protein degradation machinery is intimately linked to the UPR, cooperating both adaptive mechanisms in order to restore ER proteostasis and resolve ER stress. For this reason, we also analyzed the activity of the 20S proteasome after the treatment with the protein folding inducer 4-PBA. According to the lessening effect of the 4-PBA on the UPR signaling system (**Figure R.7**), we observed that the chymotypsin-like protease activity of the 20S proteasome was also significantly reduced by this chemical chaperone in normal and cystic human cholangiocytes (**Figure R.8**). Further supporting the concept that 4-PBA modulates the activity of this sub-complex of the UPS and attenuates ER stress levels, probably by contributing with the improvement of the ER folding capacity.

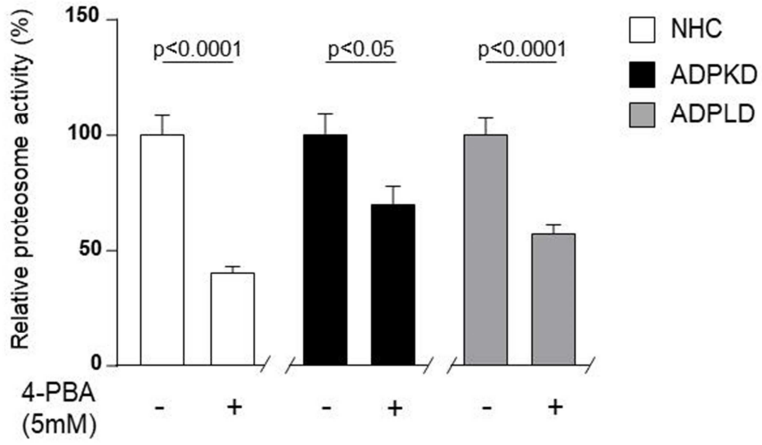

Figure R.8. 4-PBA-mediated modulation of the 20S proteasome activity in human cholangiocytes cultures. AMC fluorescence intensity in NHC, ADPKD and ADPLD cholangiocytes treated with 4-PBA (5mM) for 48 hours (n=6 per cell line). The AMC fluorescence intensity detected is proportional to the chymotrypsin-like protease activity of the 20S proteasome. Each treated condition was compared with the corresponding vehicle-treated control. **Abbrev:** 4-PBA, 4-phenylbutyric acid; ADPKD, autosomal dominant polycystic kidney disease; ADPLD, autosomal dominant polycystic liver disease; AMC, 7-amino-4-methylcoumarin; NHC, normal human cholangiocytes.

These results suggest that the UPR is a modular signaling system, which ultimately adapts both the expression levels of its main sensors and effectors, as well as, the activity of the 20S proteasome according to the un/misfolded protein burden, and therefore to the levels of ER stress.

R.2.2. Alleviation of ER stress diminishes cholangiocyte proliferation

Notably, our research group has previously reported that the aberrant hyperproliferative phenotype of cystic cholangiocytes, which is triggered by intracellular abnormalities in Ca^{2+} and cAMP levels, is responsible for hepatic cystogenesis.[82, 99] Thus, the involvement of ER stress in the proliferation rate of normal and cystic human cholangiocytes in culture was assessed after 4-PBA treatment. Interestingly, administration of 4-PBA significantly diminished the proliferation of ADPKD and ADPLD cholangiocytes (32% and 24%, respectively), compared to the vehicle-treated condition (**Figure R.9A**). Furthermore, we also noticed that 4-PBA also decreased the proliferation rate of NHC (**Figure R.9A**). In line with this, the phosphorylation levels of the mitogen-activated protein kinases (MAPK) ERK½ were markedly inhibited in human cystic cholangiocytes in the presence of this chemical chaperone (**Figure R.9B**). Hence, a significant reduction of the p-ERK½/ERK½ ratio was evidenced in ADPKD cholangiocytes treated with 4-PBA, when compared to the untreated ones (**Figure R.9B**). We conclude that the assistance on protein folding and the attenuation of ER stress levels induced by 4-PBA have an anti-proliferative impact on human cholangiocytes in culture, which is mediated by an ERK½-dependent mechanism.

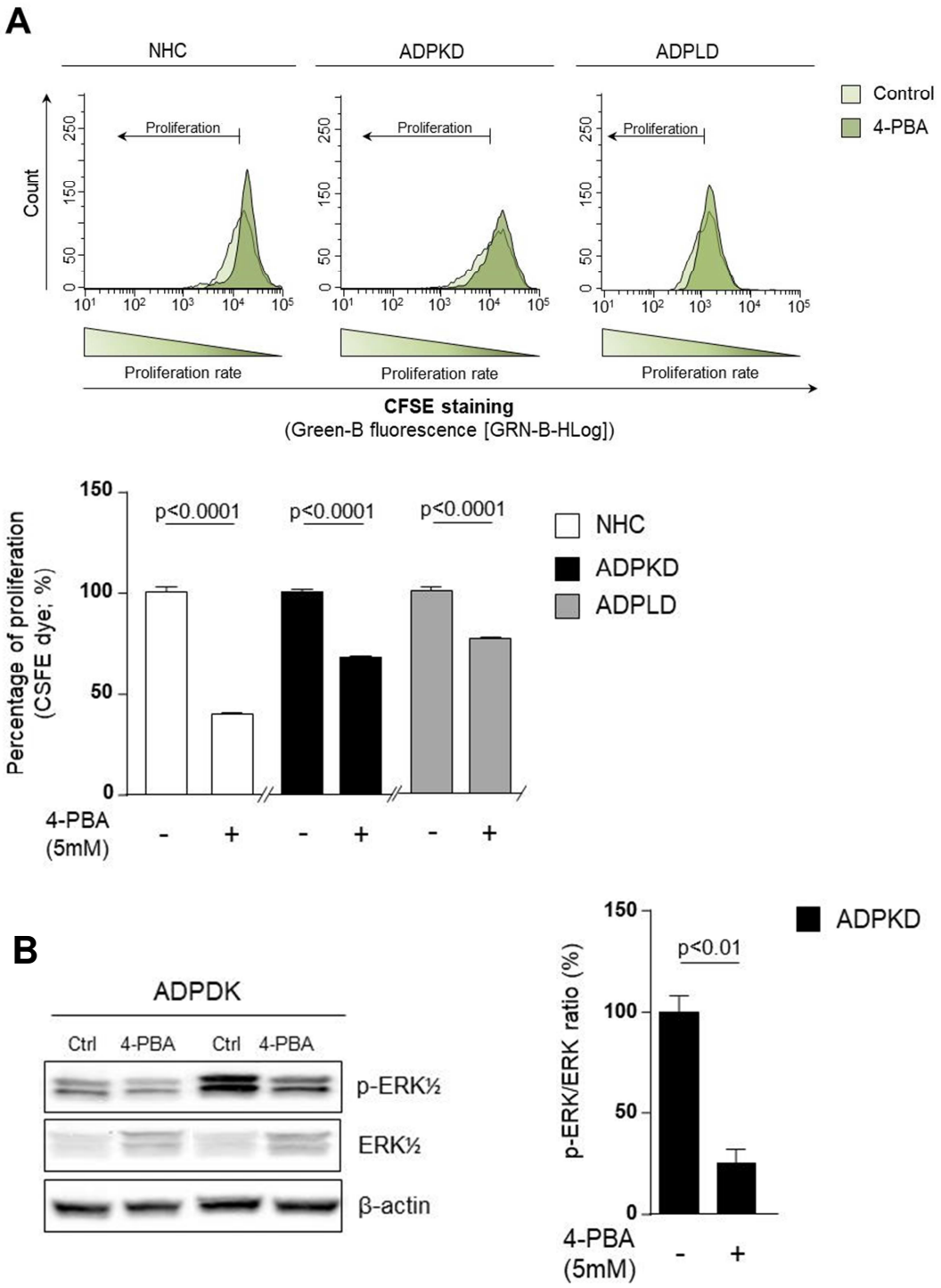

Figure R.9. Effect of 4-PBA on human cholangiocyte proliferation. (**A**) Representative histograms and quantification of the CFSE signal intensity in NHC, ADPKD and ADPLD cholangiocytes after treatment with 4-PBA or vehicle for 48 hours. (**B**) Phosphorylation of ERK½ was determined by immunoblot. (**A-B**) Each treated condition was compared with the corresponding vehicle-treated control. **Abbrev:** 4-PBA, 4-phenylbutyric acid; ADPKD, autosomal dominant polycystic kidney disease; ADPLD, autosomal dominant polycystic liver disease; CFSE, 5(6)-carboxyfluorescein N-hydroxysuccinimidyl ester; ERK½, extracellular signal-regulated kinases ½; NHC, normal human cholangiocytes; p-ERK½, phospho-extracellular signal-regulated kinases ½

R.2.3. ER stress controls cell fate

The aberrant proliferation of cystic cholangiocytes exerts a pivotal effect in hepatic cystogenesis and disease progression, albeit cell death also plays a key role in cystic growth.[211] In this regard, the intensity and duration of the ER stress stimuli govern cell fate decisions between survival and death.[142]

For this reason, we focused on modulating the ER stress levels by increasing or decreasing the burden of un/misfolded proteins within this intracellular organelle, in order to elucidate the response of human cholangiocytes. Hence, the apoptotic rate of NHC, ADPKD and ADPLD cholangiocytes was determined in the presence and/or absence of ER stress modulators (i.e., 4-PBA and TM). Indeed, administration of 4-PBA significantly decreased cell death in both cystic human cholangiocyte cell lines (i.e., ADPKD and ADPLD), not observing a significant effect in the apoptotic rate of NHC (**Figure R.10**). This could indicate that the basal cell death noticed in NHC is not caused by ER stress and that the dose of 4-PBA used is not toxic for human cholangiocytes. By contrast, TM triggered cell death of both normal and cystic cholangiocytes (**Figure R.10**). Importantly, the pro-apoptotic effect of TM was completely abolished by 4-PBA in the three analyzed human cell lines, reaching similar or even lower apoptotic rates than that the observed in the vehicle-treated conditions (**Figure R.10**).

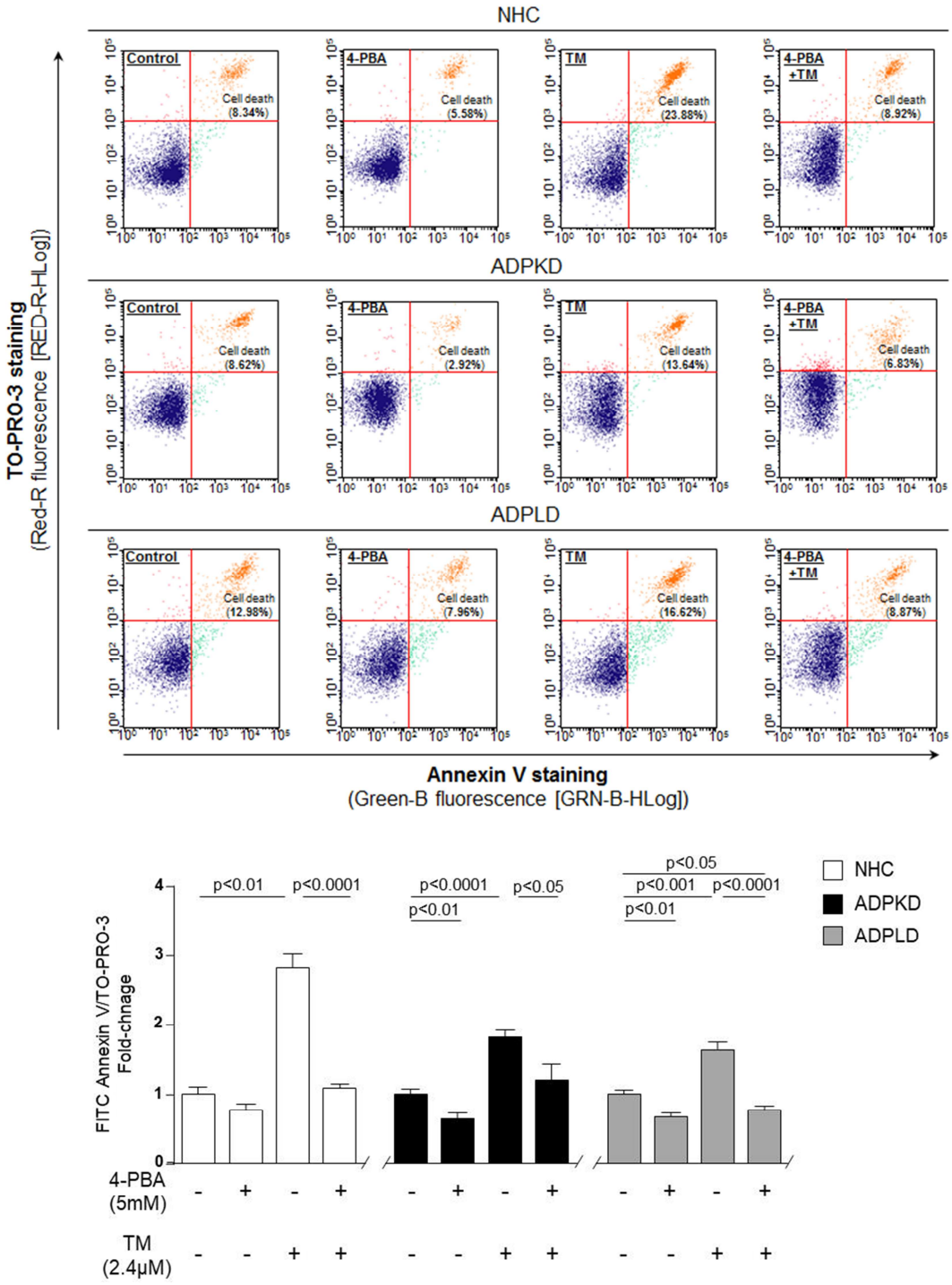

Figure R.10. Apoptotic rate of human cholangiocytes in the presence of 4-PBA and/or TM. Representative flow cytometry dot plots depicting normal and cystic human cholangiocytes dually stained with Annexin V and TO-PRO-3 (orange dots) after 48 hours of treatment with 4-PBA, TM and the combination of both compounds. Blue colored dots correspond to non-apoptotic cholangiocytes. The quantification of the amount of NHC (n=6), ADPKD (n=6) and APDLD (n=6) apoptotic cholangiocytes and significant differences between conditions are represented in the bar graph. Proliferation values are normalized to the corresponding vehicle-treated condition. **Abbrev:** 4-PBA, 4-phenylbutyric acid; ADPKD, autosomal dominant polycystic kidney disease; ADPLD, autosomal dominant polycystic liver disease; NHC, normal human cholangiocytes; TM, tunicamycin.

In consonance with these data, the cytosolic activity of caspase 3 and caspase 7, two key executioners of apoptosis, was significantly reduced in human cholangiocytes (i.e., NHC, ADPKD and ADPLD) after the treatment with 4-PBA, further substantiating the anti-apoptotic effect of this ER stress inhibitor. (**Figure R.11**). These data suggest that ER stress promotes cholangiocyte cell death via apoptosis, in which activated caspase 3/7 act as pivotal mediators.

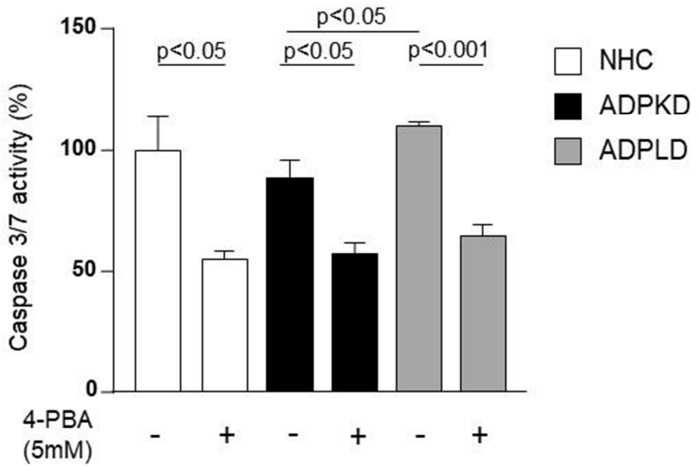

Figure R.11. Caspase 3/7 activity in human cholangiocytes in culture. Measurement of the luminescence signal of free aminoluciferin, a specific substrate of caspase 3/7, in normal (i.e., NHC) and cystic (i.e., ADPKD and ADPLD) human cholangiocytes treated with 4-PBA or with vehicle (n=4 per cell line). The luminescence intensity is proportional to caspase 3/7 activity. Caspase 3/7 activity values are normalized to NHC (100%). **Abbrev:** 4-PBA, 4-phenylbutyric acid; ADPKD, autosomal dominant polycystic kidney disease; ADPLD, autosomal dominant polycystic liver disease; NHC, normal human cholangiocytes.

Thus, we conclude that once the protein folding capacity is overhelmed, the ER stress levels become excessive and not tolerated by the human cholangiocytes in culture, leading to cellular apoptosis executed by caspase 3/7. Nevertheless, when protein folding is assisted with the chemical chaperone 4-PBA, human cholangiocytes endure the levels of ER stress preventing cell death and therefore, promoting cellular survival. Notably, cellular apoptosis could be averted by administration of 4-PBA in moderate and highly stressed cholangiocytes.

R.3. Involvement of ER stress in hepatic cystogenesis

R.3.1. ER proteostasis disturbance and stress contributes to hepatic cystogenesis in vivo

The contribution of ER stress to hepatic cystogenesis and, consequently, to PLD progression, as well as the potential therapeutic value of its modulation, was assessed in the PCK rat model. Thus, 100mM of 4-PBA and/or 0.02mg/kg of TM were administered to 8 weeks-old rats for 5 months.

In comparison to wild-type animals, control PCK rats develop a massive hepatomegaly, as revealed by a significant increase in both liver weight and volume (**Figure R.12A**). However, no difference in total body weight was detected between these two groups of animals, resulting in an increased liver/body weight ratio in the diseased rats (**Table R.1**). Moreover, some serological parameters related to cholestasis and liver injury [i.e., ALP, De Ritis ratio (AST/ALT), albumin and total protein] were significantly altered in control PCK rats compared to wild-type animals (**Table R.1**).

Furthermore, the potential therapeutic value of the aforementioned ER stress modulators was also evaluated in this *in vivo* experimental model. Of note, chronic administration of 4-PBA induced a significant reduction of liver weight and volume, almost reaching similar values to those observed in non-diseased rats (**Figure R.12A**). Likewise, treatment with 4-PBA normalized serological values of ALT, but it did not affect the levels of ALP and AST (**Table R.1**). Despite no changes in the liver area affected by cysts was detected, the volume of the hepatic cysts was significantly decreased as a result of this treatment (**Figure R.12B**). By contrast, chronic administration of TM to PCK rats did not result in any significant difference, neither in the weight nor in the volume of the liver tissue (**Figure R.12A**) or the total hepatic cystic volume (**Figure R.12B**), compared to the control PCK group, albeit a leaning towards increasing was associated with this treatment (**Figure R.12**). Nevertheless, a significant increase of the total liver/body weight ratio was observed in those animals treated with the ER stress inducer (~2%) (**Table R.1**). This is because a marked body weight loss was evidenced in the animals treated with TM (**Table R.1**), suggesting a deteriorated physical condition of the rats undergoing this treatment. Moreover, this tendency of TM to aggravate the disease progression

was reinforced by a significant increase in the hepatic cystic area (**Figure 12.B**), and a significant upregulation of the serological parameters of cholestasis and liver injury, including ALP, AST and De Ritis ratio (**Table R.1**) Noteworthy, 4-PBA was able to counteract TM-induced liver weight and volume increase (**Figure 12.A**), as well as to reduce cystic volume, when compared to rats treated with TM (**Figure 12.B**), indicating that 4-PBA inhibits TM-induced effects.

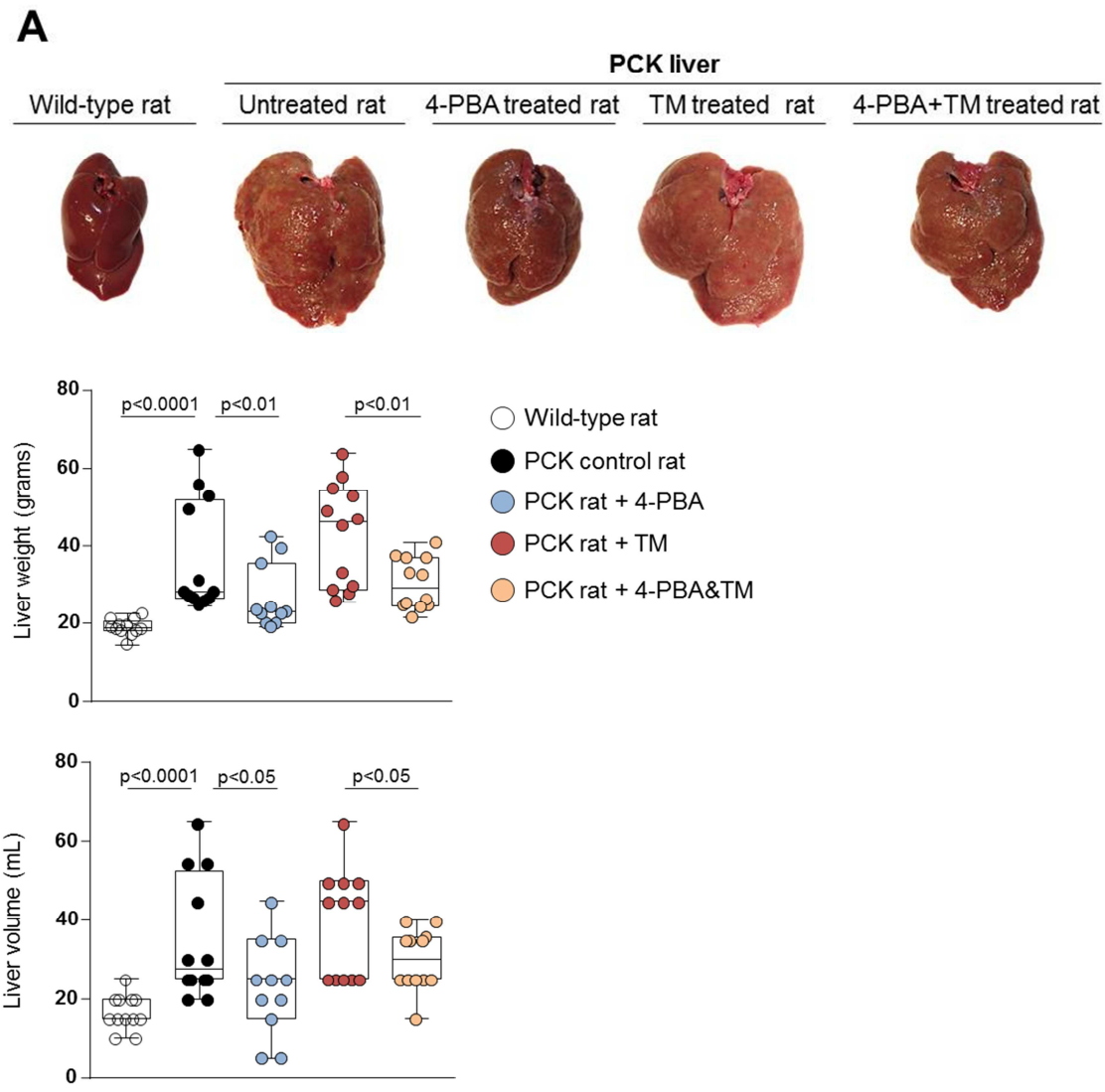

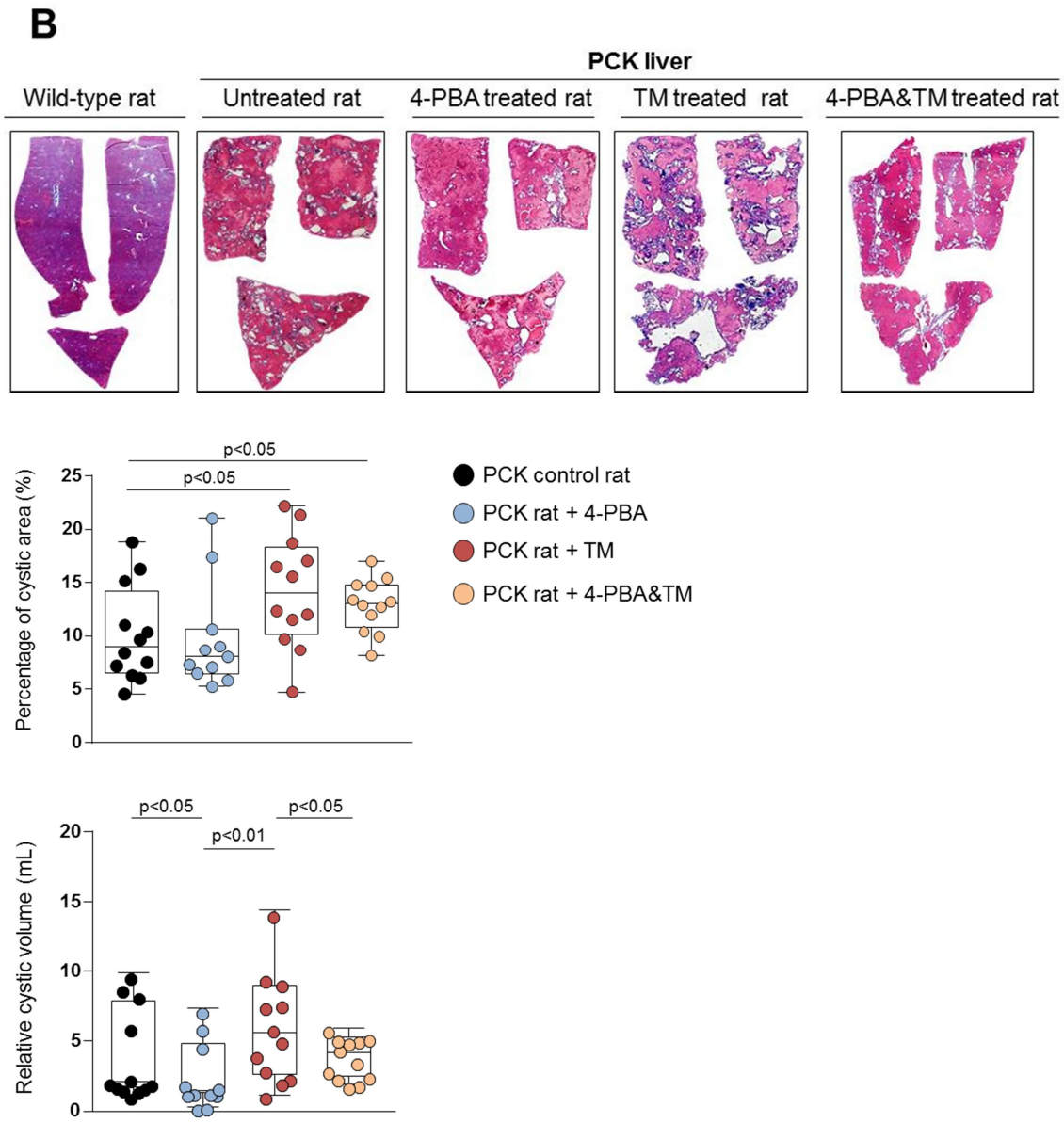

Figure R.12. Evaluation of PLD in PCK rats treated with 4-PBA and/or TM for 5 months. (**A**) Representative macroscopic photographs showing the status of the liver tissue and quantification of the weight and volume of this organ in wild-type and PCK rats, which are divided in control, 4-PBA (100mM), TM (0.02mg/kg) and 4-PBA&TM administered groups (n=12 per group). (**B**) Representative liver histological images stained with hematoxylin/eosin, and measurements of the total cystic area and the cystic volume in the aforementioned *in vivo* experimental groups (n=12 per group). **Abbrev:** 4-PBA, 4-phenylbutyric acid; TM, tunicamycin.

Table R.1. Liver biochemical and macroscopical determinations in normal and PCK rats

Parameters	A	B	C	D	E					
	Wild-type rats	PCK rats (non – treated)	PCK rats (4-PBA – treated)	PCK rats (TM – treated)	PCK rats (4-PBA&TM – treated)	*p* value (A *vs* B)	*p* value (B *vs* C)	*p* value (B *vs* D)	*p* value (B vs E)	*p* value (D *vs* E)
Body weight (g)	627.92 ± 13.81	626.96 ± 11.39	521.68 ± 15.58	549.63 ± 7.54	460.21 ± 22.62	0.8291	< 0.0001	< 0.0001	< 0.0001	0.0011
Liver/body weight (%)	3.01 ± 0.07	5.93 ± 0.75	5.20 ± 0.60	7.81 ± 0.70	6.89 ± 0.73	<0.0001	0.1643	0.0204	0.0915	0.3724
Bile flow (µl/min/g)	0.022 ± 0.0021	0.026 ± 0.0070	0.026 ± 0.0052	0.041 ± 0.0088	0.070 ± 0.020	0.9526	0.8198	0.1764	0.0708	0.4432
Alkaline phosphatase (U/L)	96.67 ± 6.98	209.33 ± 18.45	234.18 ± 22.12	323.00 ± 18.00	314.00 ± 18.17	<0.0001	0.2663	0.0006	0.0013	0.7283
Aspartate aminotransferase (U/L)	201.33 ± 25.81	228.33 ± 23.02	252.36 ± 16.68	381.67 ± 21.97	460.00 ± 45.35	0.4433	0.2664	<0.0001	<0.0001	0.1778
Alanine aminotransferase (U/L)	61.00 ± 4.52	47.33 ± 1.54	63.64 ± 4.05	62.67 ± 3.86	82.33 ± 6.54	0.0090	0.0009	0.0013	<0.0001	0.0167
De Ritis ratio (AST/ALT)	3.28 ± 0.31	4.98 ± 0.63	4.18 ± 0.46	6.41 ± 0.60	6.29 ± 0.99	0.0377	0.2032	0.0252	0.1066	0.3098
Albumin (g/L)	9.25 ± 0.24	5.84 ± 0.29	6.61 ± 0.37	7.04 ± 0.48	7.29 ± 0.60	<0.0001	0.0759	0.0433	0.0405	0.7444
Total protein (g/dL)	6.23 ± 0.12	5.71 ± 0.19	5.84 ± 0.07	6.14 ± 0.15	5.90 ± 0.16	0.0317	0.1640	0.0343	0.2977	0.2821

Abbrev: 4-PBA, 4-phenylbutyric acid; AST, aspartate aminotransferase; ALT, alanine aminotransferase; TM, tunicamycin; VS, versus.

As previously reported,[185, 186] increased expression of pro-fibrotic (i.e., *Col1a1*, *α-Sma*, *Ctgf*) and pro-inflammatory genes (i.e., *Il-6* and *Cxcl1*) was observed in the liver of PCK rats compared to wild-type animals (**Figure R.13**). Unfortunately, chronic administration of 4-PBA did not modulate the mRNA expression of any of the aforementioned pro-fibrotic (**Figure R.13A**) and pro-inflammatory genes (**Figure R.13B**). In line with this, TM-induced pro-fibrotic and pro-inflammatory gene expression was not significantly reduced after 4-PBA treatment in the liver of PCK rats (**Figure R.13A and R.13B**).

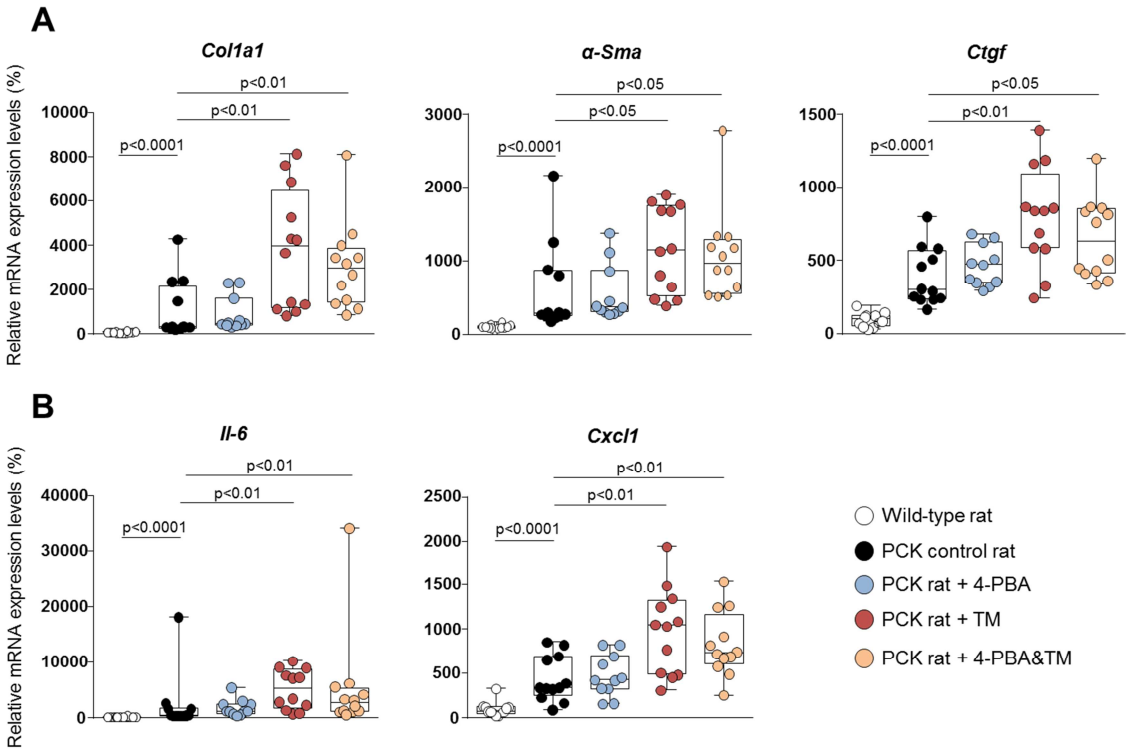

Figure R.13. Expression of pro-fibrotic and pro-inflammatory genes in rat liver tissue samples after the administration of 4-PBA and/or TM. mRNA expression levels of (**A**) pro-fibrotic (i.e., *Col1a1*, *α-Sma* and *Ctgf*) and (**B**) pro-inflammatory (i.e., *Il-6* and *Cxcl1*) genes in the liver of wild-type (n=12) and control PCK rats (n=12), as well as, in PCK rats chronically treated with 4-PBA (n=12) and/or TM (n=12). (**A-B**) mRNA expression values are normalized to the group of wild-type rats (100%). **Abbrev:** 4-PBA, 4-phenylbutyric acid; TM, tunicamycin.

On the other hand, considering that renal cystogenesis is another predominant pathological feature of this animal model, we also determined the renal function of the rats by analyzing different macroscopic and serological parameters. In this regard, the control group of PCK rats underwent a marked nephromegaly, displaying a significant increase in both kidney weigh and kidney/body weight ratio (**Table R.2**), as compared to the wild-type group. Likewise, serological levels of creatinine and urea (i.e., two commonly used indicators of the renal function) were increased in the diseased animals (**Table R.2**). Although chronic administration of 4-PBA did not exert any effect on the renal disease manifestations, the striking data were obtained from the TM-treated group, where a highly significant reduction in all the analyzed renal parameters were observed, when compared to the control group (**Table R.2**). In such a way, unlike the results observed in liver tissue, the administration of TM ameliorated kidney function of PCK rats, whereas the chemical chaperone had no effect on the kidneys.

Altogether, these data indicate that fine tuning of ER stress regulates liver and renal cystogenesis, emerging the chemical chaperone 4-PBA as a potential therapy to hamper the progression of hepatic cysts. Nevertheless, the levels of ER stress in polycystic liver and kidneys, and their role in cystic pathobiology, might be different and dependent of the type of gene found mutated, deserving further investigation.

Table R.2. Kidney biochemical and macroscopical determinations in normal and PCK rats

Parameters	A	B	C	D	E					
	Wild-type rats	PCK Rats (non – treated)	PCK Rats (4-PBA – treated)	PCK Rats (TM – treated)	PCK Rats (4-PBA&TM – treated)	*p* value (A *vs* B)	*p* value (B *vs* C)	*p* value (B *vs* D)	*p* value (B vs E)	*p* value (D *vs* E)
Kidney weight (g)	1.58 ± 0.04	3.94 ± 0.32	3.88 ± 0.20	2.41 ± 0.11	3.18 ± 0.11	<0.0001	0.5969	<0.0001	0.0165	<0.0001
Kidney/body weight (%)	0.51 ± 0.01	1.25 ± 0.09	1.52 ± 0.13	0.876 ± 0.04	1.39 ± 0.14	<0.0001	0.0454	0.0001	0.1822	0.0008
Urea (mg/dL)	35.00 ± 0.87	55.00 ± 5.59	44.36 ± 2.77	32.67 ± 2.64	40.67 ± 3.07	<0.0001	0.2038	<0.0001	0.0221	0.0070
Creatinine (mg/dL)	0.48 ± 0.02	0.69 ± 0.03	0.62 ± 0.02	0.53 ± 0.02	0.51 ± 0.02	<0.0001	0.1051	0.0002	0.0001	0.5700
UCR (Urea/Creatinine)	74.64 ± 4.24	78.01 ± 5.18	71.67 ± 3.88	61.47 ± 3.61	80.37 ± 6.68	0.6233	0.3450	0.0045	0.7828	0.0103

Abbrev: 4-PBA, 4-phenylbutyric acid; TM, tunicamycin; UCR, urea to creatinine ratio; VS, versus.

R.4. Role of UDCA in ER stress management

R.4.1. Modulatory effects of UDCA on the UPR signaling and the 20S proteasome activity in PLD murine models

As mentioned above, the hydrophilic bile acid UDCA restrains the proliferative capacity of cystic human cholangiocytes and hepatic cystogenesis in PCK rats by restoring the $[Ca^{2+}]_i$.[82] Considering the direct relationship of ER Ca^{2+} levels and protein folding activity of several ER-resident chaperones, we proposed to evaluate whether UDCA could also modulate the adaptive responses activated upon ER stress. Thus, the mRNA expression levels of the UPR sensors (i.e., *Atf6*, *Perk* and *Ire1α*) and effectors (i.e., *Chop*, *Grp78* and *Xbp1*) were firstly analyzed in normal (i.e., NRC) and cystic (i.e., PCK) rat cholangiocytes in culture. As shown in **Figure R.14A**, despite the expression of the UPR factors remained unchanged in NRC, the transcript levels of *Ire1α, Chop, Grp78* and *Xbp1* were significantly reduced after treating PCK cholangiocytes with UDCA, as compared to the vehicle-treated condition. In the same line, chronic administration (i.e., 5 months) of UDCA to PCK rats induced a marked reduction of the 20S proteasome activity (**Figure R.14B**)

These preliminary results may pinpoint another mechanism by which UDCA halts the PLD progression, emerging as a potential ER stress modulator. Nevertheless, more detailed investigations are required.

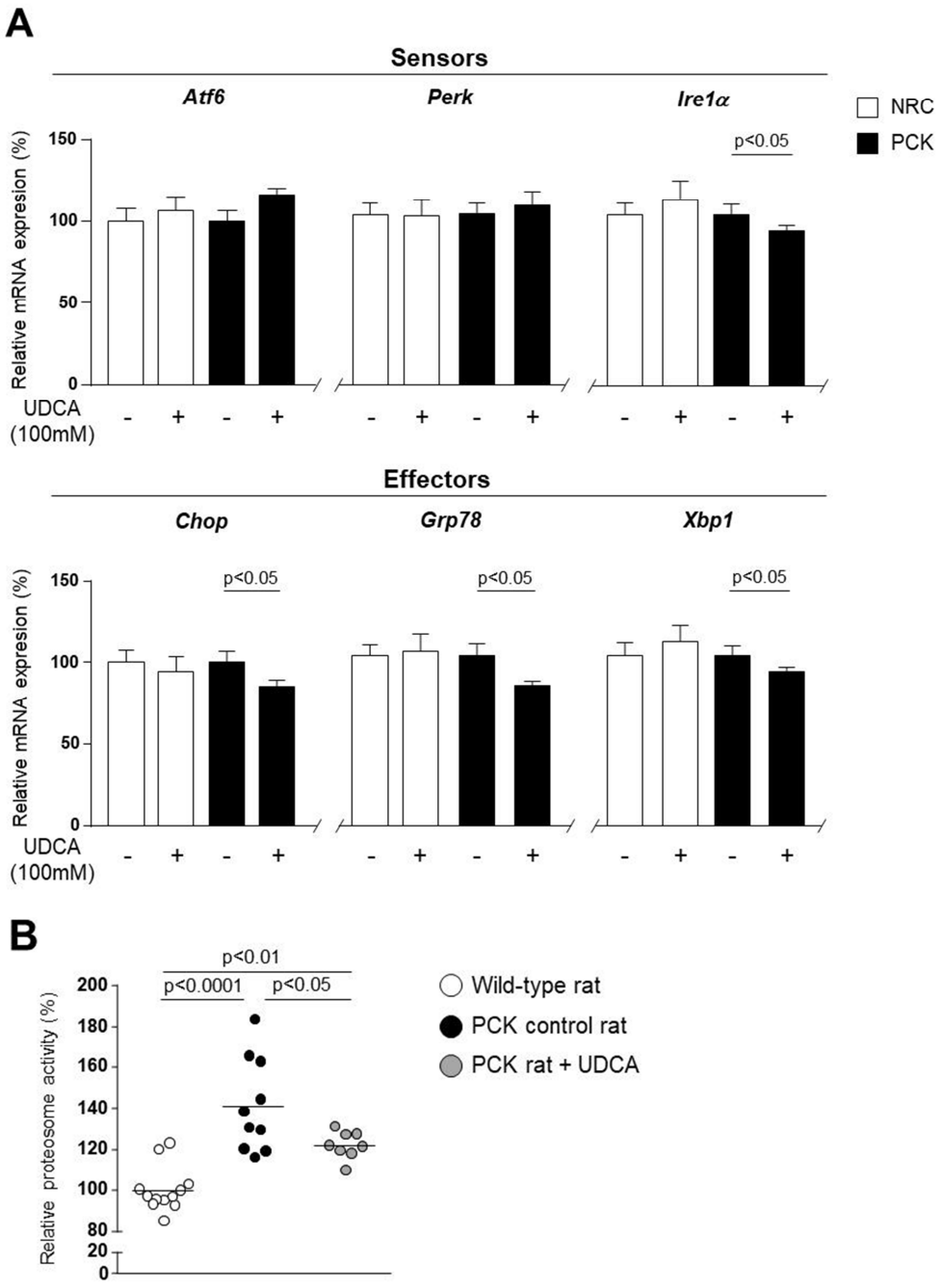

Figure R.14. UDCA-mediated impact on the UPR signaling system and the 20S proteasome activity in murine experimental models of ARPKD. (**A**) mRNA expression levels of the UPR sensors and effectors in normal (n=12) and cystic (n=11) rat cholangiocytes after 24 hours of treatment with UDCA (100mM). (**B**) AMC fluorescence intensity in liver tissue samples from wild-type (n=12), PCK control (n=10) and UDCA-treated PCK rats (n=8). (**A**) Each treated condition was compared with the corresponding vehicle-treated control. (**B**) The AMC fluorescence intensity detected is proportional to the chymotrypsin-like protease activity of the 20S proteasome. The values of AMC fluorescence signal are normalized to the group of wild-type rats (100%). **Abbrev:** AMC, 7-amino-4-methylcoumarin; ATF6, activating transcription factor 6; CHOP, C/EBP-homologous protein; GRP78, 78-kDa glucose-related protein; IRE1α, inositol-requiring enzyme 1 alpha; NRC, normal rat cholangiocytes; PCK, cystic rat cholangiocytes; PERK, pancreatic endoplasmic reticulum kinase; UDCA, ursodeoxycholic acid; XBP1, x-box binding protein 1.

Discussion

The major findings reported in this dissertation suggest that cystic cholangiocytes (i.e., ADPKD and ADPLD) are characterized by abnormal ER proteostasis, leading to the accumulation of un/misfolded proteins within the lumen of this organelle. In turn, this triggers a pathological condition termed ER stress and subsequent activation of pro-survival mechanisms. Our data indicate that: **(I)** the UPR signaling pathways are activated in different PLD experimental models, both in liver biopsies and in primary cystic cholangiocytes from humans and rats, as a result of increased expression of the main sensors and effectors of this adaptive response; **(II)** morphologically, the ER lumen of cystic human and rat cholangiocytes undergoes a marked baseline dilatation, which is characteristic of ER stress; **(III)** the treatment with the ER stress inhibitor 4-PBA significantly reduces the expression of the main UPR effectors (i.e., *CHOP*, *GRP78* and *XBP1*) in NHC and ADPKD, but not in ADPLD cholangiocytes, while TM have the opposite effect in the three cell lines; **(IV)** 4-PBA exerts anti-proliferative and anti-apoptotic effects in both normal (i.e., NHC) and cystic (i.e., ADPKD and ADPLD) human cholangiocytes. In contrast, treatment with the ER stress inducer TM promotes cell death; **(V)** the chemical chaperone 4-PBA is able to alleviate the detrimental effects induced by TM administration *in vitro*, including the mRNA expression levels of the UPR effectors and the apoptotic rate; **(VI)** cystic human cholangiocytes and PCK rat liver tissue samples sustain an hyperactivation of the 20S proteasome, compared to control conditions. This effect is markedly reduced *in vitro* after treatment with 4-PBA; **(VII)** chronic administration of 4-PBA delays disease progression by significantly reducing both the liver weight and volume, as well as, the hepatic cystic volume in PCK rats, in the presence and absence of TM; **(VIII)** the treatment with UDCA also seems to have a modulatory impact on ER stress levels both, in *in vitro* and *in vivo* murine experimental models of PLD. All these results are consistent with the notion that ER stress plays a pivotal role in the pathogenesis of PLD, while its attenuation may halt hepatic cystogenesis, ameliorating disease and thus, representing a novel and promising therapeutic strategy.

It has been widely described that several molecular mechanisms underlie the pathogenesis of PLD, including primary cilium and centrosomal dysfunctions, matrix metalloproteinase hyperactivity, epigenetic alterations, aberrant fluid secretion and dysregulated intracellular levels of cAMP and Ca^{+2},

leading to the characteristic hyperproliferative phenotype of cystic cholangiocytes, which govern the onset and progression of hepatic cystogenesis.[23, 50] Recently, some authors have suggested that the impairment in the biogenesis and trafficking of nascent proteins contained in the ER may be another pivotal event contributing to cyst growth and disease severity,[32, 151] albeit the specific pathological mechanism in PLD is still poorly understood.[22, 32] In this regard, over the last few years an interesting mechanistic interpretation has outlined the determining role of PC1 in PLD progression.[32, 84] Accordingly, mutations in the ER-associated PLD genes compromise the biosynthesis and transport of PC1 to the primary cilium reducing its functional dosage, which is the rate-limiting determinant of cystogenesis and, consequently, of the disease severity.[32, 151] Taking this into consideration, this dissertation aimed to describe the morphological and molecular alterations of the ER in cystic cholangiocytes, ascertain their role in the development and progression of PLD, and evaluate the potential therapeutic value of its regulation.

Our data indicate that, mutations in *PRKCSH*, *SEC63*, *GANAB* and *Pkhd1* genes, which are responsible for the three PLD phenotypes (i.e., ADPKD, ADPLD and ARPKD), are associated with an upregulated UPR signaling, a pronounced dilatation of the ER lumen and a hyperactivated 20S proteasome, compared to their respective normal controls. Noteworthy, *PRKCSH*, *SEC63* and *GANAB* encode for the ER-resident proteins GIIβ, translocation protein SEC63 homolog and GIIα, respectively, which play key roles in co- and post-translational modifications of nascent polypeptides.[32] Hence, a partial or a total abolishment of the function of these proteins could impair the folding, maturation and trafficking of nascent proteins, promoting their accumulation inside the ER and triggering ER stress. Of note, ADPKD (*GANAB* mutant) cholangiocytes exhibited higher levels of the UPR effectors *XBP1* and *CHOP*, as well as, a more enlarged ER lumen than ADPLD (*PRKCSH* mutant) cholangiocytes at baseline conditions. These effects were opposite to the 20S proteasome activity in both type of diseased cholangiocytes, supporting the notion that the UPS aims to relieve the levels of un/misfolded proteins and the subsequent ER stress in cystic cholangiocytes. Based on all these data, the levels of ER stress and the interplay between the ER proteostasis and the proteasomal degradation seem to be dependent on the type of gene found

mutated in PLD. In addition, *Pkhd1* encodes for FPC, a protein located in the primary cilium that participates in tubulogenesis and the maintenance of the duct lumen epithelium architecture.[23, 50] The splicing mutation of this orthologous gene found in the PCK rats could compromise the correct maturation of the protein product (i.e., FPC), being retained within the ER and rapidly degraded. This would reduce the total amount of the protein located in the primary cilium, where it usually interacts with PC2 and modulates the activity of this Ca^{2+} channel.[25, 212, 213] Indeed, a recent study has demonstrated that FPC co-localizes with CNX in the ER.[214] Furthermore, it was described that FPC also interacts with the calcium-modulating cyclophilin ligand (CAML), a primary cilia and ER-associated protein involved in the regulation of cytosolic Ca^{+2} levels.[215] Interestingly, considering that ER chaperones require an optimal Ca^{+2} concentration to preserve the correct folding and maturation of the nascent proteins,[126, 216] ER stress is also triggered when the ER-Ca^{+2} storage is depleted.[126, 217] Thus, these approaches could also explain the presence of ER stress in the experimental models of ARPKD.

Under all these pathological circumstances of ER stress, and in order to restore proteostasis and resolve this stress condition, the UPR signaling branches (i.e., IRE1α, PERK and ATF6) become activated, leading to the upregulation of genes involved in both protein folding and ERAD.[142, 149] Nevertheless, when the UPR is unable to handle the overload of un/misfolded proteins, chronic and/or excessive ER stress might result in apoptosis induction.[118, 142, 149, 152] In this regard, sustained UPR signaling have been identified as a pivotal pathogenic factor in several human diseases, such as T2DM, neurogenerative disorders, viral infections, cancer, heart failure and a wide range of liver diseases.[125, 218, 219]

In order to restore ER proteostasis, several studies have been focused on analyzing the role of 4-PBA, emphasizing the chaperone-like activity of this molecule, which boosts the capacity of protein folding and trafficking, as well as the degradation efficiency. In turn, this allows to prevent the aggregation of un/misfolded proteins within the ER and alleviate the negative outcome derived from ER stress.[126, 154] Indeed, the therapeutic effects of 4-PBA have been assessed in a variety of human pathologies including genetic,[220, 221] inflammatory and metabolic disorders,[192, 222] and neurodegenerative and liver

diseases,[223-225] exerting promising benefits in all of the aforementioned pathologies. Interestingly, the results obtained in our *in vitro* and *in vivo* experimental models of PLD are consistent with these findings. In this regard, chronic intake of 4-PBA hampers the progression of the disease, which is evidenced by significant reduction of hepatic cystic volume, accompanied by a decreased liver weight and volume. On the other hand, chronic stimulation of ER stress with TM exacerbate the hepatomegaly and the hepatic cystic area of PCK rats, probably as a consequence of the cell death process that occurs upon prolonged increased ER stress, which could promote cyst expansion and explain the aggravation of liver damage observed in this experimental group. Notably, 4-PBA shows the same aforementioned therapeutic benefits when is administered in combination with TM, but unfortunately, when both ER stress modulators are combined the serological levels of transaminases are notably increased. This could be linked to the deficiency of the liver to totally metabolize both compounds. Moreover, *in vitro* administration of 4-PBA markedly attenuates the 20S proteasome hyperactivity, due to the assistance of this chemical chaperone to protein folding, which restores ER proteostasis and resolves ER stress. Accordingly, 4-PBA inhibits the hyperproliferation, as well as the basal and TM-induced apoptosis in cystic cholangiocytes, maintaining a suitable balance between proliferation and cell death and thus, delaying the progression of PLD.[226]

In contrast, incubation of human cholangiocytes with TM induces the terminal UPR signaling, during which the adaptive responses become overshadowed by ER stress (i.e., chronic or excessive), failing to restore ER proteostasis and, ultimately, leading to programmed cell death. Of note, the transition towards this point of no return is efficiently prevented by 4-PBA. Nevertheless, it would be interesting to evaluate other potential strategies focused on reducing ER stress levels, such as UPR signaling inducers (i.e., Salubrinal), gene therapy (i.e., AAV-GRP78) or even other chemical chaperones (i.e., TUDCA).

In this regard, our data also support the notion that the previously described therapeutic benefits of UDCA for PLD treatment (both in PCK rats and patients with ADPKD),[71, 82] which were primarily linked to the ability of this bile acid to normalize the decreased $[Ca^{2+}]_i$ in cystic cholangiocytes and hinder hepatic

cystogenesis, could be also related to the inhibition of ER stress. Interestingly, its natural tauro-conjugated form (i.e., TUDCA) has been well-documented to function as an ER chaperone.[156, 227]

In summary (**Figure D.1**), this study provides evidences about the role of ER stress in the pathogenesis of PLD and the therapeutic impact of its regulation. Of note, the vast majority of mutations in the PLD-causing genes ultimately affect the folding, maturation and trafficking of nascent proteins, which are built-up within the ER, triggering ER stress and hepatic cystogenesis. Consequently, our data indicate that the lumen of this organelle becomes enlarged, as an adaptive mechanism to harbor the overload of un/misfolded proteins. In turn, the UPR signaling is induced, promoting the expression not only of factors that contribute with protein folding (i.e., XBP1 and GRP78), but also of pro-apoptotic mediators (i.e., CHOP). Additionally, the UPS-mediated degradation of structurally aberrant proteins is hyperactivated. Importantly, both mechanisms (i.e., UPR and UPS) cooperate to reduce the burden of structurally aberrant proteins accumulated within the ER, and to counteract the mild pro-apoptotic signals that are triggered by the transcriptional activation of CHOP. This allows to restore ER proteostasis and to resolve ER stress, promoting cholangiocyte survival. On the other hand, upon chronic and/or excessive ER stress, an overflowing burden of un/misfolded proteins cause the transition to the terminal UPR signaling. In this scenario, the transcription of CHOP prevails over that of factors involved in protein folding (i.e., XBP1 and GRP78), reaching levels of this pro-apoptotic mediator that are unmanageable by the adaptive responses and inducing cholangiocyte cell death, which is finally executed by the activation of caspase 3/7.[228] Interestingly, administration of the 4-PBA chaperone, aimed to improve the protein folding within the ER, promotes the reduction of ER stress and the inhibition of the hyperproliferative phenotype of cystic cholangiocytes, resulting in decreased hepatic cystogenesis. Altogether, this study indicates that ER stress, and specifically the burden of un/misfolded proteins, represent a novel and promising therapeutic target for patients with PLD.

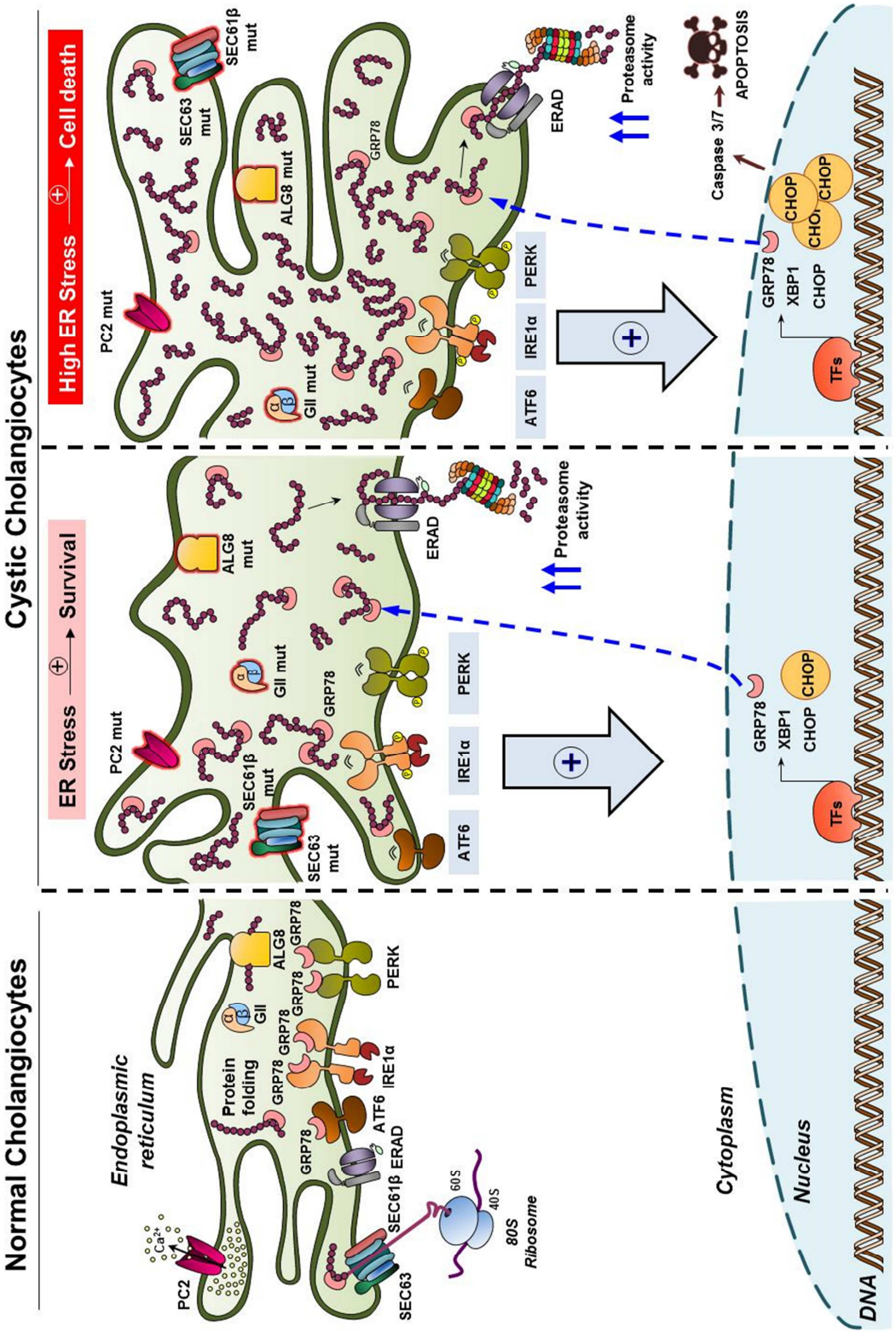

Figure D.1. Working model. Mutations in the PLD-related genes that encode for ER-resident proteins (i.e., PC2, ALG8, SEC63, SEC61B, GIIα and GIIβ) compromise the ER proteostasis and promote the build-up of un/misfolded nascent proteins within the lumen of this organelle. This induce an ensemble of adaptive responses including the activation of UPR signaling branches, enlargement of the ER lumen and hyperactivation of the cellular degradative mechanisms mediated by the UPS. Upon ER stress, the three responses cooperate to overcome protein overload, restore ER proteostasis and resolve

ER stress, leading to cholangiocyte survival. Nevertheless, upon chronic and/or excessive ER stress, the burden of structurally aberrant proteins becomes unmanageable, triggering cellular apoptosis mediated by CHOP and caspase 3/7 activation. **Abbrev:** ALG8, alpha-1,3-glucosyltransferase; ATF4, activating transcription factor 4; ATF6, activating transcription factor 6; Ca^{2+}, calcium; CHOP, C/EBP-homologous protein; DNA, deoxyribonucleic acid; ERAD, endoplasmic reticulum-associated degradation; GII, glucosidase II; GRP78, 78-kDa glucose-regulated protein; IRE1α, inositol-requiring enzyme 1 alpha; mut, mutated; PC2, polycystin-2; PERK, pancreatic endoplasmic reticulum kinase; SEC61B, SEC61 translocon beta subunit; SEC63, translocation protein SEC63 homolog; TFs, transcription factors, XBP1, X-box binding protein 1.

Conclusions

1- The mRNA expression levels of the UPR sensors and effectors are upregulated in experimental models of polycystic liver disease, both *in vivo* and *in vitro*, suggesting that ER stress constitutes a novel pathological mechanism underlying PLD progression.

2- In response to ER stress, induction of the UPR signaling pathways, ER lumen enlargement and 20S proteasome hyperactivity are evidenced in cystic cholangiocytes, which are three well-known adaptive responses to ER stress intended to restore proteostasis.

3- Treatment with the chemical chaperone 4-PBA attenuates the expression of the UPR effectors and the 20S proteasome activity *in vitro*, consequently decreasing ER stress levels in human cholangiocytes.

4- 4-PBA-mediated inhibition of ER stress exerts anti-proliferative and anti-apoptotic effects in primary human cystic cholangiocytes in culture, promoting cell survival. ER stress-mediated cystic cholangiocytes proliferation seems to be dependent on ERK½ signaling pathway.

5- Upon chronic and/or excessive ER stress conditions induced by TM, apoptosis-mediated cell death is triggered, due to the failure of the adaptive mechanisms to restore ER protein homeostasis.

6- 4-PBA protects against TM-induced ER stress in human cystic cholangiocytes *in vitro*, as shown by a reduction in the expression levels of the UPR effectors and apoptosis.

7- Chronic administration of 4-PBA in PCK rats, a model of polycystic liver and kidney disease, delays hepatic cystogenesis evidenced by a significant reduction in liver weight and volume, as well as, in liver cystic volume.

8- TM aggravates hepatic cystogenesis, induces the expression of pro-fibrotic and pro-inflammatory genes in the liver of PCK rats, and increases the serological markers of liver injury and cholestasis.

9- Treatments aimed to restore $[Ca^{2+}]_i$, such as UDCA administration, alleviates the expression of the UPR effectors and *Ire1α*, as well as the 20S proteasome hyperactivity in murine experimental models of polycystic liver disease, emerging as a potential ER stress modulator.

Therefore, inhibition of ER stress arises as a promising therapeutic strategy to tackle PLD progression.

Summary in Spanish (Resumen en Español)

Introducción

Las enfermedades biliares, también denominadas colangiopatías, constituyen un conjunto de enfermedades hepáticas crónicas que afectan a las células epiteliales de los conductos biliares (i.e., colangiocitos).[10, 11] Entre ellas, la enfermedad hepática poliquística (en inglés *polycystic liver disease*; PLD) abarca un grupo de desórdenes genéticos hereditarios, caracterizados por la dilatación del conducto biliar y/o el desarrollo de múltiples quistes biliares (>10), que son la principal causa de morbilidad.[22-24] Además, una elevada proporción de estos pacientes desarrolla enfermedad renal poliquística (en inglés *polycystic kidney disease*; PKD) concomitante.[22-24] Es importante destacar que ambos sexos son susceptibles de padecer PLD. No obstante, las mujeres de mediana edad (<48) son las principales afectadas.[24, 27, 28] A pesar de que la mayoría de los pacientes con PLD permanecen asintomáticos, la hepatomegalia masiva desarrollada por un pequeño porcentaje de ellos, desencadena diversos síntomas y complicaciones[23, 24] que limitan seriamente su calidad de vida, e incluso en algunos casos pueden llegar a ser mortales.[24] Hasta la fecha, los tratamientos quirúrgicos[24, 54] y/o farmacológicos[23, 24, 71] disponibles han mostrado efectos beneficiosos moderados y/o a corto plazo. Es por ello que el trasplante hepático se presenta como la única opción curativa para estos pacientes. [22-24]

Atendiendo a los rasgos genéticos subyacentes a la PLD, cabe mencionar que la presencia de mutaciones germinales heterocigóticas no es suficiente para desarrollar el fenotipo asociado a esta enfermedad, siendo necesaria la aparición de una mutación somática espontánea (i.e., en inglés *second-hit theory*) en el alelo funcional, que causa su inactivación y la pérdida de heterocigosidad (en inglés *loss of heterocygosity*; LOH).[29, 30, 32, 33] Aunque todas las células del organismo portan la mutación germinal, únicamente se ha evidenciado cistogénesis hepática aislada [i.e., Enfermedad Hepática Poliquística Autosómica Dominante (en inglés *Autosomal Dominant Polycystic Liver Disease*; ADPLD)] o combinada con quistes renales [i.e., Enfermedad Renal Poliquística Autosómica Dominante (en inglés *Autosomal Dominant Polycystic Kidney Disease*; ADPKD) o Enfermedad Renal Poliquística Autosómica Recesiva (en inglés *Autosomal Recessive Polycystic Kidney*

Disease; ARPKD)], sugiriendo que estos dos órganos son más sensibles a la ausencia de los productos proteicos derivados de los genes causantes de PLD.[29, 30, 33]

El fenotipo ADPLD está causado por mutaciones en una amplia variedad de genes (i.e., *PRKCSH*, *SEC63*, *GANAB*, *SEC61B* y *ALG8*) que codifican para proteínas que se localizan en el retículo endoplasmático (RE), donde participan en el plegamiento y transporte de proteínas de nueva síntesis.[23, 30, 32] A diferencia de estos genes, *LRP5* codifica para una proteína transmembrana involucrada en la transmisión de señales de la vía canónica de Wnt.[30, 41]

Por otro lado, el fenotipo ADPKD se origina como consecuencia de fallos en la función de las proteínas ciliares policistina-1 (PC1) y policistina-2 (PC2), causados por mutaciones en los genes codificantes *PKD1* y *PKD2*, respectivamente.[23, 30] Ambas proteínas forman el complejo PC1-PC2 que está involucrado en la regulación de la concentración intracelular de Ca^{2+} ($[Ca^{2+}]_i$).[23, 30, 43] Además de en el cilio primario, PC2 también se localiza en la membrana del RE donde controla directa e indirectamente los niveles de Ca^{2+} almacenado en este orgánulo.[23, 30, 43]

Finalmente, el fenotipo recesivo de PLD (i.e., ARPKD) está causado por mutaciones en el gen *PKHD1*, cuyo producto funcional es una proteína denominada fibrocistina/poliductina, que se localiza en el cilio primario donde modula la actividad de PC2, y por tanto la $[Ca^{2+}]_i$, así como también participa en procesos relacionados con la morfogénesis tubular.[30, 44, 45]

Previamente, se ha demostrado que la PLD está asociada con anomalías en diversos mecanismos moleculares entre los que se incluyen, disfunción del cilio primario,[23, 87, 88] desregulación de los niveles intracelulares de Ca^{2+} y 3', 5'-adenosina monofosfato cíclico (AMPc),[23, 50] hiper-proliferación y angiogénesis,[23, 50, 102], aumento de la actividad metaloproteolítica,[23, 50, 62, 96], hiper-secreción[9, 23, 50, 107] y alteraciones epigenéticas.[23, 50, 112, 115] Además, y como se ha mencionado anteriormente, la mayoría de los genes causantes de PLD codifican para proteínas que se localizan en el RE,[30] donde participan en el procesamiento de proteínas de nueva síntesis.[117-119] En este sentido, diversos estudios han demostrado que la biogénesis y el transporte de PC1 al cilio primario se ven afectados como consecuencia de dichas mutaciones, lo que resulta en una disminución de la dosis funcional de esta proteína, que actúa

como factor determinante de la progresión de la enfermedad y, por tanto, de la severidad de la misma.[32, 83, 84] Asimismo, alteraciones en la vía de biogénesis conducen a la acumulación de otras muchas proteínas mal plegadas en el interior del RE,[125-127] desencadenando una condición patológica denominada estrés de RE, que contribuye al desarrollo de una gran variedad de enfermedades humanas (i.e., metabólicas, neurodegenerativas, tumorales y hepáticas, entre otras).[125, 128, 129] En contrapartida a este estrés de RE, se produce la activación de la respuesta a proteínas desplegadas (en inglés *unfolded protein response*; UPR), un mecanismo adaptativo inicialmente destinado a restaurar la proteostasis del RE y eliminar dicha situación de estrés mediante la atenuación de la síntesis proteica, la mejora del tráfico, transporte y plegamiento de las proteínas mal plegadas en el RE, y la activación de procesos degradativos mediados por el proteasoma, promoviendo así la supervivencia celular[128, 142]. Para ello la UPR está constituida por tres sensores localizados en la membrana del RE [i.e., proteína 1 α requirente de inositol (en inglés *inositol-requiring protein 1 alpha*; IRE1α), quinasa pancreática del RE (en inglés *pancreatic ER kinase*; PERK) y factor de trascripción 6 activado (en inglés *activating transcription factor 6*; ATF6)], que en condiciones de no estrés de RE se encuentra inactivos.[142-144] Sin embargo, cuando se produce la acumulación de proteínas mal plegadas dentro del lumen del RE, las vías de señalización mediadas por dichos sensores se inducen para regular principalmente la expresión de factores involucrados en el plegamiento proteico (i.e., GRP78) y la degradación proteasomal,[142, 145-147]

No obstante, si los niveles de estrés de RE se vuelven crónicos y/o excesivos se produce una intensificación de la capacidad de plegamiento proteico y de la degradación proteasomal, aunque no es suficiente para restaurar la proteostasis del RE y resolver la situación de estrés de RE.[142, 149] En ese caso, se activa una señalización alternativa de la UPR, denominada UPR terminal, en la que predominan mecanismos pro-apoptóticos que finalmente causan la muerte celular. [116, 123]

Debido al papel que el estrés de RE tiene en el desarrollo y progresión de diversas enfermedades humanas, su regulación surge como una posible estrategia terapéutica. En este sentido, cuando la funcionalidad del órgano en

cuestión está afectada, se persigue favorecer la supervivencia celular mediante la disminución de los niveles de estrés de RE por medio de la administración de chaperonas químicas,[154-156, 158] inductores de la UPR [159, 160] y/o adenovirus que sobreexpresen componentes de la maquinaria degradativa.[161] Por el contrario, en procesos tumorales se busca inducir la muerte de las células cancerígenas mediante la perpetuación del estrés de RE.[152] Para ello, se han desarrollado inhibidores específicos de los tres sensores de la UPR [164, 167, 169, 172] y de GRP78,[175, 176] inhibidores del procesamiento proteico [164, 178, 179] e inhibidores del proteasoma.[180, 181]

Hipótesis y Objetivos

La mayoría de los genes mutados en PLD codifican para proteínas residentes del RE, especialmente en los fenotipos ADPKD y ADPLD. En este sentido, la pérdida parcial o total de la funcionalidad del producto proteico impide el correcto plegamiento, maduración y tráfico de las proteínas de nueva síntesis e induce estrés de RE. Por ello, postulamos la hipótesis de que el estrés de RE representa un mecanismo subyacente a la etiopatogenia de la PLD y una posible diana terapéutica para el tratamiento de esta enfermedad. Para ello se han planteado los siguientes objetivos:

I. Caracterizar molecular y ultraestructuralmente el RE en muestras de tejido sano y poliquístico de origen humano y murino, así como en colangiocitos aislados de ambas especies.

II. Analizar los niveles de expresión de los componentes de la UPR en presencia o ausencia de moduladores de estrés de RE.

III. Evaluar el impacto de la modulación del estrés de RE, con agentes tanto inhibidores como inductores del estrés de RE, en el destino final de los colangiocitos humanos en cultivo.

IV. Determinar el efecto de la modulación del estrés de RE en el desarrollo y progresión de la cistogénesis hepática en ratas PCK.

Material y Métodos

Expresión génica de los principales componentes de la UPR en biopsias hepáticas y cultivos celulares primarios de origen humano y murino

Lo niveles transcripcionales de los sensores (i.e., ATF6, PERK e IRE1α) y efectores (i.e., CHOP, GRP78 y XBP1) de la UPR fueron analizados en biopsias hepáticas y biliares procedentes de individuos sanos y pacientes con ADPLD, así como también, en muestras de tejido hepático obtenidas de ratas "wild-type" y PCK. Respecto a las muestras de tejido humano, fueron cedidas por el Biobanco Vasco (San Sebastián, España) y el Hospital Universitario Radboud (Nimega, Holanda), en cumplimiento con los respectivos Comités Éticos para la Investigación Clínica. Asimismo, la expresión de estos factores fue determinada en cultivos primarios de colangiocitos sanos y poliquísticos de origen humano (i.e., NHC, ADPKD y APDLD) y murino (i.e., NRC y PCK), tanto en condiciones basales como tras 24 horas de tratamiento con 4-PBA (5mM) y/o TM (2,4µM), en el caso de los colangiocitos humanos, y UDCA (100mM), en el caso de los colangiocitos de rata.

El análisis transcripcional se realizó mediante PCR cuantitativa (qPCR), empleando para ello el termociclador "*CFX96 Touch™*" (Bio-Rad) y el kit "iQ™ SYBR® Green Supermix" (Bio-Rad). La expresión del mRNA del gen *GAPDH* fue utilizada como control interno de carga para normalizar la expresión de cada muestra.

Modelo murino de PLD para estudiar el efecto de los modulares del estrés de RE sobre la cistogénesis hepática

La rata PCK [PCK/CrljCrl-*Pkhd1*^{pck}/Crl (Laboratorios Charles River Inc.)] es un modelo animal ampliamente utilizado para el estudio de la cistogénesis hepato-renal, debido a que porta una mutación (IVS35–2A3 T) en el gen ortólogo *PKHD1*, que hace que estos animales desarrollen un cuadro hepático y renal muy similar al que presentan los pacientes con fenotipo ARPKD y ADPKD.[183-188] Por ello, ratas PCK macho de 8 semanas de edad fueron tratadas con 4-PBA (100mM; en agua de bebida) y/o TM (0,02mg/kg; vía intraperitoneal) durante 5 meses (n=12 por grupo) para estudiar los efectos de estos agentes

modulares del estrés de RE en la cistogénesis hepáticas y, por tanto, en la progresión de la enfermedad. Al mismo tiempo, un grupo de ratas PCK (n=12) se utilizó como control de los tratamientos, mientras que un grupo de ratas "wild-type" [Crj:CD (SD) (Laboratorios Charles River Inc.)] (n=12), de la misma edad y sexo, fueron empleadas como control negativo de la enfermedad.

Además de esto, un estudio *in vivo* previamente publicado[82] fue empleado para evaluar el efecto del UDCA sobre el estrés de RE. Para ello, ratas PCK macho de 8 semanas de edad fueron tratadas con UDCA (25mg/kg/día; mezclado con la comida) durante 5 meses (n=10). Al igual que en el caso anterior, tanto un grupo de ratas PCK (n=10) como un grupo de ratas "wild-type" (n=12), de la misma edad y sexo que las ratas PCK, fueron empleadas como control del tratamiento y como control negativo de la enfermedad, respectivamente.

Mensualmente se realizó un análisis bioquímico de la sangre de los animales utilizando el aparato *COBAS Integra400Plus*, a fin de determinar el estado funcional del hígado y los riñones a lo largo de estudio. Del mismo modo, el estado físico de los animales fue monitorizado *a visu* durante todo el estudio, en ambos casos. Una vez finalizados los procedimientos, los animales fueron sacrificados para la extracción de muestras de tejido hepático y renal.

En el caso del modelo experimental tratado con 4-PBA y TM, la arquitectura del tejido hepático fue analizada histológicamente mediante la tinción de hematoxilina/eosina. Además de esto, también se realizaron análisis transcripcionales en muestras de tejido hepático mediante qPCR.

Todos los procedimientos experimentales realizados durante los estudios *in vivo* fueron aprobados por los correspondientes Comités Éticos de Experimentación Animal.

Evaluación morfológica de la estructura del RE en cultivos primarios de origen humano y murino

La morfología ultraestructural del RE de los colangiocitos sanos (i.e., NHC y NRC) y poliquísticos (ADPKD, ADPLD y PCK) en cultivo, fue visualizada utilizando el microscopio electrónico de trasmisión *JEOL JEM-1400* (JEOL), en colaboración con el grupo del profesor Nicholas F. LaRusso (Mayo Clinic,

EEUU). A partir de las imágenes obtenidas se procedió a cuantificar la superficie ocupada por este orgánulo con el programa informático ImageJ versión 1.50 (NIH, Bethesda, MA, USA).

Estudios funcionales en presencia y/o ausencia de 4-PBA y TM en colangiocitos humanos en cultivo

La tasa de proliferación de los colangiocitos humanos sanos (i.e., NHC) y poliquísticos (i.e., ADPKD y ADPLD) fue determinada mediante su marcaje con la sonda fluorescente "CellTrace™ CFSE Cell Proliferation Kit" (Thermo Fisher Scientific) y posterior tratamiento de los mismos con 4-PBA (5mM) durante 48 horas, empleando el citómetro de flujo "*Guava Easycyte 8HT"* (Merck Millipore) para detectar la intensidad final de la sonda. Además de esto, los niveles de proliferación de los colangiocitos ADPKD también fueron evaluados mediante inmunoblot, utilizando para ello anticuerpos primarios específicos para la proteína ERK½ (Cell Signaling) y su forma fosforilada (i.e., p-ERK½) (Cell Signaling), y posteriormente anticuerpos secundarios conjugados con peroxidasa (Sigma-Aldrich). La proteína β-actina (Sigma-Aldrich) se utilizó como control de carga. Las bandas de proteína se detectaron mediante quimioluminiscencia utilizando el sistema de imagen "*iBright™ FL1000"* (Thermo Fisher Scientific).

En el caso del ensayo de apoptosis celular, los colangiocitos NHC, ADPKD y ADPLD fueron marcados con las sondas fluorescentes "FITC Annexin V" (BioLegend) y "TO-PRO™-3 iodide" (Thermo Fisher Scientific), cuya intensidad fue detectada, tras 48 horas de tratamiento de los colangiocitos con 4-PBA (5mM) y/o TM (2,4µM), en el citómetro de flujo "*Guava Easycyte 8HT*" (Merck Millipore). Asimismo, la actividad de los ejecutores apoptóticos caspasa 3 y caspasa 7, fue cuantificada en colangiocitos NHC, ADPKD y ADPLD tratados con 4-PBA (5mM) durante 48 horas, utilizando para ello el kit "Caspase-Glo® 3/7 Assay" y el luminómetro "*PHERAstar"* (BMG Labtech).

Determinación de la actividad del proteasoma en colangiocitos humanos en cultivo

La actividad tipo quimotripsina de la partícula central 20S del proteasoma (proteasoma 20S) fue analizada en extractos proteicos obtenidos a partir de cultivos primarios de colangiocitos humanos (i.e., NHC, ADPKD y ADPLD) en condiciones basales y tratados con 4-PBA (5mM) durante 48 horas. Asimismo, dicha actividad también fue cuantificada en muestras de tejido hepático procedentes de ratas "wild-type", y ratas PCK (i.e., no tratadas y tratadas crónicamente con UDCA). Para ello, las muestras fueron lisadas con el detergente "Nonidet P-40 (NP40) Cell Lysis Buffer" (Thermo Fisher Sicentific) y los extractos proteicos obtenidos fueron cuantificados con el kit "Pierce™ BCA Protein Assay" (Thermo Fisher Scientific). Posteriormente, las muestras de proteína (i.e., 5µg) fueron incubadas con el kit "Proteasome Activity Assay" (Abnova), el cual contiene un sustrato específico de esta subunidad del proteasoma eucariótico. La fluorescencia emitida por el compuesto generado de la proteólisis de dicho sustrato, fue detectada en intervalos de 5 minutos (24 intervalos) utilizando el lector de placas "*Infinite® 200 PRO"* (Tecan). Es importante mencionar que, la intensidad de fluorescencia es proporcional a la actividad del proteasoma 20S, y que durante todo el procedimiento las muestras se mantuvieron a 37ºC.

Análisis estadístico

Todos los parámetros cuantitativos del estudio fueron incluidos en tablas de MS Excel para su posterior análisis estadístico con el programa "GraphPad Prism" versión 6.01 (GraphPad Software). Para comparaciones entre dos grupos se emplearon los tests estadísticos "T de Student" o "Mann Whitney", atendiendo a si las variables de estudio cumplían una distribución paramétrica o no paramétrica, respectivamente. Para comparaciones entre dos o más grupos se utilizó el test paramétrico de análisis de varianza unidireccional (ANOVA) seguido del test *a posteriori* de "Bonferroni" o el test no paramétrico "Kruskal Wallis" seguido del test *a posteriori* "Dunns". Los datos estás representados como la media ± error estándar de la media. Las diferencias fueron consideradas significativas cuando el valor de $p < 0.05$.

Resultados y Discusión

Caracterización molecular y morfológica del RE en modelos experimentales poliquísticos de origen humano y murino

Expresión de los sensores y efectores de la UPR en biopsias hepáticas y cholangiocitos en cultivo

Para determinar si en la PLD existe una situación de estrés de RE, nos propusimos analizar el estado de la UPR en muestras obtenidas, tanto de individuos sanos y pacientes con ADPLD, como de un modelo murino de ARPKD. En este sentido, pudimos observar que la expresión génica de los sensores (i.e., *ATF6*, *PERK* e *IRE1α*) y los efectores (i.e., *CHOP*, *GRP78* y *XBP1*) de la UPR estaba significativamente aumentada en las muestras aisladas de pacientes con PLD, en comparación con las muestras de vesícula biliar y tejido hepático sano, empleadas como grupos control. Las diferencias fueron especialmente evidentes en la comparativa PLD *vs* vesicular biliar, debido a la similitud de las células de este órgano con los colangiocitos,[204] mientras que en el caso de las muestras de hígado sano, estas diferencias fueron ligeramente enmascaradas posiblemente debido a su alto contenido de hepatocitos. Respecto al modelo animal, también pudimos observar una clara sobreexpresión de los distintos componentes de las vías de señalización de la UPR en el tejido hepático procedente de las ratas PCK, en comparación con las de ratas "wild-type", aunque en el caso del eje IRE1α-XBP1 dichas diferencias no llegaron a ser significativas.

Además de esto, la expresión de cada uno de los factores de la UPR también fue cuantificada en cultivos primarios de colangiocitos humanos (i.e., NHC, ADPKD y ADPLD) y de rata (i.e., NRC y PCK) detectando, de nuevo, un incremento significativo de su expresión en la condición patológica (i.e., ADPKD, ADPLD y PCK), respecto a la condición sana (i.e., NHC y NRC).

Estos datos indican, que los tres fenotipos de PLD (i.e., ADPKD, ADPLD y ARPKD) están caracterizados por una situación de estrés de RE, manifestada molecularmente por una fuerte activación de las vías de señalización de la UPR.

Análisis morfológico del RE de los colangiocitos humanos y de rata

Debido a que uno de los mecanismos desencadenantes de estrés de RE es la acumulación masiva de proteínas mal plegadas en el interior de este orgánulo,[145] decidimos estudiar su morfología en colangiocitos sanos (i.e., NHC y NRC) y poliquísticos (i.e., ADPKD, ADPLD y PCK) en cultivo. Esto nos permitió identificar un lumen reticular notoriamente dilatado en los colangiocitos ADPKD, ADPLD y PCK, cuya superficie era significativamente mayor (i.e., 1,79, 1,47 y 1,62 veces, respectivamente) que la del RE observado en los colangiocitos NHC y NRC.

Estos resultados refuerzan la teoría de que en los tres fenotipos de PLD (i.e., ADPKD, ADPLD y ARPKD) existe una situación de estrés de RE, posiblemente causada por la acumulación de proteínas mal plegadas en el lumen de este orgánulo, lo que explicaría las alteraciones morfológicas observadas en los colangiocitos poliquísticos de humano y de rata.

Efectos del 4-PBA y la TM sobre las respuestas adaptativas inducidas frente al estrés de RE

Modulación de la señalización de la UPR mediante la exposición de los colangiocitos humanos a 4-PBA y TM

Dado que la activación de las vías de señalización de la UPR constituye la primera línea de respuesta frente al estrés de RE, nos plantemos analizar la expresión de los sensores (i.e., *ATF6*, *PERK* e *IRE1α*) y de los efectores (i.e., *CHOP*, *GRP78* y *XBP1*) que integran dicho mecanismo adaptativo, en presencia de un inhibidor (i.e., 4-PBA) y un inductor (i.e., TM) de estrés de RE ampliamente descritos en la literatura.[154, 155, 179] El tratamiento de los colangiocitos humanos sanos (i.e., NHC) y poliquísticos (i.e., ADPKD y ADPLD) con 4-PBA y TM, indujo de manera uniforme la expresión de *IRE1α* respecto al correspondiente grupo tratado con vehículo. No obstante, la expresión de los otros dos sensores de la UPR no se vio alterada por estos agentes moduladores del estrés de RE en los colangiocitos NHC y ADPKD.

Por el contrario, los niveles transcripcionales de *CHOP*, *GRP78* y *XBP1* se vieron significativamente disminuidos como consecuencia de la acción del 4-

PBA sobre los colangiocitos ADPKD, efecto que también se observó en los niveles de expresión de *GRP78* y *XBP1* en los colangiocitos NHC. Sin embargo, el 4-PBA no fue capaz de inhibir la expresión de los efectores de la UPR en los colangiocitos ADPLD. A diferencia del 4-PBA, la TM produjo una marcada sobreexpresión de los efectores de la UPR en las tres líneas celulares analizadas, con la única excepción de que los niveles de *XBP1* en los colangiocitos NHC no alcanzaron diferencias significativas respecto al grupo tratado con vehículo, aunque la tendencia era al alza. No obstante, dicha sobreexpresión inducida por la TM fue eficientemente atenuada por el 4-PBA en NHC, ADPKD y ADPLD, alcanzando valores cercanos a los del grupo tratado con vehículo.

Estos datos sugieren que el 4-PBA reduce los niveles de estrés de RE en colangiocitos humanos al regular la señalización de las vías de la UPR.

Papel compensatorio del sistema ubiquitina proteasoma en colangiocitos poliquísticos humanos

Puesto que la capacidad degradativa del sistema ubiquitina proteasoma (en inglés *ubiquitin proteasome system*; UPS) está modulada por las vías de señalización de la UPR,[205] nos propusimos, en primer lugar, evaluar el estado basal del proteasoma 20S en colangiocitos NHC, ADPKD y ADPLD en cultivo, así como en muestras de tejido hepático obtenidas de ratas “wild-type” y PCK. En este sentido, pudimos detectar una clara hiperactividad del proteasoma 20S, tanto en los colangiocitos humanos poliquísticos (i.e., ADPKD y ADPLD) como en el tejido hepático de las ratas PCK, en comparación con los correspondientes controles (i.e., NHC y tejido hepático de ratas “wild-type”, respectivamente).

A continuación, nos planteamos analizar el efecto del 4-PBA sobre la actividad del proteasoma 20S en cultivos primarios de colangiocitos humanos sanos y poliquísticos. Así, observamos una disminución significativa (~30-60%) de dicha actividad en las tres líneas celulares analizadas (i.e., NHC, ADPDK y ADPLD), en comparación con su correspondiente control tratado con vehículo.

Todo ello, sugiere que la actividad proteolítica del proteasoma 20S se adecúa a las necesidades degradativas y además es modulada por la acción del 4-PBA, posiblemente de manera indirecta al mejorar la capacidad de

plegamiento del RE, contribuyendo así a reducir la carga de proteínas mal plegadas en el interior de este orgánulo y, por tanto, los niveles de estrés de RE.

Análisis de la funcionalidad de los colangiocitos humanos en cultivo tras la modulación del estrés de RE

Determinación de las tasas de proliferación y apoptosis in vitro en presencia de 4-PBA y TM

El fenotipo hiperproliferativo de los colangiocitos poliquísticos es el principal factor implicado en la progresión de la cistogénesis hepática y, por tanto, en la aparición de los síntomas que padecen los pacientes con PLD.[50, 99] Por este motivo, quisimos determinar si el estrés de RE juega un papel en la progresión de esta enfermedad. Para ello, determinamos la tasa de proliferación de los colangiocitos humanos sanos (i.e., NHC) y poliquísticos (i.e., ADPKD y ADPLD) en presencia de 4-PBA, observando una disminución significativa de su capacidad proliferativa (25-60%), como consecuencia de este tratamiento. Además de esto, el tratamiento con 4-PBA también redujo significativamente el ratio p-ERK½/ERK½ en los colangiocitos ADPKD.

Posteriormente, quisimos descartar que dicha disminución de la tasa de proliferación de los colangiocitos humanos fuera consecuencia de un aumento de la muerte celular de los mismos, causada por efectos tóxicos del 4-PBA. De tal manera que, analizamos la tasa de apoptosis en las tres líneas celulares de interés, observando que la administración de 4-PBA redujo significativamente la apoptosis de los colangiocitos poliquísticos (i.e., ADPKD y ADPLD), sin afectar a los colangiocitos NHC. Esto podría indicar que, en condiciones basales, la muerte celular detectada en NHC no está causada por estrés de RE y que la dosis empleada de 4-PBA no es tóxica para los colangiocitos humanos. Por el contrario, la TM aumentó de manera significativa la muerte celular de los colangiocitos NHC, ADPKD y ADPLD, aunque dicho efecto fue eficientemente contrarrestado por la acción del 4-PBA, alcanzando tasas de apoptosis similares o incluso inferiores a las observadas en los controles tratados con vehículo. Asimismo, el tratamiento con 4-PBA disminuyó la actividad de Caspasa 3 y Caspasa 7 en los colangiocitos humanos sanos y poliquísticos.

En conjunto, estos datos sugieren que la chaperona química 4-PBA reduce la proliferación de los colangiocitos humanos a través de la vía de señalización de ERK½ y previene su apoptosis, promoviendo así la supervivencia celular. Por el contrario, la TM induce la muerte celular de los colangiocitos mediante un mecanismo de apoptosis en el que las caspasas 3 y 7 actúan como principales ejecutores.

Determinación del potencial terapéutico de la regulación del estrés de RE *in vivo*

Papel del estrés de RE en la cistogénesis hepática

Debido a que el estrés de RE surge como un mecanismo molecular capaz de controlar la capacidad proliferativa de los colangiocitos poliquísticos, nos planteamos estudiar el impacto terapéutico asociado a la modulación de los niveles de estrés de RE en un modelo animal de ARPKD. Para ello, las ratas PCK fueron tratadas durante 5 meses con 4-PBA (100mM) y/o TM (0,02mg/kg).

En primer lugar observamos que, a diferencia de los animales “wild-type”, las ratas PCK control sufrieron hepatomegalia masiva, manifestada por un aumento significativo tanto del peso como del volumen hepático total. Asimismo, los animales enfermos experimentaron un incremento del “liver/body weight ratio”, debido a la ausencia de diferencias en el peso corporal entre ambos grupos. Asociado a esto, en las ratas PCK control también pudimos detectar cambios significativos en los valores serológicos de FA, albumina, proteína total y “De Ritis ratio” (i.e., AST/ALT), que son indicativos de colestasis y daño hepático.

Por otro lado, el tratamiento crónico de las ratas PCK con 4-PBA redujo significativamente el peso y el volumen del tejido hepático hasta niveles cercanos a los mostrados por las ratas “wild-type”. Este efecto también se vio reflejado en una disminución del volumen de los quistes hepáticos. Además de esto, la administración de la chaperona química normalizó los niveles de ALT en suero. No obstante, el 4-PBA no mostró ningún efecto sobre los valores serológicos de FA y AST, ni sobre el área de los quistes hepáticos.

Por el contrario, la administración de TM no afectó significativamente al peso ni al volumen hepático, así como tampoco al volumen quístico, en comparación con el grupo de ratas PCK control. Sin embargo, como consecuencia de este tratamiento los animales experimentaron un incremento del "liver/body weight ratio" debido a la notable pérdida de peso corporal observada en los mismo. Además, esta tendencia de la TM a agravar la progresión de la enfermedad fue reforzada por un aumento significativo del área hepática ocupada por quistes y por una elevación de los niveles en suero de FA y AST, y del indicador de daño hepático "De Ritis ratio".

Cabe destacar que, la combinación de ambos compuesto (i.e., 4-PBA&TM) produjo una reducción del peso y volumen hepático, así como del volumen de los quistes hepáticos, en comparación con el grupo tratado únicamente con TM. Desafortunadamente, la combinación de 4-PBA y TM elevó significativamente los niveles serológicos de las transaminasas en comparación con los valores detectados en las ratas PCK control. Esto puede ser una manifestación de daño hepático posiblemente ocasionado por la incapacidad del hígado de metabolizar ambos compuestos.

Además de esto, la expresión de diferentes genes pro-fibróticos (i.e., *Col1a1*, *α-Sma* y *Ctgf*) y pro-inflamatorios (i.e., *Il-6* y *Cxcl1*) se indujo como consecuencia de la administración de TM, no siendo capaz el 4-PBA de contrarrestarla.

Por último, a nivel renal pudimos observar que el grupo de ratas PCK control experimentó una notable nefromegalia, que se tradujo en un aumento significativo del "kidney/body weight ratio", en comparación con las ratas "wild-type". Además, los niveles serológicos de creatinina y urea (i.e., dos marcadores de la función renal) también estaban elevados en las ratas PCK control. Curiosamente, al contrario de lo que sucedía a nivel hepático, el 4-PBA no tuvo efectos relevantes sobre los riñones, mientras que la TM mejoró la función renal de los animales al provocar una disminución significativa de los parámetros renales analizados.

Todos estos datos sugieren que el 4-PBA retrasa la progresión de la enfermedad hepática, pudiendo representar una estrategia terapéutica eficaz para los pacientes con PLD.

Regulación del estrés de RE mediada por UDCA

Efecto del UDCA sobre las respuestas adaptativas frente al estrés de RE

Debido a la relación que existe entre la concentración de Ca^{2+} reticular y la actividad de plegamiento de muchas chaperonas del RE, nos propusimos evaluar si el UDCA, un ácido biliar endógeno capaz de restaurar la $[Ca^{2+}]_i$ en colangiocitos poliquísticos,[82] puede modular las respuestas adaptativas activadas frente al estrés de RE. En este sentido, observamos que los niveles transcripcionales de *Ire1α*, *Chop*, *Grp78* y *Xbp1* estaban significativamente disminuidos tras el tratamiento de los colangiocitos PCK con este ácido biliar, en comparación con el grupo tratado con vehículo. A su vez, las muestras de tejido hepático obtenidas de las ratas PCK tratadas crónicamente con UDCA mostraron una reducción significativa de la actividad del proteasoma 20S, en comparación con el tejido hepático de las ratas PCK control.

Estos datos apuntan ligeramente a un nuevo mecanismo por el que el UDCA podría detener el progreso de la PLD, al surgir como un posible modulador del estrés de RE.

Conclusiones

1- Los niveles de expresión (mRNA) de los sensores y efectores de la UPR están aumentados en modelos experimentales de enfermedad hepática poliquística, tanto *in vivo* como *in vitro*, sugiriendo que el estrés de RE constituye un nuevo mecanismo patológico subyacente a la progresión de la PLD.

2- En respuesta al estrés de RE, los colangiocitos poliquísticos muestran activación de las vías de señalización de la UPR, dilatación del lumen del RE e hiperactividad del proteasoma 20S, las cuales constituyen tres respuestas adaptativas frente al estrés de RE destinadas a restaurar la proteostasis.

3- El tratamiento con la chaperona química 4-PBA disminuye la expresión de los efectores de la UPR y la actividad del proteasoma 20S *in vitro*, y en consecuencia, también los niveles de estrés de RE en colangiocitos humanos.

4- La inhibición del estrés de RE inducida por el 4-PBA tiene efectos anti-proliferativos y anti-apoptóticos en cultivos primarios de colangiocitos poliquísticos humanos, promoviendo la supervivencia celular. La proliferación de los colangiocitos poliquísticos mediada por el estrés de RE parece ser dependiente de la vía de señalización de ERK½.

5- En condiciones de estrés de RE crónico y/o excesivo inducido por la TM, se desencadenan mecanismos apoptóticos, debido a la incapacidad de las respuestas adaptativas de restaurar la homeostasis proteica del RE.

6- El 4-PBA protege frente al estrés de RE inducido por la TM en colangiocitos humanos poliquísticos *in vitro*, lo que se manifiesta por la reducción de los niveles de expresión de los efectores de la UPR y de la tasa de apoptosis.

7- La administración crónica de 4-PBA en ratas PCK, un modelo de poliquistosis hepática y renal, retrasa la cistogénesis hepática al reducir el peso y volumen hepático, así como el volumen de los quistes hepáticos.

8- La TM agrava la cistogénesis hepática, induce la expresión de genes pro-fibróticos y pro-inflamatorios en el tejido hepático de ratas PCK, y aumenta los marcadores serológicos de daño hepático y colestasis.

9- Los tratamientos destinados a restaurar la $[Ca^{2+}]_i$, como la administración de UDCA, atenúan la expresión de los efectores de la UPR y de *Ire1α*, así como la hiperactividad del proteasoma 20S en modelos murinos de enfermedad hepática poliquística, surgiendo como un posible modulador del estrés de RE.

Por todo ello, la inhibición del estrés de RE emerge como una prometedora estrategia terapéutica frente a la progresión de la PLD.

References

1. Juza RM, Pauli EM. Clinical and surgical anatomy of the liver: a review for clinicians. Clin Anat 2014;27:764-769.
2. Trefts E, Gannon M, Wasserman DH. The liver. Curr Biol 2017;27:R1147-R1151.
3. Boyer JL. Bile formation and secretion. Compr Physiol 2013;3:1035-1078.
4. Kubes P, Jenne C. Immune responses in the liver. Annu Rev Immunol 2018;36:247-277.
5. Bhatia SN, Underhill GH, Zaret KS, et al. Cell and tissue engineering for liver disease. Sci Transl Med 2014;6:245sr2.
6. Cotoi C QA. Normal liver anatomy and introduction to liver histology. Textbook of pediatric gastroenterology, hepatology and nutrition. Springer, Cham 2016:4.
7. Mescher AL. Junqueira's basic histology: text and atlas. McGraw-Hill Medical 2013.
8. Han Y, Glaser S, Meng F, et al. Recent advances in the morphological and functional heterogeneity of the biliary epithelium. Exp Biol Med 2013;238:549-565.
9. Tabibian JH, Masyuk AI, Masyuk TV, et al. Physiology of cholangiocytes. Compr Physiol 2013;3:541-565.
10. Rajapaksha IG, Angus PW, Herath CB. Current therapies and novel approaches for biliary diseases. World J Gastrointest Pathophysiol 2019;10:1-10.
11. KM B. The clinical burden of biliary disease: a global perspective. Textbook "Biliary disease from science to clinic". Springer, Cham 2017:15.
12. Marcellin P, Kutala BK. Liver diseases: a major, neglected global public health problem requiring urgent actions and large-scale screening. Liver Int 2018;38 Suppl 1:2-6.
13. Lazaridis KN, LaRusso NF. The cholangiopathies. Mayo Clin Proc 2015;90:791-800.
14. Tam PKH, Yiu RS, Lendahl U, et al. Cholangiopathies - towards a molecular understanding. EBioMedicine 2018;35:381-393.
15. De Assuncao TM, Jalan-Sakrikar N, Huebert RC. Regenerative medicine and the biliary tree. Semin Liver Dis 2017;37:17-27.
16. Nakanuma Y. Tutorial review for understanding of cholangiopathy. Int J Hepatol 2012;2012:547840.
17. Horsley-Silva JL, Carey EJ, Lindor KD. Advances in primary sclerosing cholangitis. Lancet Gastroenterol Hepatol 2016;1:68-77.
18. Ehlken H, Schramm C. Primary sclerosing cholangitis and cholangiocarcinoma: pathogenesis and modes of diagnostics. Dig Dis 2013;31:118-125.
19. Naseer M, Dailey FE, Juboori AA, et al. Epidemiology, determinants, and management of AIDS cholangiopathy: a review. World J Gastroenterol 2018;24:767-774.
20. Padda MS, Sanchez M, Akhtar AJ, et al. Drug-induced cholestasis. Hepatology 2011;53:1377-1387.
21. Deltenre P, Valla DC. Ischemic cholangiopathy. Semin Liver Dis 2008;28:235-246.
22. Perugorria MJ, Banales JM. Genetics: Novel causative genes for polycystic liver disease. Nat Rev Gastroenterol Hepatol 2017;14:391-392.
23. Santos-Laso A, Izquierdo-Sanchez L, Lee-Law PY, et al. New Advances in Polycystic Liver Diseases. Semin Liver Dis 2017;37:45-55.
24. van Aerts RMM, van de Laarschot LFM, Banales JM, et al. Clinical management of polycystic liver disease. J Hepatol 2017;4:827-837.
25. Bergmann C, Guay-Woodford LM, Harris PC, et al. Polycystic kidney disease. Nat Rev Dis Primers 2018;4:50.
26. Lanktree MB, Haghighi A, Guiard E, et al. Prevalence estimates of polycystic kidney and liver disease by population sequencing. J Am Soc Nephrol 2018;29:2593-2600.
27. D'Agnolo HM, Drenth JP. Risk factors for progressive polycystic liver disease: where do we stand? Nephrol Dial Transplant 2016;31:857-859.
28. Gevers TJ, Drenth JP. Diagnosis and management of polycystic liver disease. Nat Rev Gastroenterol Hepatol 2013;10:101-108.

29. Janssen MJ, Waanders E, Te Morsche RH, et al. Secondary, somatic mutations might promote cyst formation in patients with autosomal dominant polycystic liver disease. Gastroenterology 2011;141:2056-2063 e2.

30. Lee-Law PY, van de Laarschot LFM, Banales JM, et al. Genetics of polycystic liver diseases. Curr Opin Gastroenterol 2019;35:65-72.

31. Knudson AG, Jr. Mutation and cancer: statistical study of retinoblastoma. Proc Natl Acad Sci U S A 1971;68:820-823.

32. Besse W, Dong K, Choi J, et al. Isolated polycystic liver disease genes define effectors of polycystin-1 function. J Clin Invest 2017;127:1772-1785.

33. Banales JM, Munoz-Garrido P, Bujanda L. Somatic second-hit mutations leads to polycystic liver diseases. World J Gastroenterol 2013;19:141-143.

34. Drenth JP, te Morsche RH, Smink R, et al. Germline mutations in PRKCSH are associated with autosomal dominant polycystic liver disease. Nat Genet 2003;33:345-347.

35. Davila S, Furu L, Gharavi AG, et al. Mutations in SEC63 cause autosomal dominant polycystic liver disease. Nat Genet 2004;36:575-577.

36. Porath B, Gainullin VG, Cornec-Le Gall E, et al. Mutations in GANAB, encoding the glucosidase IIalpha subunit, cause autosomal-dominant polycystic kidney and liver disease. Am J Hum Genet 2016;98:1193-1207.

37. Wang Q, Groenendyk J, Michalak M. Glycoprotein quality control and endoplasmic reticulum stress. Molecules 2015;20:13689-13704.

38. Linxweiler M, Schick B, Zimmermann R. Let's talk about Secs: Sec61, Sec62 and Sec63 in signal transduction, oncology and personalized medicine. Signal Transduct Target Ther 2017;2:17002.

39. Falcone D, Henderson MP, Nieuwland H, et al. Stability and function of the Sec61 translocation complex depends on the Sss1p tail-anchor sequence. Biochem J 2011;436:291-303.

40. Van den Berg B, Clemons WM, Jr., Collinson I, et al. X-ray structure of a protein-conducting channel. Nature 2004;427:36-44.

41. Cnossen WR, te Morsche RH, Hoischen A, et al. Whole-exome sequencing reveals LRP5 mutations and canonical Wnt signaling associated with hepatic cystogenesis. Proc Natl Acad Sci U S A 2014;111:5343-5348.

42. Perugorria MJ, Olaizola P, Labiano I, et al. Wnt-beta-catenin signalling in liver development, health and disease. Nat Rev Gastroenterol Hepatol 2019;16:121-136.

43. Wu M, Yu S. New insights into the molecular mechanisms targeting tubular channels/transporters in PKD development. Kidney Dis 2016;2:128-135.

44. Bergmann C, von Bothmer J, Ortiz Bruchle N, et al. Mutations in multiple PKD genes may explain early and severe polycystic kidney disease. J Am Soc Nephrol 2011;22:2047-2056.

45. Kim I, Fu Y, Hui K, et al. Fibrocystin/polyductin modulates renal tubular formation by regulating polycystin-2 expression and function. J Am Soc Nephrol 2008;19:455-468.

46. Roskams T, Desmet V. Embryology of extra- and intrahepatic bile ducts, the ductal plate. Anat Rec 2008;291:628-635.

47. Carpentier R, Suner RE, van Hul N, et al. Embryonic ductal plate cells give rise to cholangiocytes, periportal hepatocytes, and adult liver progenitor cells. Gastroenterology 2011;141:1432-1438.

48. Raynaud P, Carpentier R, Antoniou A, et al. Biliary differentiation and bile duct morphogenesis in development and disease. Int J Biochem Cell Biol 2011;43:245-256.

49. Wills ES, Roepman R, Drenth JP. Polycystic liver disease: ductal plate malformation and the primary cilium. Trends Mol Med 2014;20:261-270.

50. Perugorria MJ, Masyuk TV, Marin JJ, et al. Polycystic liver diseases: advanced insights into the molecular mechanisms. Nat Rev Gastroenterol Hepatol 2014;11:750-761.

51. Hand NJ, Master ZR, Eauclaire SF, et al. The microRNA-30 family is required for vertebrate hepatobiliary development. Gastroenterology 2009;136:1081-1090.

52. Moore KL P, TVN. The developing human: clinically oriented embryology (10th ed). Saunders 2015:560.

53. Raynaud P, Tate J, Callens C, et al. A classification of ductal plate malformations based on distinct pathogenic mechanisms of biliary dysmorphogenesis. Hepatology 2011;53:1959-1966.

54. Drenth JP, Chrispijn M, Nagorney DM, et al. Medical and surgical treatment options for polycystic liver disease. Hepatology 2010;52:2223-2230.

55. van Keimpema L, de Koning DB, Strijk SP, et al. Aspiration-sclerotherapy results in effective control of liver volume in patients with liver cysts. Dig Dis Sci 2008;53:2251-2257.

56. Moorthy K, Mihssin N, Houghton PW. The management of simple hepatic cysts: sclerotherapy or laparoscopic fenestration. Ann R Coll Surg Engl 2001;83:409-414.

57. Patel C, Tchan M, Savige J, et al. KHA-CARI autosomal dominant polycystic kidney disease guideline: genetics and genetic counseling. Semin Nephrol 2015;35:550-556.

58. van Keimpema L, Ruurda JP, Ernst MF, et al. Laparoscopic fenestration of liver cysts in polycystic liver disease results in a median volume reduction of 12.5%. J Gastrointest Surg 2008;12:477-482.

59. Yang J, Ryu H, Han M, et al. Comparison of volume-reductive therapies for massive polycystic liver disease in autosomal dominant polycystic kidney disease. Hepatol Res 2016;46:183-191.

60. Schindl MJ, Redhead DN, Fearon KC, et al. The value of residual liver volume as a predictor of hepatic dysfunction and infection after major liver resection. Gut 2005;54:289-296.

61. Coquillard C, Berger J, Daily M, et al. Combined liver-kidney transplantation for polycystic liver and kidney disease: analysis from the United Network for Organ Sharing dataset. Liver Int 2016;36:1018-1025.

62. Urribarri AD, Munoz-Garrido P, Perugorria MJ, et al. Inhibition of metalloprotease hyperactivity in cystic cholangiocytes halts the development of polycystic liver diseases. Gut 2014;63:1658-1667.

63. Masyuk TV, Radtke BN, Stroope AJ, et al. Inhibition of Cdc25A suppresses hepato-renal cystogenesis in rodent models of polycystic kidney and liver disease. Gastroenterology 2012;142:622-633.

64. Gradilone SA, Habringer S, Masyuk TV, et al. HDAC6 is overexpressed in cystic cholangiocytes and its inhibition reduces cystogenesis. Am J Pathol 2014;184:600-608.

65. Lorenzo Pisarello M, Masyuk TV, Gradilone SA, et al. Combination of a histone deacetylase 6 inhibitor and a somatostatin receptor agonist synergistically reduces hepatorenal cystogenesis in an animal model of polycystic liver disease. Am J Pathol 2018;188:981-994.

66. Spirli C, Okolicsanyi S, Fiorotto R, et al. ERK1/2-dependent vascular endothelial growth factor signaling sustains cyst growth in polycystin-2 defective mice. Gastroenterology 2010;138:360-371.

67. Amura CR, Brodsky KS, Groff R, et al. VEGF receptor inhibition blocks liver cyst growth in pkd2(WS25/-) mice. Am J Physiol Cell Physiol 2007;293:C419-C428.

68. Gradilone SA, Masyuk TV, Huang BQ, et al. Activation of Trpv4 reduces the hyperproliferative phenotype of cystic cholangiocytes from an animal model of ARPKD. Gastroenterology 2010;139:304-314.

69. Chrispijn M, Gevers TJ, Hol JC, et al. Everolimus does not further reduce polycystic liver volume when added to long acting octreotide: results from a randomized controlled trial. J Hepatol 2013;59:153-159.

70. Walz G, Budde K, Mannaa M, et al. Everolimus in patients with autosomal dominant polycystic kidney disease. N Engl J Med 2010;363:830-840.

71. D'Agnolo HM, Kievit W, Takkenberg RB, et al. Ursodeoxycholic acid in advanced polycystic liver disease: A phase 2 multicenter randomized controlled trial. J Hepatol 2016;65:601-607.

72. Hogan MC, Masyuk T, Bergstralh E, et al. Efficacy of 4 years of octreotide long-acting release therapy in patients with severe polycystic liver disease. Mayo Clin Proc 2015;90:1030-1037.

73. Chrispijn M, Nevens F, Gevers TJ, et al. The long-term outcome of patients with polycystic liver disease treated with lanreotide. Aliment Pharmacol Ther 2012;35:266-274.

74. Hogan MC, Masyuk TV, Page LJ, et al. Randomized clinical trial of long-acting somatostatin for autosomal dominant polycystic kidney and liver disease. J Am Soc Nephrol 2010;21:1052-1061.

75. Hogan MC, Masyuk TV, Page L, et al. Somatostatin analog therapy for severe polycystic liver disease: results after 2 years. Nephrol Dial Transplant 2012;27:3532-3539.

76. van Aerts RMM, Kolkman M, Kievit W, et al. Drug holiday in patients with polycystic liver disease treated with somatostatin analogues. Therap Adv Gastroenterol 2018;11:1-11.

77. Beuers U, Trauner M, Jansen P, et al. New paradigms in the treatment of hepatic cholestasis: from UDCA to FXR, PXR and beyond. J Hepatol 2015;62:S25-S37.

78. Marin JJ, Macias RI, Briz O, et al. Bile acids in physiology, pathology and pharmacology. Curr Drug Metab 2015;17:4-29.

79. De Marco G, Sordino D, Bruzzese E, et al. Early treatment with ursodeoxycholic acid for cholestasis in children on parenteral nutrition because of primary intestinal failure. Aliment Pharmacol Ther 2006;24:387-394.

80. Rost D, Rudolph G, Kloeters-Plachky P, et al. Effect of high-dose ursodeoxycholic acid on its biliary enrichment in primary sclerosing cholangitis. Hepatology 2004;40:693-698.

81. Angulo P, Dickson ER, Therneau TM, et al. Comparison of three doses of ursodeoxycholic acid in the treatment of primary biliary cirrhosis: a randomized trial. J Hepatol 1999;30:830-835.

82. Munoz-Garrido P, Marin JJ, Perugorria MJ, et al. Ursodeoxycholic acid inhibits hepatic cystogenesis in experimental models of polycystic liver disease. J Hepatol 2015;4:952-961.

83. Fedeles SV, Tian X, Gallagher AR, et al. A genetic interaction network of five genes for human polycystic kidney and liver diseases defines polycystin-1 as the central determinant of cyst formation. Nat Genet 2011;43:639-647.

84. Fedeles SV, Gallagher AR, Somlo S. Polycystin-1: a master regulator of intersecting cystic pathways. Trends Mol Med 2014;20:251-260.

85. Jiang ST, Chiou YY, Wang E, et al. Defining a link with autosomal-dominant polycystic kidney disease in mice with congenitally low expression of Pkd1. Am J Pathol 2006;168:205-220.

86. Garcia-Gonzalez MA, Menezes LF, Piontek KB, et al. Genetic interaction studies link autosomal dominant and recessive polycystic kidney disease in a common pathway. Hum Mol Genet 2007;16:1940-1950.

87. Mansini AP, Peixoto E, Thelen KM, et al. The cholangiocyte primary cilium in health and disease. Biochim Biophys Acta Mol Basis Dis 2018;1864:1245-1253.

88. Saternos HC, AbouAlaiwi WA. Implications of dysfunction of mechanosensory cilia in polycystic kidney disease. Polycystic Kidney Disease. 2015.

89. Masyuk AI, Masyuk TV, LaRusso NF. Cholangiocyte primary cilia in liver health and disease. Dev Dyn 2008;237:2007-2012.

90. Tomilin V, Reif GA, Zaika O, et al. Deficient transient receptor potential vanilloid type 4 function contributes to compromised [Ca(2+)]i homeostasis in human autosomal-dominant polycystic kidney disease cells. FASEB J 2018;32:4612-4623.

91. Masyuk TV, Masyuk AI, Lorenzo Pisarello M, et al. TGR5 contributes to hepatic cystogenesis in rodents with polycystic liver diseases through cyclic adenosine monophosphate/Galphas signaling. Hepatology 2017;66:1197-1218.

92. Mangolini A, de Stephanis L, Aguiari G. Role of calcium in polycystic kidney disease: from signaling to pathology. World J Nephrol 2016;5:76-83.

93. Lemos FO, Ehrlich BE. Polycystin and calcium signaling in cell death and survival. Cell Calcium 2018;69:37-45.

94. Pochynyuk O, Zaika O, O'Neil RG, et al. Novel insights into TRPV4 function in the kidney. Pflugers Arch 2013;465:177-186.

95. Li Y, Santoso NG, Yu S, et al. Polycystin-1 interacts with inositol 1,4,5-trisphosphate receptor to modulate intracellular Ca2+ signaling with implications for polycystic kidney disease. J Biol Chem 2009;284:36431-36441.

96. Masyuk TV, Masyuk AI, LaRusso NF. Therapeutic targets in polycystic liver disease. Curr Drug Targets 2017;18:950-957.

97. Chebib FT, Sussman CR, Wang X, et al. Vasopressin and disruption of calcium signalling in polycystic kidney disease. Nat Rev Nephrol 2015;11:451-464.

98. Cheng X, Ji Z, Tsalkova T, et al. Epac and PKA: a tale of two intracellular cAMP receptors. Acta Biochim Biophys Sin 2008;40:651-662.

99. Banales JM, Masyuk TV, Gradilone SA, et al. The cAMP effectors Epac and protein kinase a (PKA) are involved in the hepatic cystogenesis of an animal model of autosomal recessive polycystic kidney disease (ARPKD). Hepatology 2009;49:160-174.

100. Spirli C, Mariotti V, Villani A, et al. Adenylyl cyclase 5 links changes in calcium homeostasis to cAMP-dependent cyst growth in polycystic liver disease. J Hepatol 2017;66:571-580.

101. Fabris L, Cadamuro M, Fiorotto R, et al. Effects of angiogenic factor overexpression by human and rodent cholangiocytes in polycystic liver diseases. Hepatology 2006;43:1001-1012.

102. Strazzabosco M, Somlo S. Polycystic liver diseases: congenital disorders of cholangiocyte signaling. Gastroenterology 2011;140:1855-1859.

103. Theocharis AD, Skandalis SS, Gialeli C, et al. Extracellular matrix structure. Adv Drug Deliv Rev 2016;97:4-27.

104. Klaas M, Kangur T, Viil J, et al. The alterations in the extracellular matrix composition guide the repair of damaged liver tissue. Sci Rep 2016;6:27398.

105. Afroze S, Meng F, Jensen K, et al. The physiological roles of secretin and its receptor. Ann Transl Med 2013;1:29.

106. Glaser S, Meng F, Han Y, et al. Secretin stimulates biliary cell proliferation by regulating expression of microRNA 125b and microRNA let7a in mice. Gastroenterology 2014;146:1795-1808.

107. Banales JM, Masyuk TV, Bogert PS, et al. Hepatic cystogenesis is associated with abnormal expression and location of ion transporters and water channels in an animal model of autosomal recessive polycystic kidney disease. Am J Pathol 2008;173:1637-1646.

108. Li Q, Dutta A, Kresge C, et al. Bile acids stimulate cholangiocyte fluid secretion by activation of transmembrane member 16A Cl(-) channels. Hepatology 2018;68:187-199.

109. Perugorria MJ, Labiano I, Esparza-Baquer A, et al. Bile acids in polycystic liver diseases: triggers of disease progression and potential solution for treatment. Dig Dis 2017;35:275-281.

110. Chuang JC, Jones PA. Epigenetics and microRNAs. Pediatr Res 2007;61:24R-29R.

111. Lee SO, Masyuk T, Splinter P, et al. MicroRNA15a modulates expression of the cell-cycle regulator Cdc25A and affects hepatic cystogenesis in a rat model of polycystic kidney disease. J Clin Invest 2008;118:3714-3724.

112. Masyuk T, Masyuk A, LaRusso N. MicroRNAs in cholangiociliopathies. Cell Cycle 2009;8:1324-1328.

113. Hajarnis S, Lakhia R, Yheskel M, et al. microRNA-17 family promotes polycystic kidney disease progression through modulation of mitochondrial metabolism. Nat Commun 2017;8:14395.

114. Patel V, Williams D, Hajarnis S, et al. miR-17~92 miRNA cluster promotes kidney cyst growth in polycystic kidney disease. Proc Natl Acad Sci U S A 2013;110:10765-10770.

115. Li X. Epigenetics and autosomal dominant polycystic kidney disease. Biochim Biophys Acta 2011;1812:1213-1218.

116. Liu W, Fan LX, Zhou X, et al. HDAC6 regulates epidermal growth factor receptor (EGFR) endocytic trafficking and degradation in renal epithelial cells. PLoS One 2012;7:e49418.

117. Schwarz DS, Blower MD. The endoplasmic reticulum: structure, function and response to cellular signaling. Cell Mol Life Sci 2016;73:79-94.

118. Bravo R, Parra V, Gatica D, et al. Endoplasmic reticulum and the unfolded protein response: dynamics and metabolic integration. Int Rev Cell Mol Biol 2013;301:215-290.

119. Xu H, Martinoia E, Szabo I. Organellar channels and transporters. Cell Calcium 2015;58:1-10.

120. Smith M, Wilkinson S. ER homeostasis and autophagy. Essays Biochem 2017;61:625-635.

121. Afonso MS, Machado RM, Lavrador MS, et al. Molecular pathways underlying cholesterol homeostasis. Nutrients 2018;10.

122. Ott CM, Lingappa VR. Integral membrane protein biosynthesis: why topology is hard to predict. J Cell Sci 2002;115:2003-2009.

123. Qi L, Tsai B, Arvan P. New insights into the physiological role of endoplasmic reticulum-associated degradation. Trends Cell Biol 2017;27:430-440.

124. Carreras-Sureda A, Pihan P, Hetz C. Calcium signaling at the endoplasmic reticulum: fine-tuning stress responses. Cell Calcium 2018;70:24-31.

125. Oakes SA, Papa FR. The role of endoplasmic reticulum stress in human pathology. Annu Rev Pathol 2015;10:173-194.

126. Lebeaupin C, Vallee D, Hazari Y, et al. Endoplasmic reticulum stress signalling and the pathogenesis of non-alcoholic fatty liver disease. J Hepatol 2018;69:927-947.

127. Mahdi AA, Rizvi SH, Parveen A. Role of endoplasmic reticulum stress and unfolded protein responses in health and diseases. Indian J Clin Biochem 2016;31:127-137.

128. Lindholm D, Korhonen L, Eriksson O, et al. Recent insights into the role of unfolded protein response in ER stress in health and disease. Front Cell Dev Biol 2017;5.

129. Manalo RVM MP. The endoplasmic reticulum stress response in disease pathogenesis and pathophysiology. Egyptian Journal of Medical Human Genetics 2018;19:59-68.

130. Back SH, Kaufman RJ. Endoplasmic reticulum stress and type 2 diabetes. Annu Rev Biochem 2012;81:767-793.

131. Ly LD, Xu S, Choi SK, et al. Oxidative stress and calcium dysregulation by palmitate in type 2 diabetes. Exp Mol Med 2017;49.

132. Cabral-Miranda F, Hetz C. ER stress and neurodegenerative disease: a cause or effect relationship? Curr Top Microbiol Immunol 2018;414:131-157.

133. Omura T, Kaneko M, Okuma Y, et al. Endoplasmic reticulum stress and Parkinson's disease: the role of HRD1 in averting apoptosis in neurodegenerative disease. Oxid Med Cell Longev 2013;2013:1-7.

134. Cheung KH, Mei L, Mak DO, et al. Gain-of-function enhancement of IP3 receptor modal gating by familial Alzheimer's disease-linked presenilin mutants in human cells and mouse neurons. Sci Signal 2010;3.

135. Cheung KH, Shineman D, Muller M, et al. Mechanism of Ca2+ disruption in Alzheimer's disease by presenilin regulation of InsP3 receptor channel gating. Neuron 2008;58:871-883.

136. Mercado G, Castillo V, Soto P, et al. ER stress and Parkinson's disease: pathological inputs that converge into the secretory pathway. Brain Res 2016;1648:626-632.

137. Cho HJ, Yu J, Xie C, et al. Leucine-rich repeat kinase 2 regulates Sec16A at ER exit sites to allow ER-Golgi export. EMBO J 2014;33:2314-2331.

138. Walczak A, Gradzik K, Kabzinski J, et al. The role of the ER-induced UPR pathway and the efficacy of its inhibitors and inducers in the inhibition of tumor progression. Oxid Med Cell Longev 2019;2019:1-15.

139. Koritzinsky M, Levitin F, van den Beucken T, et al. Two phases of disulfide bond formation have differing requirements for oxygen. J Cell Biol 2013;203:615-627.

140. Lind NR QQ, Yang L. ER stress and autophagy in obesity and nonalcoholic fatty liver disease. Current Pathobiology Reports 2017;5:289-299.

141. Lambert JE, Ramos-Roman MA, Browning JD, et al. Increased de novo lipogenesis is a distinct characteristic of individuals with nonalcoholic fatty liver disease. Gastroenterology 2014;146:726-735.

142. Hetz C, Papa FR. The unfolded protein response and cell fate control. Mol Cell 2018;69:169-181.

143. Adams CJ, Kopp MC, Larburu N, et al. Structure and molecular mechanism of ER stress signaling by the unfolded protein response signal activator IRE1. Front Mol Biosci 2019;6.

144. Carrara M, Prischi F, Ali MM. UPR signal activation by luminal sensor domains. Int J Mol Sci 2013;14:6454-6466.

145. Corazzari M, Gagliardi M, Fimia GM, et al. Endoplasmic reticulum stress, unfolded protein response, and cancer cell fate. Front Oncol 2017;7.

146. Todd DJ, Lee AH, Glimcher LH. The endoplasmic reticulum stress response in immunity and autoimmunity. Nat Rev Immunol 2008;8:663-674.

147. Jain BP. An Overview of unfolded protein response signaling and its role in cancer. Cancer Biother Radiopharm 2017;32:275-281.

148. Gardner BM, Pincus D, Gotthardt K, et al. Endoplasmic reticulum stress sensing in the unfolded protein response. Cold Spring Harb Perspect Biol 2013;5:1-15.

149. Hetz C, Chevet E, Oakes SA. Proteostasis control by the unfolded protein response. Nat Cell Biol 2015;17:829-838.

150. Glembotski CC. Endoplasmic reticulum stress in the heart. Circ Res 2007;101:975-984.

151. Fedeles SV, So JS, Shrikhande A, et al. Sec63 and Xbp1 regulate IRE1alpha activity and polycystic disease severity. J Clin Invest 2015;125:1955-1967.

152. Schonthal AH. Endoplasmic reticulum stress: its role in disease and novel prospects for therapy. Scientifica 2012;2012:1-26.

153. Uppala JK, Gani AR, Ramaiah KVA. Chemical chaperone, TUDCA unlike PBA, mitigates protein aggregation efficiently and resists ER and non-ER stress induced HepG2 cell death. Sci Rep 2017;7.

154. Kolb PS, Ayaub EA, Zhou W, et al. The therapeutic effects of 4-phenylbutyric acid in maintaining proteostasis. Int J Biochem Cell Biol 2015;61:45-52.

155. Ma W, Goldberg E, Goldberg J. ER retention is imposed by COPII protein sorting and attenuated by 4-phenylbutyrate. Elife 2017;6.

156. Li P, Fu D, Sheng Q, et al. TUDCA attenuates intestinal injury and inhibits endoplasmic reticulum stress-mediated intestinal cell apoptosis in necrotizing enterocolitis. Int Immunopharmacol 2019;74.

157. Berger E, Haller D. Structure-function analysis of the tertiary bile acid TUDCA for the resolution of endoplasmic reticulum stress in intestinal epithelial cells. Biochem Biophys Res Commun 2011;409:610-615.

158. Yoon YM, Lee JH, Yun SP, et al. Tauroursodeoxycholic acid reduces ER stress by regulating of Akt-dependent cellular prion protein. Sci Rep 2016;6.

159. Matsuoka M, Komoike Y. Experimental evidence shows salubrinal, an eIF2alpha dephosphorylation inhibitor, reduces xenotoxicant-induced cellular damage. Int J Mol Sci 2015;16:16275-16287.

160. Liu MQ, Chen Z, Chen LX. Endoplasmic reticulum stress: a novel mechanism and therapeutic target for cardiovascular diseases. Acta Pharmacol Sin 2016;37:425-443.

161. Valenzuela V, Jackson KL, Sardi SP, et al. Gene therapy strategies to restore ER proteostasis in disease. Mol Ther 2018;26:1404-1413.

162. Cabral-Miranda F HC. ER stress in neurodegenerative disease: from disease mechanisms to therapeutic interventions. Endoplasmic reticulum stress in disease 2017;4:11-26.

163. Ha Y, Liu W, Liu H, et al. AAV2-mediated GRP78 transfer alleviates retinal neuronal injury by downregulating ER stress and Tau oligomer formation. Invest Ophthalmol Vis Sci 2018;59:4670-4682.

164. Wang M, Law ME, Castellano RK, et al. The unfolded protein response as a target for anticancer therapeutics. Crit Rev Oncol Hematol 2018;127:66-79.

165. Riha R, Gupta-Saraf P, Bhanja P, et al. Stressed Out - Therapeutic implications of ER stress related cancer research. Oncomedicine 2017;2:156-167.

166. Zhao N, Cao J, Xu L, et al. Pharmacological targeting of MYC-regulated IRE1/XBP1 pathway suppresses MYC-driven breast cancer. J Clin Invest 2018;128:1283-1299.

167. Logue SE, McGrath EP, Cleary P, et al. Inhibition of IRE1 RNase activity modulates the tumor cell secretome and enhances response to chemotherapy. Nat Commun 2018;9.

168. Jiang D, Niwa M, Koong AC. Targeting the IRE1alpha-XBP1 branch of the unfolded protein response in human diseases. Semin Cancer Biol 2015;33:48-56.

169. Atkins C, Liu Q, Minthorn E, et al. Characterization of a novel PERK kinase inhibitor with antitumor and antiangiogenic activity. Cancer Res 2013;73:1993-2002.

170. Pytel D, Gao Y, Mackiewicz K, et al. PERK is a haploinsufficient tumor suppressor: gene dose determines tumor-suppressive versus tumor promoting properties of PERK in melanoma. PLoS Genet 2016;12.

171. Yadav RK, Chae SW, Kim HR, et al. Endoplasmic reticulum stress and cancer. J Cancer Prev 2014;19:75-88.

172. Gallagher CM, Garri C, Cain EL, et al. Ceapins are a new class of unfolded protein response inhibitors, selectively targeting the ATF6alpha branch. Elife 2016;5.

173. Okada T, Haze K, Nadanaka S, et al. A serine protease inhibitor prevents endoplasmic reticulum stress-induced cleavage but not transport of the membrane-bound transcription factor ATF6. J Biol Chem 2003;278:31024-31032.

174. Lee AS. GRP78 induction in cancer: therapeutic and prognostic implications. Cancer Res 2007;67:3496-3499.

175. Cerezo M, Lehraiki A, Millet A, et al. Compounds triggering ER stress exert anti-melanoma effects and overcome BRAF inhibitor resistance. Cancer Cell 2016;29:805-819.

176. Kosakowska-Cholody T, Lin J, Srideshikan SM, et al. HKH40A downregulates GRP78/BiP expression in cancer cells. Cell Death Dis 2014;5.

177. Ma Z, Fan C, Yang Y, et al. Thapsigargin sensitizes human esophageal cancer to TRAIL-induced apoptosis via AMPK activation. Sci Rep 2016;6.

178. Ferreira RB, Wang M, Law ME, et al. Disulfide bond disrupting agents activate the unfolded protein response in EGFR- and HER2-positive breast tumor cells. Oncotarget 2017;8:28971-28989.

179. Nami B, Donmez H, Kocak N. Tunicamycin-induced endoplasmic reticulum stress reduces in vitro subpopulation and invasion of CD44+/CD24- phenotype breast cancer stem cells. Exp Toxicol Pathol 2016;68:419-426.

180. Manasanch EE, Orlowski RZ. Proteasome inhibitors in cancer therapy. Nat Rev Clin Oncol 2017;14:417-433.

181. Dou QP, Zonder JA. Overview of proteasome inhibitor-based anti-cancer therapies: perspective on bortezomib and second generation proteasome inhibitors versus future generation inhibitors of ubiquitin-proteasome system. Curr Cancer Drug Targets 2014;14:517-536.

182. Waanders E, te Morsche RH, de Man RA, et al. Extensive mutational analysis of PRKCSH and SEC63 broadens the spectrum of polycystic liver disease. Hum Mutat 2006;27:830-839.

183. Katsuyama M, Masuyama T, Komura I, et al. Characterization of a novel polycystic kidney rat model with accompanying polycystic liver. Exp Anim 2000;49:51-55.

184. Sanzen T, Harada K, Yasoshima M, et al. Polycystic kidney rat is a novel animal model of Caroli's disease associated with congenital hepatic fibrosis. Am J Pathol 2001;158:1605-1612.

185. Masyuk TV, Huang BQ, Masyuk AI, et al. Biliary dysgenesis in the PCK rat, an orthologous model of autosomal recessive polycystic kidney disease. Am J Pathol 2004;165:1719-1730.

186. Mason SB, Liang Y, Sinders RM, et al. Disease stage characterization of hepatorenal fibrocystic pathology in the PCK rat model of ARPKD. Anat Rec (Hoboken) 2010;293:1279-1288.

187. Ward CJ, Hogan MC, Rossetti S, et al. The gene mutated in autosomal recessive polycystic kidney disease encodes a large, receptor-like protein. Nat Genet 2002;30:259-269.

188. Lager DJ, Qian Q, Bengal RJ, et al. The pck rat: a new model that resembles human autosomal dominant polycystic kidney and liver disease. Kidney Int 2001;59:126-136.

189. Mohammed-Ali Z, Lu C, Marway MK, et al. Endoplasmic reticulum stress inhibition attenuates hypertensive chronic kidney disease through reduction in proteinuria. Sci Rep 2017;7.

190. Jones FE, Murray LS, McNeilly S, et al. 4-Sodium phenyl butyric acid has both efficacy and counter-indicative effects in the treatment of Col4a1 disease. Hum Mol Genet 2019;28:628-638.

191. Liu J, Lee J, Salazar Hernandez MA, et al. Treatment of obesity with celastrol. Cell 2015;161:999-1011.

192. Montane J, de Pablo S, Castano C, et al. Amyloid-induced beta-cell dysfunction and islet inflammation are ameliorated by 4-phenylbutyrate (PBA) treatment. FASEB J 2017;31:5296-5306.

193. Jellbauer S, Perez Lopez A, Behnsen J, et al. Beneficial effects of sodium phenylbutyrate administration during infection with salmonella enterica serovar typhimurium. Infect Immun 2016;84:2639-2652.

194. Han X, Zhang X, Li H, et al. Tunicamycin enhances the antitumor activity of trastuzumab on breast cancer in vitro and in vivo. Oncotarget 2015;6:38912-38925.

195. Willot S, Uhlen S, Michaud L, et al. Effect of ursodeoxycholic acid on liver function in children after successful surgery for biliary atresia. Pediatrics 2008;122:e1236-e1241.

196. Harnois DM, Angulo P, Jorgensen RA, et al. High-dose ursodeoxycholic acid as a therapy for patients with primary sclerosing cholangitis. Am J Gastroenterol 2001;96:1558-1562.

197. Kotb MA. Molecular mechanisms of ursodeoxycholic acid toxicity & side effects: ursodeoxycholic acid freezes regeneration & induces hibernation mode. Int J Mol Sci 2012;13:8882-8914.

198. Banales JM, Saez E, Uriz M, et al. Up-regulation of microRNA 506 leads to decreased Cl-/HCO3- anion exchanger 2 expression in biliary epithelium of patients with primary biliary cirrhosis. Hepatology 2012;56:687-697.

199. Muff MA, Masyuk TV, Stroope AJ, et al. Development and characterization of a cholangiocyte cell line from the PCK rat, an animal model of Autosomal Recessive Polycystic Kidney Disease. Lab Invest 2006;86:940-950.

200. Huang BQ, Masyuk TV, Muff MA, et al. Isolation and characterization of cholangiocyte primary cilia. Am J Physiol Gastrointest Liver Physiol 2006;291:G500-G509.

201. Chen Q, Kang J, Fu C. The independence of and associations among apoptosis, autophagy, and necrosis. Signal Transduct Target Ther 2018;3.

202. Adan A, Alizada G, Kiraz Y, et al. Flow cytometry: basic principles and applications. Crit Rev Biotechnol 2017;37:163-176.

203. Poon IK, Hulett MD, Parish CR. Molecular mechanisms of late apoptotic/necrotic cell clearance. Cell Death Differ 2010;17:381-397.

204. Yoo KS, Lim WT, Choi HS. Biology of cholangiocytes: from bench to cedside. Gut Liver 2016;10:687-698.

205. Hwang J, Qi L. Quality control in the endoplasmic reticulum: crosstalk between ERAD and UPR pathways. Trends Biochem Sci 2018;43:593-605.

206. Christianson JC, Ye Y. Cleaning up in the endoplasmic reticulum: ubiquitin in charge. Nat Struct Mol Biol 2014;21:325-335.

207. Menendez-Benito V, Verhoef LG, Masucci MG, et al. Endoplasmic reticulum stress compromises the ubiquitin-proteasome system. Hum Mol Genet 2005;14:2787-2799.

208. Latham MP, Sekhar A, Kay LE. Understanding the mechanism of proteasome 20S core particle gating. Proc Natl Acad Sci USA 2014;111:5532-5537.

209. Vilchez D, Saez I, Dillin A. The role of protein clearance mechanisms in organismal ageing and age-related diseases. Nat Commun 2014;5.

210. Ben-Nissan G, Sharon M. Regulating the 20S proteasome ubiquitin-independent degradation pathway. Biomolecules 2014;4:862-884.

211. Onori P, Franchitto A, Mancinelli R, et al. Polycystic liver diseases. Dig Liver Dis 2010;42:261-271.

212. Masyuk TV, Huang BQ, Ward CJ, et al. Defects in cholangiocyte fibrocystin expression and ciliary structure in the PCK rat. Gastroenterology 2003;125:1303-1310.

213. Ward CJ, Yuan D, Masyuk TV, et al. Cellular and subcellular localization of the ARPKD protein; fibrocystin is expressed on primary cilia. Hum Mol Genet 2003;12:2703-2710.

214. Outeda P, Menezes L, Hartung EA, et al. A novel model of autosomal recessive polycystic kidney questions the role of the fibrocystin C-terminus in disease mechanism. Kidney Int 2017;92:1130-1144.

215. Nagano J, Kitamura K, Hujer KM, et al. Fibrocystin interacts with CAML, a protein involved in Ca2+ signaling. Biochem Biophys Res Commun 2005;338:880-889.

216. Torres M, Encina G, Soto C, et al. Abnormal calcium homeostasis and protein folding stress at the ER: A common factor in familial and infectious prion disorders. Commun Integr Biol 2011;4:258-261.

217. Liu XG, M.R. Endoplasmic reticulum stress and liver diseases. Liver research 2019;3:55-64.

218. Dara L, Ji C, Kaplowitz N. The contribution of endoplasmic reticulum stress to liver diseases. Hepatology 2011;53:1752-1763.

219. Lin JH, Walter P, Yen TS. Endoplasmic reticulum stress in disease pathogenesis. Annu Rev Pathol 2008;3:399-425.

220. Besio R, Iula G, Garibaldi N, et al. 4-PBA ameliorates cellular homeostasis in fibroblasts from osteogenesis imperfecta patients by enhancing autophagy and stimulating protein secretion. Biochim Biophys Acta Mol Basis Dis 2018;1864:1642-1652.

221. Zode GS, Kuehn MH, Nishimura DY, et al. Reduction of ER stress via a chemical chaperone prevents disease phenotypes in a mouse model of primary open angle glaucoma. J Clin Invest 2015;121:3542-3553.

222. Kim HJ, Jeong JS, Kim SR, et al. Inhibition of endoplasmic reticulum stress alleviates lipopolysaccharide-induced lung inflammation through modulation of NF-kappaB/HIF-1alpha signaling pathway. Sci Rep 2013;3.

223. Zhao Z, Cao L, Reece EA. Formation of neurodegenerative aggresome and death-inducing signaling complex in maternal diabetes-induced neural tube defects. Proc Natl Acad Sci USA 2017;114:4489-4494.

224. Ren LP, Song GY, Hu ZJ, et al. The chemical chaperon 4-phenylbutyric acid ameliorates hepatic steatosis through inhibition of de novo lipogenesis in high-fructose-fed rats. Int J Mol Med 2013;32:1029-1036.

225. Liu Y, Pan X, Li S, et al. Endoplasmic reticulum stress restrains hepatocyte growth factor expression in hepatic stellate cells and rat acute liver failure model. Chem Biol Interact 2017;277:43-54.

226. Lee EJ. Cell Proliferation and Apoptosis in ADPKD. Adv Exp Med Biol 2016;933:25-34.

227. Rani S, Sreenivasaiah PK, Kim JO, et al. Tauroursodeoxycholic acid (TUDCA) attenuates pressure overload-induced cardiac remodeling by reducing endoplasmic reticulum stress. PLoS One 2017;12.

228. Hu H, Tian M, Ding C, et al. The C/EBP Homologous protein (CHOP) transcription factor functions in endoplasmic reticulum stress-induced apoptosis and microbial infection. Front Immunol 2018;9.

Appendix

Publications during the PhD

1. **Santos-Laso A**, Izquierdo-Sánchez L, Rodrigues PM, Huang BQ, Munoz-Garrido P, Arbelaiz A, Caballero FJ, Fernandez-Barrena MG, Jimenez-Agüero R, Argemi J, Aragon T, Marzioni M, Drenth JPH, LaRusso NF, Bujanda L, Perugorria MJ, Banales JM. Proteaostasis improvement in cystic cholangiocytes alleviates endoplasmic reticulum stress and halts polycystic liver disease. Under preparation.
2. Banales JM, Iñarrairaegui M, Arbelaiz A, Milkiewicz P, Muntane J, Muñoz-Bellvis L, La Casta A, Gonzalez LM, Arretxe E, Alonso C, Martínez-Arranz I, Lapitz A, **Santos-Laso A**, Avila MA, Martínez-Chantar ML, Bujanda L, Marin JJG, Sangro B, Macias RIR. Serum metabolites as diagnostic biomarkers for cholangiocarcinoma, hepatocellular carcinoma and primary sclerosing cholangitis. *Hepatology*. (2019) 70(2); 547-562.
3. Perugorria MJ, Esparza-Baquer A, Oakley F, Labiano I, Korosec A, Jais A, Mann J, Tiniakos D, **Santos-Laso A**, Arbelaiz A, Gawish R, Sampedro A, Fontanellas A, Hijona E, Jimenez-Agüero R, Esterbauer H, Stoiber D, Bujanda L, Banales JM, Knapp S, Sharif O, Mann DA. Non-parenchymal TREM-2 protects the liver from immune-mediated hepatocellular damage. *Gut*. (2018) 68(3); 533-546.
4. Bárcena-Varela M, Caruso S, Llerena S, Álvarez-Sola G, Uriarte I, Latasa MU, Urtasun R, Rebouissou S, Alvarez L, Jimenez M, Santamaría E, Rodriguez-Ortigosa C, Mazza G, Rombouts K, José-Eneriz ES, Rabal O, Agirre X, Iraburu M, **Santos-Laso A**, Banales JM, Zucman-Rossi J, Prósper F, Oyarzabal J, Berasain C, Ávila MA, Fernández-Barrena MG. Dual targeting of histone methyltransferase G9a and DNA-methyltransferase 1 for the treatment of experimental hepatocellular carcinoma. *Hepatology*. (2019) 69(2); 587-603.
5. Ampuero J, Aller R, Gallego-Durán R, Banales JM, Crespo J, García-Monzón C, Pareja MJ, Vilar-Gómez E, Caballería J, Escudero-García D, Gomez-Camarero J, Calleja JL, Latorre M, Albillos A, Salmeron J, Aspichueta P, Lo Iacono O, Francés R, Benlloch S, Fernández-Rodríguez C, García-Samaniego J, Estévez P, Andrade RJ, Turnes J, Romero-Gómez M; **HEPAmet Registry**. The effects of metabolic status on non-alcoholic fatty liver disease-related outcomes, beyond the presence of obesity. *Alimentary Pharmacology & Therapeutics*. (2018) 48(11-12); 1260-1270.
6. Rodrigues PM, Perugorria MJ, **Santos-Laso A**, Bujanda L, Beuers U, Banales JM. Primary biliary cholangitis: A tale of epigenetically-induced secretory failure? *Journal of Hepatology*. (2018) 69(6); 1371-1393. REVIEW.
7. Erice O, Munoz-Garrido P, Vaquero J, Perugorria MJ, Fernandez-Barrena MG, Saez E, **Santos-Laso A**, Arbelaiz A, Jimenez-Agüero R, Fernandez-Irigoyen J, Santamaria E, Torrano V, Carracedo A, Ananthanarayanan M, Marzioni M, Prieto J, Beuers U, Oude Elferink RP, LaRusso NF, Bujanda L, Marin JJG, Banales JM. MiRNA-506 promotes primary biliary cholangitis-like features in cholangiocytes and immune activation. *Hepatology*. (2018) 67(4); 1420-1440.
8. Erice O, Labiano I, Arbelaiz A, **Santos-Laso A**, Munoz-Garrido P, Jimenez-Agüero R, Olaizola P, Caro-Maldonado A, Martín-Martín N, Carracedo A, Lozano E, Marin JJ, O'Rourke CJ, Andersen JB, Llop J, Gómez-Vallejo V, Padro D, Martin A,

Marzioni M, Adorini L, Trauner M, Bujanda L, Perugorria MJ, Banales JM. Differential effects of FXR or TGR5 activation in cholangiocarcinoma progression. *Biochimica et Biophysica Acta Molecular Basis of Disease*. (2018) 1864(4 Pt B); 1335-1344.

9. Arbelaiz A, Azkargorta M, Krawczyk M, **Santos-Laso A**, Lapitz A, Perugorria MJ, Erice O, Gonzalez E, Jimenez-Agüero R, Lacasta A, Ibarra C, Sanchez-Campos A, Jimeno JP, Lammert F, Marzioni M, Macias RIR, Marin JJ, Patel T, Gores GJ, Martinez I, Elortza F, Falcon-Perez JM, Bujanda L, Banales JM. Serum extracellular vesicles contain protein biomarkers for primary sclerosing cholangitis and cholangiocarcinoma. *Hepatology*. (2017) 66(4); 1125-1143.
10. **Santos-Laso A**, Perugorria MJ, Banales JM. O-GlcNAcylation: undesired tripmate but an opportunity for treatment in NAFLD-HCC. *Journal of Hepatology*. (2017) 67 (2); 218-220. EDITORIAL.
11. Merino-Azpitarte M, Lozano E, Perugorria MJ, Esparza-Baquer A, Erice O, **Santos-Laso A**, O'Rourke CJ, Andersen JB, Jiménez-Agüero R, Lacasta A, D'Amato M, Briz O, Jalan-Sakrikar N, Huebert RC, Thelen KM, Gradilone SA, Aransay AM, Lavín JL, Fernández-Barrena MG, Matheu A, Marzioni M, Gores GJ, Bujanda L, Marin JJ, Banales JM. SOX17 regulates cholangiocyte differentiation and acts as a tumour supressor in cholangiocarcinoma. *Journal of Hepatology*. (2017) 67 (1); 72-83.
12. **Santos-Laso A**, Izquierdo-Sanchez L, Lee-Law PY, Perugorria MJ, Marzioni M, Marin JJ, Bujanda L, Banales JM. New advances in polycystic liver diseases. *Seminars Liver Disease*. (2017) 37 (1); 45-55. REVIEW.
13. **Santos-Laso A**, Munoz- Garrido P, Felipe Agirre M, Bujanda L, Banales JM, Perugorria MJ. New advances in the molecular mechanisms driving biliary fibrosis and emerging molecular targets. *Current Drug Targets*. (2017) 18(8); 908-920. REVIEW.
14. Munoz-Garrido P, Marin JJG, Perugorria MJ, Urribarri AD, Sáez E, Uriz M, Sarvide S, Portu A, Concepcion AR, Romero MR, Monte MJ, **Santos-Laso A**, Hijona E, Jimenez-Agüero R, Marzioni M, Beuers U, Masyuk TV, LaRusso NF, Prieto J, Bujanda L, Drenth JPH, Banales JM. Ursodeoxycholic acid inhibits hepatic cystogenesis in experimental models of polycystic liver disease. *Journal of Hepatology*. (2015) 63(4); 952-961.